Water Resources Management in the Atacama Desert: pivotal insights into arid Andean groundwater systems of northern Chile

vorgelegt von
M. Sc.
Konstantin W. Scheihing
geb. in Duisburg

von der Fakultät VI - Planen Bauen Umwelt -
der Technischen Universität Berlin
zur Erlangung des akademischen Grades

Doktor der Ingenieurwissenschaften
– Dr.-Ing. –
genehmigte Dissertation

Promotionsausschuss:

Vorsitzender:	Prof. Dr. Matthias Barjenbruch
Gutachter:	Prof. Dr. Uwe Tröger
Gutachter:	Prof. Dr. Stefan Wohnlich

Tag der wissenschaftlichen Aussprache: 07. November 2017

Berlin 2018

To the people of Chile.

Abstract

Different stakeholders depend on the depleting groundwater resources in the Atacama Desert of northern Chile. Endeavors in water resources management encounter the arduous task of balancing the often-opposing poles of societal, economic, political and environmental interests. Finding – at best – sustainable solutions to modern challenges is aggravated by a lack of understanding of hydrological processes in the arid Andean environment. The presented dissertation aims to shed light on several long-lived questions concerning hydrogeological uncertainties in the Tarapacá Region. Accordingly, it challenges established concepts and describes so far unconsidered hydrological mechanisms that hold relevance for the Atacama Desert.

A statistical assessment of long-term monitoring data in the arid Andean Laguna Lagunillas basin – where groundwater is being overexploited since the early-1990s – reveals that shallow groundwater can have a substantial regulating function on the associated local climate. These unknown groundwater-climate feedbacks hold strong importance for managing future and existing water production sites in the high, arid Andes.

Furthermore, the often-discussed existence of an inter-basin groundwater flow from the Andean Altiplano to the Pampa del Tamarugal (PdT) – through deep basement fractures – was investigated. For the most prominent geological complex, where such an inter-basin flow could occur (Salar del Huasco basin-Pica Oasis), a hydrological time series analysis, as well as reflection seismic data and geothermal investigations, demonstrate, that the concept cannot be proven true. In this context, it is shown, that pressure signals induced by recharge in the Andean Precordillera can propagate rapidly over tens of kilometers with a constant lag down to the Andean foothills.

Finally, a reassessment of a sizeable stable isotope dataset of meteoric water provides evidence that local topographic features of western Andean slope catchments, can control vapor mixing processes of easterly and westerly air masses with different isotope characteristics. This effect is reflected in basin-specific isotope value ranges in surface and groundwater and hence can be used to trace the regional groundwater flow regime and respective recharge areas. The primary recharge facilitated into the PdT-Aquifer infiltrates in the investigated cases very likely along the lower stream segments of intermittently discharging rivers, while the established idea of a significant alluvial fan recharge after flash-floods is challenged.

The developed insights have implications for other, hydrologically-akin groundwater systems in the Atacama Desert and strengthen the basis for rational decision-making when managing respective water resources in the Tarapacá region.

Zusammenfassung

Verschiedene Akteure sind von den zurückgehenden Grundwasserressourcen in der Atacama Wüste Nordchiles abhängig. Derzeitige Bestrebungen im Bereich des Wasserressourcenmanagements treffen auf die schwierige Aufgabe, die oft gegensätzlichen gesellschaftlichen, ökonomischen, politischen und ökologischen Interessen zu einen. Das Finden von - im besten Falle - nachhaltigen Lösungen ist oft erschwert durch die Unkenntnis über hydrologische Prozesse in den ariden Anden. Das Ziel der vorliegenden Dissertation war es, neue Einsichten zu langjährigen, offenen hydrogeologischen Fragestellungen in der Tarapacá Region zu erarbeiten. Dabei wurden gefestigte Erklärungsmodelle hinterfragt und bisher vollkommen unbeachtete hydrologische Funktionsweisen aufgezeigt, die in der Atacama Wüste von Bedeutung sind.

Die statistische Analyse von Langzeit-Monitoringdaten des ariden Laguna Lagunillas Einzugsgebietes, wo sich der Grundwasserspiegel durch Übernutzung seit den Neunzigern mehrere Meter abgesenkt hat, zeigt auf, dass oberflächennahes Grundwasser eine stark regulierende Funktion auf das betroffene lokale Klima haben kann. Diese bis dato unbekannten Grundwasser-Klima-Kopplungen sind von hoher Bedeutung für das Management zukünftiger und gegenwärtiger Wasserproduktionsstätten in den ariden Anden.

Darüber hinaus wurde das oft diskutierte Konzept eines unterirdischen Grundwasserflusses von dem andinen Altiplano des Salar del Huasco Beckens zur Pampa del Tamarugal (PdT) durch tiefe Störungszonen untersucht. Hydrologische Zeitreihenanalysen, sowie reflektionsseismische Daten und geothermische Untersuchungen konnten aufzeigen, dass für ein solches konzeptionelles Modell keine Belege existieren. In diesem Zusammenhang kann gezeigt werden, dass hydraulische Drucksignale, die durch Grundwasserneubildung im andinen Vorgebirge erzeugt werden, in kürzester Zeit über zehner Kilometer und mit einem konstanten Zeitversatz zum Fußgebirge der Atacama Wüste übertagen werden.

Schlussendlich ließ sich durch die Analyse eines großen Datensatzes stabiler Isotope in Grundwasser darlegen, dass lokale topographische Ausprägungen westlicher, andiner Einzugsgebiete eine zentrale Rolle bei der Mischung von westlichen und östlichen Luftmassen haben, die jeweils unterschiedliche Isotopenzusammensetzungen aufweisen. Dieser Effekt spiegelt sich wider im Wertespektrum stabiler Isotope im Grundwasser und kann daher genutzt werden,

um die langjährige, regionale Grundwasserfließrichtung zu identifizieren und die jeweiligen Neubildungszonen einzugrenzen. Die Hauptgrundwasserneubildung für den PdT-Aquifer findet sehr wahrscheinlich entlang der Endsegmente ephemerer Flüsse statt, wobei das Konzept einer signifikanten Neubildung im Bereich alluvialer Fächer nach Flutungsereignissen in den untersuchten Fällen hinterfragt werden muss.

Die entwickelten Erkenntnisse sind von Bedeutung auch für andere, hydrologisch vergleichbare Grundwassersysteme in der Atacama Wüste und stärken die Basis für ein evidenzbasiertes Wasserressourcenmanagement in der Tarapacá Region.

Resumen

Diferentes grupos de interés dependen de los recursos hídricos subterráneos decrecientes del desierto de Atacama, en el norte de Chile. Los esfuerzos actuales en la gestión del agua se enfrentan con la tarea desafiante de contrapesar los intereses sociales, económicos, políticos y ecológicos. Encontrar - en el caso mejor - soluciones sustentables, es muchas veces agravado por la falta de entendimiento de procesos hidrológicos en el ambiente de los Andes áridos. La meta de la presente disertación es generar nuevos conocimientos acerca de preguntas hidrogeológicas aún sin respuesta en la región de Tarapacá. En ella, se analiza críticamente modelos conceptuales establecidos y demuestra la existencia de funcionamientos hidrológicos no considerados, que son de relevancia por el desierto de Atacama.

El análisis estadístico de datos de monitoreo de 29 años medidos en la cuenca árida Laguna Lagunillas, dónde el agua subterránea ha sido sobreexplotada desde hace décadas, demuestra que, agua subterránea somera puede tener una función regulatorio esencial con respecto al clima local. Estas desconocidas interacciones entre agua subterránea y el clima son de alta importancia para la gestión de futuros y presentes proyectos de extracción de agua en los Andes áridos.

Además, se investigó el concepto controvertido de un flujo subterráneo de agua desde el Altiplano andino hacia la Pampa del Tamarugal (PdT) a través de una red de fracturas muy profundas. El análisis de series temporales, tal como la interpretación de datos sísmicos y consideraciones geotérmicas, demuestran que este tipo de flujo profundo no se pudo verificar para el caso del complejo geológico discutido (Salar del Huasco-Oasis de Pica). En este contexto es posible justificar que las señales de presión hidráulica, generadas por eventos de recarga en la Precordillera andina, se transmiten rápidamente a través de decenas de kilómetros con un retraso constante hacia las estribaciones andinas.

Finalmente, en el marco de un análisis de un registro sustancial de datos isotópicos estables de agua subterránea, se pudo mostrar que las diferentes condiciones topográficas locales de las cuencas en la Precordillera, controlan significativamente la mezcla de masas de aire occidental y oriental, las cuales muestran distintas características isotópicas. Este efecto se refleja en los valores isotópicos de agua subterránea y, por lo tanto, es posible utilizarlo para rastrear flujos subterráneos de agua e identificar las zonas de recarga respectivas.

La recarga principal del acuífero de la PdT ocurre más probablemente en los segmentos finales de ríos efímeros, mientras que es necesario reconsiderar el concepto aceptado de una recarga significativa en el área de los abanicos aluviales investigados después de inundaciones intermitentes.

Las comprensiones desarrolladas son de importancia para otros sistemas parecidos de agua subterráneas en el Atacama y apoyan la base para una gestión racional de los recursos hídricos vitales en la región de Tarapacá.

Contents

1. Introduction

1.1. Motivation: Vital groundwater resources in the hyper-arid to arid environment of the Atacama Desert

The Atacama Desert expands from the Pacific coastline of northern Chile to the arid Andes with altitudes above 5500 m above sea level and is famously known to exhibit some of the driest places on earth (Moreno 2007). Despite its aridity particularly the sedimentary basins which fill respective Andean valleys, can hold significant groundwater resources. These serve for human consumption, as drinking water, for mining purposes or in the local agriculture (Valdés-Pineda et al. 2014; Chávez et al. 2016). At the same time, the growing water demand, as well as climate change, threaten and continuously diminish available resources (Chávez et al. 2016; Valdés-Pineda et al. 2014; Ribeiro et al. 2015; Minvielle and Garreaud 2011). Both factors have negative impacts on the long-term water supply security as well as groundwater-fed ecosystems. In many cases, Andean hydrogeological systems lack a profound and scientific functional understanding, due to their complex geology as well as often remote and vastly extended areas which complicate data collection. Respective hydrogeological research has only recently begun to intensify (Houston 2006a, 2007, 2009; Acosta and Custodio 2008; Herrera et al. 2016; Kikuchi and Ferré 2016; Magaritz et al. 1990; Montgomery et al. 2003; Oyarzún et al. 2017; Uribe et al. 2015). However, such an understanding is the very basis for optimizing water management schemes. In particular, high Andean aquifers in northern Chile hold hitherto mostly untouched but attractive groundwater resources in an otherwise water-scarce environment (PUC 2009). These resources will likely gain in importance regionally in the coming years to compensate eventual water usage constraints

imposed on conventionally-exploited aquifers (PUC 2009; Valdés-Pineda et al. 2014). In this context, the presented thesis aims to advance the knowledge on the functional hydrogeology of arid Andean groundwater systems, while focusing on the regional Pampa del Tamarugal (PdT) Aquifer and the associated high Andean basins (Figure 1.1a, b).

1.2. From the Andes to the Pampa del Tamarugal: Hydrogeological interdependence of two complex geological systems

The broader area of work can be subdivided geographically into four major units. Beginning in the west, these are (Figure 1.1a): (1) the Chilean Coastal Cordillera; (2) the sedimentary forearc basin of the PdT (also termed Central Depression); followed east by (3) the Andean Precordillera; and subsequently the (4) Andean Altiplano Plateau (Jordan and Nester 2012). The PdT-Aquifer (Figure 1.1b) is the largest known aquifer of northern Chile and its resources serve for human consumption to more than 300,000 inhabitants of the Tarapacá Region, as well as in the local mining industry and agriculture (Jica 1995; Chávez et al. 2016). The aquifer superficially spreads over a north-south extension of more than 150 km. While sedimentary deposits in the PdT exhibit a total depth of up to ~1700 m below ground level (bgl) (Nester 2008), the primary exploited aquifer reaches a maximum depth of ~300 m bgl (Jica 1995). Its groundwater storage was estimated in 1995 at ~27 km^3 (Jica 1995). However, available water resources are being persistently overexploited with drawdown rates of on average ~5-40 cm/a in the central western part of the PdT (Jica 1995; Chávez et al. 2016; Lictevout et al. 2013).

The hydrology of the area of work is dominated by east-west heading, mainly ephemeral rivers, flowing through narrow ravines (Quebradas) downslope, from parts of the Andean Altiplano and Precordillera (at >4000 m asl) to the plane sedimentary basin (at ~1000 m asl). The relevant catchments are (from north to south, Figure 1.1b): Aroma, Tarapacá, Quipisca, Juan de Morales, Quisma, Chacarillas, and Ramada.

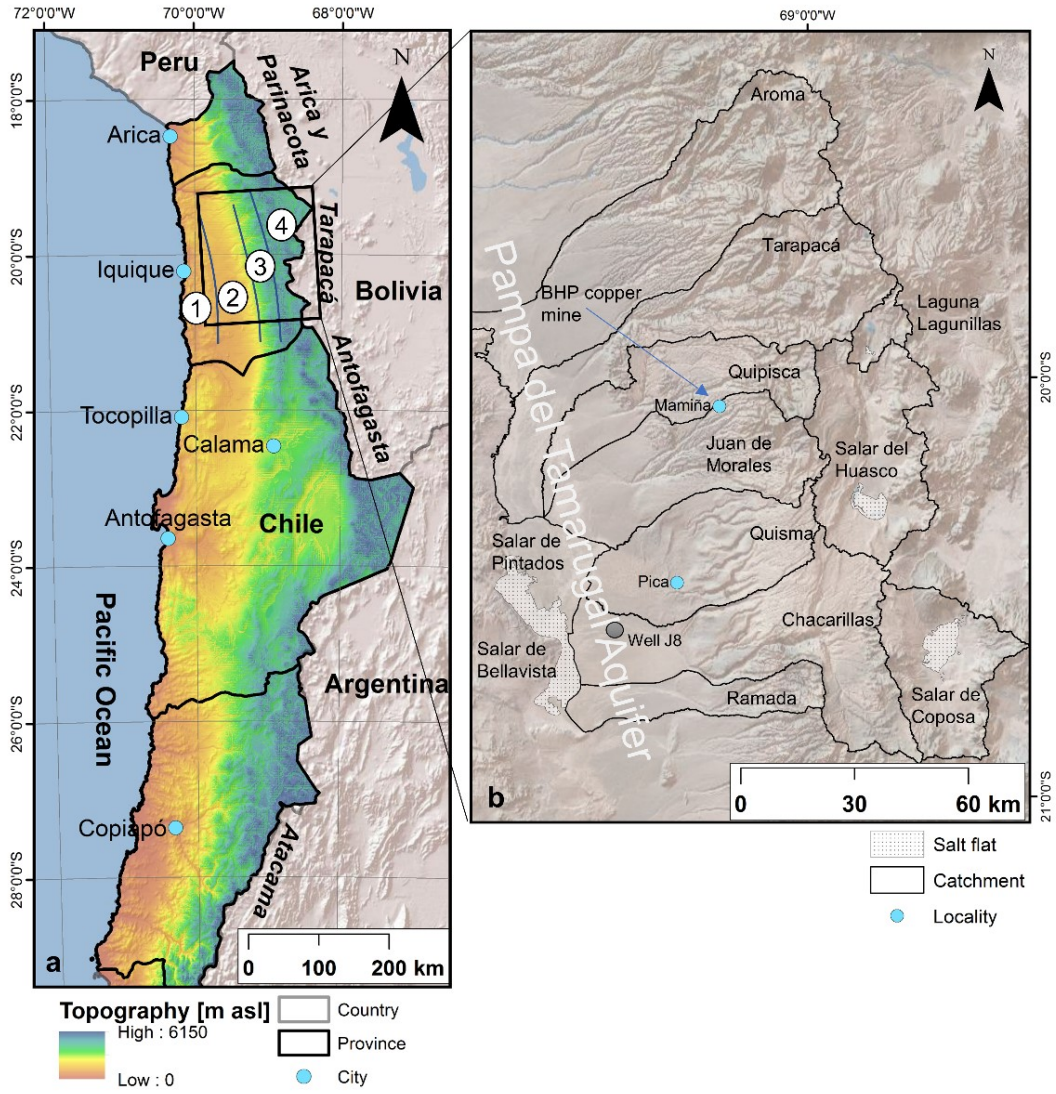

Figure 1.1 **(a)** Topography of the Atacama Desert in central South America (1: Coastal Cordillera, 2: Pampa del Tamarugal, 3: Andean Precordillera, 4: Andean Altiplano Plateau and high Andes), **(b)** Catchments of the area of work

Groundwater and surface water finally reaches the sinks of the PdT at its western margin, where the magmatic rocks of the Coastal Cordillera behave as an impermeable barrier (Jordan and Nester 2012). These sinks form terminal water traps and – due to extensive evaporation – exhibit extensive salt flats (Pintados- and Bellavista-Salar) (Nester 2008; Jordan and Nester 2012). Mean annual rainfall (R_m *[mm/a]*) in the region increases exponentially with altitude (*A [m asl]*) according to Eq. 1-1 (Houston 2006b):

$$R_m = e^{0.0012A} \qquad \text{Eq. 1-1}$$

Precipitation amounts below 2000 m asl are negligible but can reach ~120 mm/a and more above 4000 m asl. Occasional storm events in the Andes – which occur particularly during austral summer, when more than 80% of annual precipitation falls – can lead to flash-floods, which finally reach the widespread alluvial fans of the PdT (Houston 2006b, 2002). At the same time, potential evaporation during austral summer months accounts for ~250-350 mm/month in the plane Atacama Desert (DGA 2015).

Despite the strategic and vital importance of the PdT-Aquifer, to date, no reliable hydrogeological model has been established for long-term groundwater management (Rojas et al. 2010). This restraint is due to conceptual uncertainties regarding the model set up. Recharge areas and amounts along with groundwater inflows are not sufficiently understood (Rojas et al. 2010).

The encountered uncertainties are facilitated by the complex hard-rock geology in the transition zone from the Andes to the PdT, as well as due to a low number of respective field studies (Houston 2002; Rojas and Dassargues 2007). The complexity of the groundwater system is reflected in the heterogenic distribution of the electrical conductivity, which ranges between 5000 µS/cm and 300 µS/cm (Jica 1995), as well as the wide spectrum of $\delta^{18}O$ values, spanning from -13 to -6 ‰ (Fritz et al. 1981; Salazar et al. 1998; Magaritz et al. 1989; Aravena 1995). These findings are particularly surprising because the lowest $\delta^{18}O$ values correspond with measurements in the Andean Altiplano.

To explain these phenomena a most controversially discussed recharge concept was proposed, namely a deep basement fracture flow, that supposedly guides water subsurface from the adjacent Andean Altiplano (Salar del Huasco basin) to the PdT-Aquifer and some thermal springs at the Andean foothills (Pica Oasis) (Magaritz et al. 1990; Magaritz et al. 1989; Uribe et al. 2015; Rojas et al. 2010; Fritz et al. 1981; Salazar et al. 1998; Jica 1995; Jayne et al. 2016). This concept was still considered during the latest attempt to model the PdT-Aquifer (Rojas et al. 2010; Rojas and Dassargues 2007). However, a first convincing argument to reject this hypothesis was recently made based on water balance calculations in the framework of the calibration of a hydrological model for the Salar del Huasco basin (Uribe et al. 2015). Altogether, this open conceptual question holds strong political importance for the region, because to date several attempts by mining companies to obtain water production rights from the Salar del Huasco basin have been denied by the Chilean water directorate (DGA), including due to the unresolved issue. Local inhabitants – particularly of the touristy Pica Oasis – fear

that permission for water extractions could lead to a reduced discharge of respective springs at the Andean foothills.

However, the observed wide spectrum of stable isotope values in the PdT-Aquifer has also kindled different other assumptions, such as a recharge occurring at different elevations along the western Andean slope accompanied by altitude effects affecting relevant precipitations, or thermal water-rock interactions and a change of climatic conditions (Aravena 1995; Magaritz et al. 1989; Jayne et al. 2016). Moreover, another commonly accepted recharge concept was introduced based on the assessment of groundwater-level fluctuations at well J8, situated at the distant alluvial fan of the Chacarillas catchment (Figure 1.1b, Houston 2002). Here, it was argued that a direct recharge would occur from alluvial fans due to flash-flood events. Houston (2002) estimated the return period of such flash-floods at four years and derived a continuous recharge amount of 200 l/s on average from the concerned alluvial fan. By contrast, a publication by Aravena et al. (1989) demonstrated, that flood water from the Chacarillas catchment is isotopically strongly enriched (>-4‰ $\delta^{18}O$) due to isotope fractionation processes caused by evaporation occurring in the open desert. They pointed out that the enriched $\delta^{18}O$ values of flood water could not be correlated with groundwater of wells that existed at that time and hence drew the conclusion that alluvial fan recharge is probably a negligible source of recharge. Houston (2002) was not aware of the study by Aravena et al. (1989) (no citation).

Despite the few scientific publications on groundwater recharge in the PdT, some governmentally-financed reports intended to determine provided inflow amounts (DICUC 1988; DICTUC 2006, 2007; Jica 1995). Total recharge was generally approximated based on the statistical distribution of rainfall along the different slope catchments that host the Pampa del Tamarugal and a jointed runoff estimation. However, such attempts were restricted by the fact that there is only one catchment (Tarapacá basin) that exhibits gauging stations (Lictevout et al. 2013). Nevertheless, the mentioned reports accounted for a total mean recharge of roughly 800-1200 l/s to the PdT-Aquifer.

Paleo-hydrological studies are indispensable for understanding recharge mechanisms in the Atacama Desert. While the PdT remained very likely arid during the Late Quaternary, the Altiplano area went through stages of prominent variations in mean precipitation amounts during the last 20 ka (Central Andean Pluvial Event) (Placzek et al. 2009; Placzek et al. 2006). It was demonstrated that these periods indirectly influenced water availability in the PdT, mainly triggered

by stream discharge from the Andean Altiplano and Precordillera (Gayo et al. 2012b; Gayo et al. 2012a; Rech et al. 2002). At ~21°S latitude, age-dated ancient riparian vegetation indicates that during the periods 17.6-14.2 ka before present (BP), 12.1-11.4 ka BP and 2.5-2 ka BP, regional groundwater recharge events fed the PdT-Aquifer (Gayo et al. 2012b). Relating to this, mean groundwater residence times in the PdT were roughly estimated to range from a few hundred to a few thousand years BP (Fritz et al. 1981).

Having said this, it remains clear that the Andean Altiplano plays a vital role in the hydrological understanding of the low-elevation Atacama Desert and the PdT. Both topographically- and climatically-distinct areas interact hydrologically by means of either surface runoff or – as described above – an eventual inter-basin flow of groundwater.

In most recent times, another linking factor should be considered, namely anthropogenic water demand and consumption. One of the most prominent examples of this is the case of the Andean Laguna Lagunillas basin. The closed Laguna Lagunillas basin abuts on the western catchments that discharge into the PdT (Figure 1.1b). Its unconfined aquifer has served since 1992 for water withdrawals to the mining company BHP Billiton (100-300 l/s), which directs the water to the copper mine Cerro Colorado in the Quipisca catchment, at the western Andean slope (BHP Billiton 2015; Larraín and Poo 2010; Yáñez Fuenzalida and Molina Otárola 2008). Therefore, it is understood that water fluxes between the Andean Altiplano and the PdT can also have human-induced reasons. The mentioned case holds particular interest because an apparent mismanagement led to a severe dropping of the formerly shallow water table in the Laguna Lagunillas basin (by several meters), consequently causing springs to become dry, which destroyed the associated wetland (Yáñez Fuenzalida and Molina Otárola 2008; Larraín and Poo 2010). While such mismanagement must be partly attributed to sheer ignorance, another essential factor is the lack of hydrogeological understanding of the concerned groundwater system. Another nearby closed Andean basin (Salar de Coposa basin) equally serves for water withdrawals to a mining company (Collahuasi Mining), although in this case, a sustainable use of water resources appears to be more successful (Acosta et al. 2009).

In conclusion, all aspects elaborated here form part of the difficulties encountered associated with water resources management in the area of work

and demonstrate the high hydrological interdependence between the arid Andes and the PdT.

Recent decades have demonstrated that water extractions from the PdT-Aquifer have increased steadily from round about 400 l/s in the 1980's to almost 4000 l/s in 2013 (Chávez et al. 2016). When compared with estimated recharge amounts, the current deficit accounts for roughly 3000 l/s. The flourishing of the copper mining sector in northern Chile actively contributed to this development, through either direct consumption or indirectly due to economic growth and hence population growth in the region. Although today there is not much development to be expected in the regions mining sector, because most profitable pits have been operating since the 1990s, agricultural water consumption has doubled since 2005 and nowadays exceeds the water use in mining (Chávez et al. 2016). The hitherto constant increment of the water demand and the associated overexploitation of available resources, emphasizes the urgent need for a reasonably accurate conceptual and contextual understanding of the particular hydrogeological framework, as well as an integrated water resources management that can count on reliable hydrogeological models to predict water availability and aquifer responses to modern challenges. While the exploitation of untapped high Andean aquifers promises short-term relief, the frivolous use of these resources will only prolong future social and environmental problems that arise due to the increasing imbalance in the region's water budget. Due to the fundamental importance of water in every aspect of society, the situation has the potential to stimulate severe conflicts. This is also true for most parts of northern Chile, like the Antofagasta Region and the Atacama Region (Figure 1.1 a), where the pressure on water resources poses even more urgent problems due to the absence of abundant aquifers (Valdés-Pineda et al. 2014). To prevent a water crisis in northern Chile, in recent years a controversial 15 billion US$ project has been proposed, with the title 'Aquatacama,' for which a feasibility study is currently being carried out (BNamericas 2016). The idea is to build an (at least) 1600 km submarine freshwater pipeline from Chiles water-rich south to the arid north (there are other similar proposals) (Via Marina 2013; CNN Chile 2017). The argumentation is that such a project would be more cost-effective in the long term than desalinization plants, which are already successfully in use in the Antofagasta region (Petry et al. 2007). Apparently, the highest risk of such a project lies in the high societal dependence on distant supply sources and –

related to that – the projects vulnerability regarding natural hazards like earth- or seaquakes. However, the successful management of scarce water resources in northern Chile is only possible when all human endeavors – in the field of either water sciences or engineering – work together for assuring a sustainable and balanced human development.

1.3. Outline of the thesis

The presented thesis features three self-contained articles that focus on the functional hydrogeological understanding of the PdT and the adjacent Andean Altiplano. The publications finally aim to enhance the basis for rational and optimized water resources management in the region by investigating and clarifying the earlier elaborated hydrogeological problems and uncertainties.

Chapter 2: Local climate change induced by groundwater overexploitation in a high Andean arid watershed, Laguna Lagunillas basin, northern Chile

Scheihing K, Tröger U (2017) Local climate change induced by groundwater overexploitation in a high Andean arid watershed, Laguna Lagunillas basin, northern Chile. Hydrogeol J 16:1817. doi: 10.1007/s10040-017-1647-4

The Laguna Lagunillas basin is a closed arid Andean catchment at elevations above 4000 m asl that serves for water withdrawals to a copper mine (situated in the PdT) owned by BHP Billiton. Since 1992 groundwater levels have fallen from near-surface to several meters below ground level. The first presented publication uses this case of groundwater mismanagement to investigate unstudied effects of feedbacks between shallow groundwater and air temperatures in the arid Andes. It was published as part of the topical collection 'Climate-change research by early-career hydrogeologists' initiated by the International Association of Hydrogeologists (IAH) and the UNESCO-IHP GRAPHIC project (Groundwater Resources Assessment under the Pressures of Humanity and Climate Change). Based on a statistical time series analysis of mean minimum and maximum temperature data over a period of 29 years, the case study can prove that the ongoing decline of the water table in the Laguna Lagunillas basin has caused a severe local climatic change. Linear and non-linear

effects are being quantified. Due to the similar hydrogeological setting of other closed arid Andean basins, yielded results are very likely transferable to similar watersheds. The findings allow deriving a best-practice recommendation for existing and future water production projects in the arid Andean Altiplano, to prevent adverse impacts on local climates.

Chapter 3: Insights into Andean slope hydrology: reservoir characteristics of the thermal Pica spring system, Pampa del Tamarugal, northern Chile

Scheihing KW, Moya CE, Tröger U (2017) Insights into Andean slope hydrology: Reservoir characteristics of the thermal Pica spring system, Pampa del Tamarugal, northern Chile. Hydrogeol J 119(2):33. doi: 10.1007/s10040-017-1533-0

The second paper inquiries into the long-lived question of the existence or non-existence of an inter-basin fracture flow from the Andean Altiplano to the plane Atacama Desert. Based on an integrated analysis of reflection-seismic data, hydrological time series and hydrochemical data, it can be demonstrated, that the water in question is being recharged at the Andean Precordillera at elevations of ~3800 m asl and circulates to maximum depths of ~950 m bgl. Consequently, in the given case an inter-basin flow is highly unlikely to occur. Furthermore, insights into the geothermal setting of the thermal Pica springs are being derived along with hydraulic slope reservoir characteristics and corrected mean residence times of groundwaters that reach the Andean foothills between 20.4°-20.6°S latitude.

Chapter 4: Reassessing hydrological processes that control stable isotope tracers in groundwater of the Atacama Desert (northern Chile)

Scheihing K, Moya C, Struck U, Lictevout E, Tröger U (2018) Reassessing Hydrological Processes That Control Stable Isotope Tracers in Groundwater of the Atacama Desert (Northern Chile). Hydrology 5:3. doi: 10.3390/hydrology5010003

The third article was published in the Journal Hydrology (MDPI). It is based on a geostatistical assessment of 514 $\delta^{18}O$ and $\delta^{2}H$ samples from the regional PdT-Aquifer and the adjacent Andes. The examination brings to light the fact that water of each Precordilleran basin exhibits a characteristic range of isotope values in meteoric waters. A novel explanation for processes that cause this

phenomenon is introduced. In addition, the effect is used to trace the regional groundwater flow regime of the PdT-Aquifer which allows for identifying different recharge zones of the given groundwater resources. Hence, conceptual hydrogeological uncertainties of the PdT-Aquifer can be reduced. Overall, the results challenge the established idea of groundwater recharge through alluvial fans after flash-floods.

Chapter 5: 'Synthesis'

The final chapter of this thesis discusses the applied methodologies and resulting findings of the three stand-alone articles. Yielded insights are set into the context of conceptual hydrogeological uncertainties, regional water resources management considerations and topics of further research.

1.4. References

Acosta O, Custodio E (2008) Impactos ambientales de las extracciones de agua subterránea en el Salar del Huasco (norte de Chile) (Environmental impacts of groundwater production in the Salar del Huasco basin (Northern Chile)). Boletín Geológico y Minero(119):33–50

Acosta O, Rengifo P, Dzogolyk E, Muñoz JF (2009) De la exploración hidrogeológica a la gestión hídrica avanzada, Salar de Coposa, norte de Chile (From hydrogeological exploration to an advanced water resources management, Salar de Coposa, northern Chile). GEOMIN 2009 Antofagasta, Chile

Aravena R (1995) Isotope Hydrology and Geochemistry of Northern Chile Groundwaters. Bull. Inst. fr. études andines(24)

BHP Billiton (2015) BHP Billiton Chile Sustainability report 2014. http://www.bhpbilliton.com/~/media/bhp/documents/society/reports/2014/csr-eng150518sustainabilityreport2014bhpbillitonchileoperations.pdf. Accessed 17 May 2016

BNamericas (2016) Chile's Aquatacama water pipeline project still in the works. https://www.bnamericas.com/en/news/waterandwaste/chiles-aquatacama-water-pipeline-project-still-in-the-works1. Accessed 5 May 2017

Chávez RO, Clevers J, Decuyper M, Bruin S de, Herold M (2016) 50 years of water extraction in the Pampa del Tamarugal basin: Can Prosopis tamarugo trees survive in the hyper-arid Atacama Desert (Northern Chile)? Journal of Arid Environments 124:292–303. doi: 10.1016/j.jaridenv.2015.09.007

CNN Chile (2017) Agenda Agrícola: Más riego y electricidad para Chile, ¿es posible? http://www.cnnchile.com/noticia/2017/06/24/agenda-agricola-mas-riego-y-electricidad-para-chile-es-posible. Accessed 25 June 2017

DGA (2015) Información Oficial Hidrometeorológica y de Calidad de Aguas en Línea - Oficial online information; hydrometeorology and water quality. http://snia.dga.cl/BNAConsultas/reportes. Accessed 20 December 2015

DICTUC (2006) Actualización de la estimación de la recarga acuíferos de Pampa del Tamarugal y LLamara (Reassessing aquifer recharge of the Pampa del Tamarugal and the Llamara Salar), Dirección de Investigaciónes Científicas y Tecnologicas de la Pontificia Universidad Católica de Chile

DICTUC (2007) Modelación de la evolución del nivel de la napa en la Pampa del Tamarugal (Modelling the development of the groundwater level in the Pampa del Tamarugal), Dirección de Investigaciónes Científicas y Tecnologicas de la Pontificia Universidad Católica de Chile

Fritz P, Suzuki O, Silva C, Salati E (1981) Isotope hydrology of groundwaters in the Pampa del Tamarugal, Chile. Journal of Hydrology 53(1-2):161–184. doi: 10.1016/0022-1694(81)90043-3

Gayo EM, Latorre C, Santoro CM, Maldonado A, Pol-Holz R de (2012a) Hydroclimate variability in the low-elevation Atacama Desert over the last 2500 yr. Clim. Past 8(1):287–306. doi: 10.5194/cp-8-287-2012

Gayo EM, Latorre C, Jordan TE, Nester PL, Estay SA, Ojeda KF, Santoro CM (2012b) Late Quaternary hydrological and ecological changes in the hyperarid core of the northern Atacama Desert (~21°S). Earth-Science Reviews 113(3-4):120–140. doi: 10.1016/j.earscirev.2012.04.003

Herrera C, Custodio E, Chong G, Lamban LJ, Riquelme R, Wilke H, Jodar J, Urrutia J, Urqueta H, Sarmiento A, Gamboa C, Lictevout E (2016) Groundwater flow in a closed basin with a saline shallow lake in a volcanic area: Laguna Tuyajto, northern Chilean Altiplano of the Andes. Sci Total Environ 541:303–318. doi: 10.1016/j.scitotenv.2015.09.060

Houston J (2002) Groundwater recharge through an alluvial fan in the Atacama Desert, northern Chile: mechanisms, magnitudes and causes. Hydrol. Process. 16(15):3019–3035. doi: 10.1002/hyp.1086

Houston J (2006a) The great Atacama flood of 2001 and its implications for Andean hydrology. Hydrol. Process. 20(3):591–610. doi: 10.1002/hyp.5926

Houston J (2006b) Variability of precipitation in the Atacama Desert: its causes and hydrological impact. Int. J. Climatol. 26(15):2181–2198. doi: 10.1002/joc.1359

Houston J (2007) Recharge to groundwater in the Turi Basin, northern Chile: An evaluation based on tritium and chloride mass balance techniques. Journal of Hydrology 334(3-4):534–544. doi: 10.1016/j.jhydrol.2006.10.030

Houston J (2009) A recharge model for high altitude, arid, Andean aquifers. Hydrol. Process. 23(16):2383–2393. doi: 10.1002/hyp.7350

Jayne RS, Pollyea RM, Dodd JP, Olson EJ, Swanson SK (2016) Spatial and temporal constraints on regional-scale groundwater flow in the Pampa del Tamarugal Basin, Atacama Desert, Chile. Hydrogeol J. doi: 10.1007/s10040-016-1454-3

Jica (1995) The study on the development of water resources in Northern Chile. http://sad.dga.cl/. Accessed 13 May 2016

Jordan TE, Nester PL (2012) The Pampa del Tamarugal forearc basin in Northern Chile. Tectonics of Sedimentary Basins - Recent Advances:369–381

Kikuchi CP, Ferré TPA (2016) Analysis of subsurface temperature data to quantify groundwater recharge rates in a closed Altiplano basin, northern Chile. Hydrogeol J. doi: 10.1007/s10040-016-1472-1

Larraín S, Poo P (2010) Conflictos por el agua en Chile - Entre los derechos humanos y las reglas de mercado (Water conflicts in Chile - between human rights and the rules of the free market), 1a ed. [s.n], Santiago, Chile

Lictevout E, Maas C, Córdoba D, Herrera V, Payano R (2013) Recursos Hídricos Región de Tarapacá - Diagnóstico y Sistematización de Información [Water resources in the region Tarapacá - Diagnosis and systematisation of existing information]. Universidad Arturo Prat, Iquique, Iquique

Magaritz M, Aravena R, Peña H, Suzuki O, Grilli A (1989) Water chemistry and isotope study of streams and springs in northern Chile. Journal of Hydrology 108:323–341. doi: 10.1016/0022-1694(89)90292-8

Magaritz M, Aravena R, Peña H, Suzuki O, Grilli A (1990) Source of Ground Water in the Deserts of Northern Chile: Evidence of Deep Circulation of Ground Water from the Andes. Groundwater(4). doi: 10.1111/j.1745-6584.1990.tb01706.x

Minvielle M, Garreaud RD (2011) Projecting Rainfall Changes over the South American Altiplano. J. Climate 24(17):4577–4583. doi: 10.1175/JCLI-D-11-00051.1

Montgomery E, Rosko M, Castro S (2003) Interbasin Underflow Between Closed Altiplano Basins in Chile. Groundwater 41(4)

Moreno T (ed) (2007) The geology of Chile. Geological Society, London u.a.

Nester PL (2008) Basin and Paleoclimate Evolution of the Pampa del Tamarugal Forearc Valley, Atacama Desert, Northern Chile. https://ecommons.cornell.edu/bitstream/handle/1813/10484/Nester2008.pdf?sequence=1&isAllowed=y. Accessed 5 May 2017

Oyarzún R, Oyarzún J, Fairley JP, Núñez J, Gómez N, Arumí JL, Maturana H (2017) A simple approach for the analysis of the structural-geologic control of groundwater in an arid rural, mid-mountain, granitic and volcanic-sedimentary terrain: The case of the Coquimbo Region, North-Central Chile. Journal of Arid Environments 142:31–35. doi: 10.1016/j.jaridenv.2017.03.003

Petry M, Sanz MA, Langlais C, Bonnelye V, Durand J-P, Guevara D, Nardes WM, Saemi CH (2007) The El Coloso (Chile) reverse osmosis plant. Desalination 203(1-3):141–152. doi: 10.1016/j.desal.2006.05.007

Placzek C, Quade J, Patchett PJ (2006) Geochronology and stratigraphy of late Pleistocene lake cycles on the southern Bolivian Altiplano: Implications for causes of tropical climate change. Geological Society of America Bulletin 118(5-6):515–532. doi: 10.1130/B25770.1

Placzek C, Quade J, Betancourt JL, Patchett PJ, Rech JA, Latorre C, Matmon A, Holmgren C, English NB (2009) Climate in the dry central Andes over geologic, millennial and interannual timescales. Annals of the Missouri Botanical Garden 96(3):386–397. doi: 10.3417/2008019

PUC (2009) Levantamiento Hidrogeológico para el Desarrollo de nuevas fuentes de Agua en áreas prioritarias de la zona norte de Chile, Regiones XV, I, II y III (Hydrogeological study for the development of new water resources in northern zones of Chile, regiones XV, I, II and III). documentos.dga.cl/REH5161v4.pdf. Accessed 13 May 2016

Rech JA, Quade J, Betancourt JL (2002) Late Quaternary paleohydrology of the central Atacama Desert (lat 22°–24°S), Chile. Geological Society of America Bulletin 114(3):334–348. doi: 10.1130/0016-7606(2002)114<0334:LQPOTC>2.0.CO;2

Ribeiro L, Kretschmer N, Nascimento J, Buxo A, Rötting T, Soto G, Señoret M, Oyarzún J, Maturana H, Oyarzún R (2015) Evaluating piezometric trends using the Mann-Kendall test on the alluvial aquifers of the Elqui River basin, Chile. Hydrological Sciences Journal 60(10):1840–1852. doi: 10.1080/02626667.2014.945936

Rojas R, Dassargues A (2007) Groundwater flow modelling of the regional aquifer of the Pampa del Tamarugal, northern Chile. Hydrogeol J 15(3):537–551. doi: 10.1007/s10040-006-0084-6

Rojas R, Batelaan O, Feyen L, Dassargues A (2010) Assessment of conceptual model uncertainty for the regional aquifer Pampa del Tamarugal – North Chile. Hydrol. Earth Syst. Sci. 14(2):171–192. doi: 10.5194/hess-14-171-2010

Salazar C, Rojas L, Pollastri A (1998) Evaluación de Recursos Hidricos en el Sector de Pica - Evaluation of water resources in the Pica area: Hoya de la Pampa del Tamarugal I Region. http://documentos.dga.cl/SUB1658.djvu. Accessed 30 May 2016

Uribe J, Muñoz JF, Gironás J, Oyarzún R, Aguirre E, Aravena R (2015) Assessing groundwater recharge in an Andean closed basin using isotopic characterization and a rainfall-runoff model: Salar del Huasco basin, Chile. Hydrogeol J. doi: 10.1007/s10040-015-1300-z

Valdés-Pineda R, Pizarro R, García-Chevesich P, Valdés JB, Olivares C, Vera M, Balocchi F, Pérez F, Vallejos C, Fuentes R, Abarza A, Helwig B (2014) Water governance in Chile: Availability, management and climate change. Journal of Hydrology 519:2538–2567. doi: 10.1016/j.jhydrol.2014.04.016

Via Marina (2013) Informe Proyecto Acquatacama (Project summary Acquatacama). http://www.acquatacama.cl/sites/default/files/ResumenProyecto.pdf. Accessed 5 May 2017

Yáñez Fuenzalida N, Molina Otárola R (2008) La gran minería y los derechos indígenas en el norte de Chile [The big mining and the rights of indiginous people in northern Chile], 1. ed. Ciencias humanas. Estado y pueblos indígenas. LOM, Santiago

2. Local climate change induced by groundwater overexploitation in a high Andean arid watershed, Laguna Lagunillas basin, northern Chile

Konstantin W. Scheihing[a,*], Uwe Tröger[a]

[a] Department of Applied Geosciences, Hydrogeology Research Group, Technische Universität Berlin, Berlin 10587, Germany

[*]corresponding author: kscheihing@gmx.de

Citation:

Scheihing K, Tröger U (2017) Local climate change induced by groundwater overexploitation in a high Andean arid watershed, Laguna Lagunillas basin, northern Chile. Hydrogeol J 16:1817. doi: 10.1007/s10040-017-1647-4

Article history:

Received: 03 November 2016 / First Online: 14 August 2017

This is a postprint-version. The final publication is available at Springer via https://doi.org/10.1007/s10040-017-1647-4.

Abstract

The Laguna Lagunillas basin in the arid Andes of northern Chile exhibits a shallow aquifer and is exposed to extreme air temperature variations from 20 to -25°C. Between 1991 and 2012, groundwater levels in the Pampa Lagunillas aquifer fell from near-surface to ~15 m below ground level (bgl) due to severe overexploitation. In the same period, local mean monthly minimum temperatures started a declining trend, dropping by 3-8°C relative to a nearby reference station. Meanwhile, mean monthly maximum summer temperatures shifted abruptly upwards by 2.7°C on average in around 1996. The observed air temperature downturns and upturns are in accordance with detected anomalies in land-surface temperature imagery. Two major factors may be causing the local climate change. One is related to a water-table decline below the evaporative energy potential extinction depth of ~2 m bgl, which causes an up-heating of the bare soil surface and, in turn, influences the lower atmosphere. At the same time, the removal of near-surface groundwater reduces the thermal conductivity of the upper sedimentary layer, which consequently diminishes the heat exchange between the aquifer (constant heat source of ~10°C) and the lower atmosphere during nights, leading to a severe dropping of minimum air temperatures. The observed critical water-level drawdown was 2–3 m bgl. Future and existing water-production projects in arid high Andean basins with shallow groundwater, should avoid a decline of near-surface groundwater below 2 m bgl and take groundwater-climate interactions into account when identifying and monitoring potential environmental impacts.

2.1. Introduction

The Pampa Lagunillas and the related wetland Laguna Lagunillas are situated in the remote arid Andes of northern Chile at an elevation of >4000 m above sea level (asl), at 19.55 °S, 68.5 °W (Figure 2.1a, b). In 1982 the Chilean central water directorate (DGA) granted BHP Billiton (BHP) instantaneous water withdrawal rights from the respective aquifer of 300 l/s (DGA resolution Nº425) (Yáñez Fuenzalida and Molina Otárola 2008).

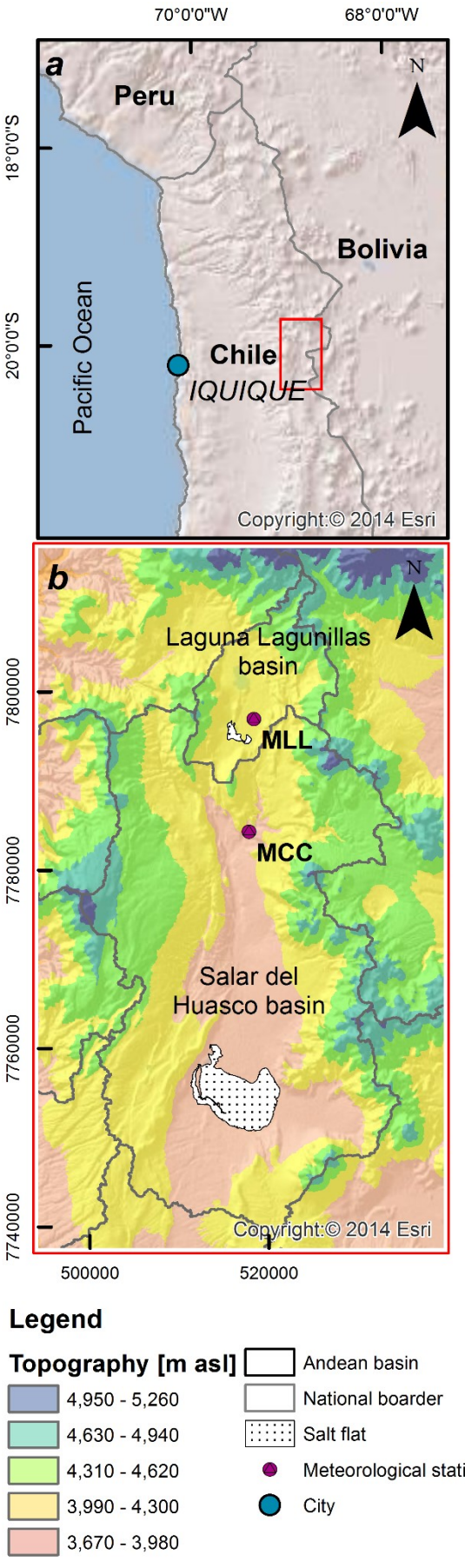

Figure 2.1 **(a)** Map of central South America (study area marked by red rectangle), **(b)** Topographic map of the area of work together with relevant meteorological stations

Groundwater was intended to be used in the Cerro Colorado copper mine, situated 45 km further west, which started commercial production in 1994. Water withdrawals started after the year 1991.

In 2002 it was noted by the local community (Aymara) that the wetland of the Laguna Lagunillas basin together with the 5 related springs had dried out, due to a severe decrease of the water table (Yáñez Fuenzalida and Molina Otárola 2008; Larraín and Poo 2010). As part of the penalty imposed on BHP, the company agreed to irrigate the wetland artificially (with water from the same aquifer, ~25 l/s, starting in ~2006) and to take care of its full restoration on a long-term basis (Yáñez Fuenzalida and Molina Otárola 2008; BHP Billiton 2015). However, as part of the actual water management plan, water withdrawals from the aquifer continue. BHP reports today's water withdrawals to be ~130 l/s (BHP Billiton 2015). At the same time, BHP wants to extend the operation of the Cerro Colorado mine up to the year 2023, for which an environmental impact study is still being carried out and which also includes the Laguna Lagunillas watershed (BHP Billiton 2015; SEA 2014). While direct impacts on flora and fauna due to water shortage are usually considered in such impact studies, under the given extreme weather conditions in the arid Andes, climatic implications should also be taken into account, as demonstrated by this study. Maximum and minimum daily air temperatures in austral summer can reach up to 20°C and can fall in winter down to -25°C (this study). At the same time, land surface temperatures (LST) of relevant sedimentary basins fluctuate between 50°C and <-20°C (this study).

Determining the interplay between groundwater withdrawals, soil moisture, atmospheric water vapor, and land-surface and lower atmosphere temperatures, was the objective of earlier studies (Boucher et al. 2004; Lo and Famiglietti 2013; Zou et al. 2014; Alkhaier et al. 2012b; Alkhaier et al. 2012a; Zeng et al. 2016; Zeng et al. 2017; Maxwell and Kollet 2008). Shallow groundwater is associated with wetter soil profiles because of upward water and vapor fluxes (Alkhaier et al. 2012b). Solar energy absorption due to evaporation, by soil moisture and near-surface groundwater, is known to have a regulating impact on both land-surface temperatures and maximum air temperatures in the lower atmosphere (Lakshmi et al. 2003; Whan et al. 2015; Berg et al. 2014; Alkhaier et al. 2012b; Alkhaier et al. 2012a). Apart from that, near-surface groundwater increases the thermal conductivity of top-soil layers (Alkhaier et al. 2012b).

Therefore, although it is understood theoretically that near-surface groundwater plays a vital role in energy balances between the lower atmosphere, the ground surface and the subsurface, in practice (in terms of environmental management), there is seldom awareness regarding its regulating function on local climates. This may also be due to numerous climate change studies that rely on large-scale modelling approaches which are understandably limited in complexity and often hard to test for accuracy and impact in relation to a specific site. Opposed to that, this case study is based on long-term monitoring data and hence is able to examine the concrete relation between a decrease of water tables and changes in daily and monthly minimum and maximum air temperatures at a mismanaged arid Andean water-production site. By a statistical analysis of time series from two nearby meteorological stations over 29 years, tangible climatic changes can be quantified.

As far as the authors are aware, the given publication investigates unstudied effects of prominent feedbacks between shallow groundwater and air temperatures in the arid Andes. Based on the observed phenomenon, a recommendation for groundwater management practices in akin Andean environments is proposed.

2.2. Study area

The Laguna Lagunillas (LL) basin is a typical Altiplano sedimentary basin in the arid Andes of northern Chile (Figure 2.1a, b). It is enclosed by Oligocene to Miocene volcanic and plutonic rocks with a longitudinal Miocene to Quaternary sedimentary fill called Pampa Lagunillas (Sernageomin 2003; Kikuchi and Ferré 2016). The latter makes up the exploited unconfined shallow aquifer which originally (prior to 1992) exhibited a total water saturated thickness of ~30 m (at well LA-4) to ~135 m (at well LA-3) with a hydraulic conductivity of 0.3 to 30 m/day (Kikuchi and Ferré 2016; Errol L. Montgomery & Associates 2005) (Figure 2.2a, b).

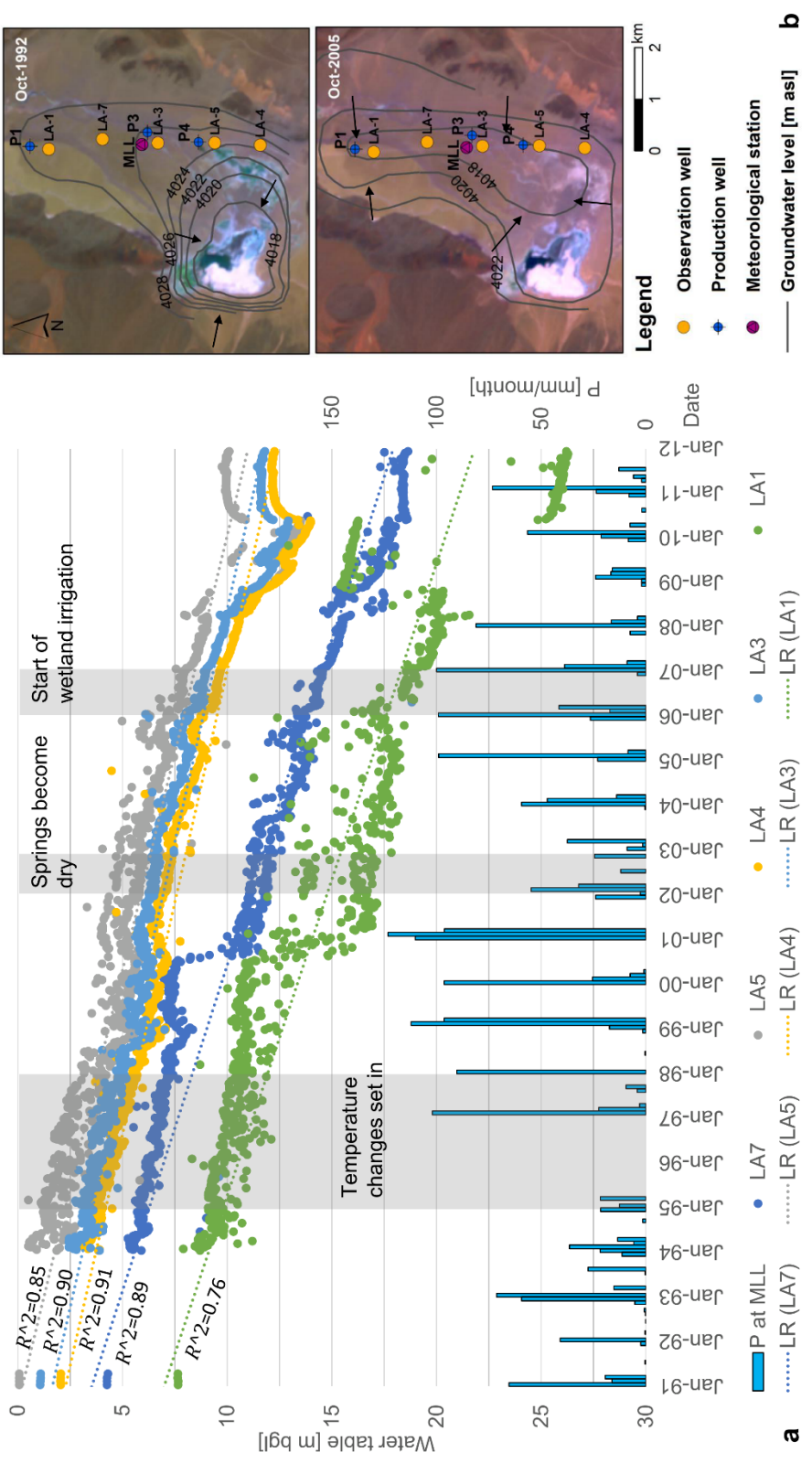

Figure 2.2 **(a)** Precipitation (P, blue bars) and water-table depth (colored circles) in 5 observation wells in the Laguna Lagunillas basin, 1991-2012 **(b)** Comparison of resulting groundwater-level contour lines between October 1992 (undisturbed conditions) and October 2005, based on data reported by Errol L. Montgomery & Associates (2005) (arrows mark approximate groundwater flow direction)

Around the wetland Lagunilllas, in the south of the basin, a salar (salt flat) can be found. In total the basin stretches over an elevation range of 4000-4800 m asl and covers an area of 194 km^2. Mean annual precipitation is ~140 mm (at ~4050 m asl); more than 80% of the precipitation falls during austral summer (Houston 2006b). Due to its remote locality, few relevant scientific studies have been published on the area of work so far.

Groundwater temperatures in the shallow Pampa Lagunillas aquifer are around 8-13 °C (Montgomery and Rosko 1996; Kikuchi and Ferré 2016). Similar shallow groundwater temperatures are associated with the Salar del Huasco basin (Figure 2.1b). However, deeper groundwater and rising springs in the Salar del Huasco basin can reach 15-20°C (PUC 2009; Scheihing et al. 2017; Uribe et al. 2015). These groundwater temperatures lie notably above the annual mean air temperatures in the region of 5°C (9°C during summer months) (Risacher et al. 2003), which is commonly a threshold for expected groundwater temperatures. The Andean Altiplano of northern Chile is known for its steep geothermal gradients, therefore geothermal energy sources can influence groundwater temperatures (Herrera et al. 2016; Sanchez-Alfaro et al. 2015; Reyes and Vidal 2011; Tassi et al. 2010; Aravena et al. 2016). However, such high groundwater temperatures are not proven for the Laguna Lagunillas basin.

2.3. Data and methodology

2.3.1. Hydrological data

Daily meteorological data used in this study originate from station Lagunillas (MLL, ~4030 m asl); the data are collected by DGA. Temperature data were available for the period Jan 1983 to Dec 2011. As a reference, temperature data from the Collacagua station (MCC, ~4013 m asl) were used for the same period. The MCC station is likewise maintained by DGA and it is situated in the adjacent Salar del Huasco basin approximately 12 km south of station MLL, close to a perennial stream.

Time-series data of water table depth for the LL were collected by BHP and were usually measured twice a month, beginning in 1991. By Chilean law, all relevant data are available to the public (ODEA 2016; DGA 2015).

Unfortunately, there are a few periods where precipitation and temperature data are missing. Monthly precipitation data for station MLL are missing for (DGA 2015): Apr to Jun 1993, Apr 1995 to Jan 1997, Nov 1999, March 2010 and Dec 2011. Missing daily temperature data from station MCC and MLL are summarized in Table 2.1. The times series show that 10% of the potential total number of days are associated with missing data and that the missing data points are randomly distributed over the whole dataset. Only at station MLL is a larger data gap present, between Apr 1995 and Jan 1997. However, the missing data points have little impact on the overall evaluation, as the observation period is in total 29 years and discussed temperature changes are being reflected strongly in the data.

To quantify trends in the water-level time series data, linear regression (LR) was applied. To identify statistically the significant change points in relevant time series, two non-parametric homogeneity tests (Pettitt's test and Buishand's test) were used (Pettitt 1979; Buishand 1982). Neither test requires assumptions about the distribution of the analyzed data, and missing data points were ignored in the assessment. The Pettitt's test is based on the null hypothesis (H_0) that the respective time series is homogeneous. It assess whether the variables follow one or more distributions that have the same location parameter (Pettitt 1979).

Table 2.1 Descriptive statistics of daily minimum (dmin) and maximum (dmax) temperature datasets of station MCC and MLL (1983-2012)

	Station MCC		**Station MLL**	
	Tdmin	*Tdmax*	*Tdmin*	*Tdmax*
No. of days (1983-2012)	10592	10592	10592	10592
No. of days with missing data	1088	918	1079	1339
No. of available data points	9504	9674	9513	9253
Min	-19.6	-0.5	-26.0	-3.8
Max	13.0	25.5	14.8	23.8
Mean	-5.9	15.0	-7.8	13.5
Std. deviation	4.8	3.8	6.1	3.5

If this is proved false, the alternative hypothesis (H_a) is true, that there is a time t from which the variables show a change of the location parameter. Then the change point t can be determined. The null hypothesis of Buishand's test is that the variables follow one or more distributions that have the same mean. If this is proved false, the alternative hypothesis is true, that there exists a time t from which the variables change in terms of the mean. The respective change point t can then be identified.
Both tests work with a significance level α of 5 % (meaning a confidence interval 95 %). Indicated p-values are a measure of risk of being wrong when rejecting the null hypothesis. If the p-value is higher than the significance level, the null hypothesis cannot be rejected.

Further, the Mann-Kendall test was executed to identify long-term trends in respective time series (Kendall and Gibbons 1990; Yue and Wang 2004; Lehmann 2006). When analyzing autoregressive temperature time series, an adjusted form of the Mann-Kendall test is usually applied (Yue and Wang 2004).

The cross-correlation of two time-series was quantified by the Pearson correlation coefficient (Lehmann 2006; Kendall and Gibbons 1990). It measures the degree of linear correlation between two variables for a preset number of time steps (lag), to explain how much of the variability of a variable is explained by another variable.

2.3.2. Thermal infrared bands and land-surface temperature data from remote sensing devices

To verify changes detected in air temperature time series, an assessment of thermal infrared and land-surface temperature (LST) data was carried out by a qualitative comparison of different spectral images of different years and under different seasonal conditions. A detailed quantitative assessment of respective data was impeded by the sporadic unavailability of respective imagery. Occasionally occurring cloud cover also reduced the applicable dataset.

The presented data for 2000-2014 were based on measurements taken by the ASTER remote sensory devices on board NASA's Terra satellite which started

observations in 1999 (NASA 2017). Imagery prior to 2000 originated from the Landsat 5 satellite (USGS 2017). Both satellites possess thermal infrared (TIR) sensors which detect land-surface temperature anomalies. However, to calculate absolute surface temperatures from this data, atmospheric correction parameters need to be obtained from atmospheric models, typically made available by NASA (NASA 2014; Barsi et al. 2005; Jiménez-Muñoz and Sobrino 2003). However, NASA does not provide this data for dates prior to 2000, which inhibits the conversion of TIR-band data from Landsat 5 imagery into absolute temperature values (NASA 2014). Nevertheless, a comparison of TIR-data from Landsat 5 was carried out based on a rescaling of raster data values from 0 to 1. Presented absolute LST values from the ASTER data were retrieved as a standard product from NASA (NASA LP DAAC 2017). Absolute accuracy of used imagery is indicated as 1.5°C in an environment with surface temperatures of ~27°C and ±2°C globally (Barsi et al. 2005; NASA 2002).

For data from the ASTER TIR-sensors, it is also possible to compare day and night imagery (spatial resolution 90 m). Landsat 5 TIR-data provide only day imagery in the area of work (spatial resolution 120 m, resampled to 30 m by NASA).

2.4. Results

2.4.1. Water-level drawdowns from 1991 to 2012

Figure 2.2a displays the water-table decline in the LL from 1991 to 2012 (no data available between June 1991 and January 1994; the positions of observation wells in the LL are displayed in Figure 2.2b). While water tables measured in 1991 reflected natural conditions in the watershed, during the following two decades the water levels fell severely. At the end of 2011, well LA-1 showed a net decline of 18.5 m, LA-3 of 10.8 m, LA-4 of 10.4 m, LA-5 of 10 m and levels at LA-7 fell by 13.5 m. Hence the water table fell on average by 0.5–1 m/a. The declining trend is approximated by respective linear regression trend lines (Figure 2.2a).

Years of increased precipitation dampened the decline a little (e.g. 1999 and 2001; Figure 2.2a). The slight groundwater recovery in 2005 is likely explained by a copper production decrease (as reported by BHP), induced by an earthquake

in the region of the Cerro Colorado mine (GFZ 2015). Jumps in the time-series probably reflect the operational management of the respective production wells (Figure 2.2). Between 1995 and 1999, when temperature changes begin to be detectable (see next section), drawdowns totaled 2-3 m compared to natural conditions (Figure 2.2a).

Figure 2.2b documents the change of the groundwater flow direction and groundwater contour lines between the years 1992 and 2005 (based on data from Errol L. Montgomery & Associates (2005)). At the same time, false color Landsat imagery depicts the general retreat of surface vegetation associated with the wetland area where groundwater levels were found originally not more than ~0.2 m bgl (observation well LA-5). The groundwater level at the local meteorological station in 1991 stood at ~1 m bgl (LA-3). Comparing groundwater-level contour lines between 1992 and 2005 demonstrates that the whole sedimentary basin experienced a water-level decline of ~6 m compared to natural conditions in this period (groundwater-level contour line 4028 m asl in 1992 compared to contour line 4022 m asl in 2005). The strongest water-level declines were associated with the production wells.

2.4.2. Daily and monthly minimum and maximum temperatures at stations MLL and MCC between 1983 to 2012

Figure 2.3 displays daily and monthly minimum and maximum air temperature data for the meteorological stations MLL and MCC. MCC serves as a reference station due to its location only 12 km south of station MLL, and its similar elevation and hydrological environment (see section 2.3). Both datasets are separated into two sub datasets, 1983-1995 (subset 1) and 1997-2012 (subset 2), in Figure 2.3. This is because there is a 2-year data gap in the time series of station MLL between 1995 and 1997. At the same time, it is approximately in this period where a change in the time series is seen to begin (see also section 2.4.4).

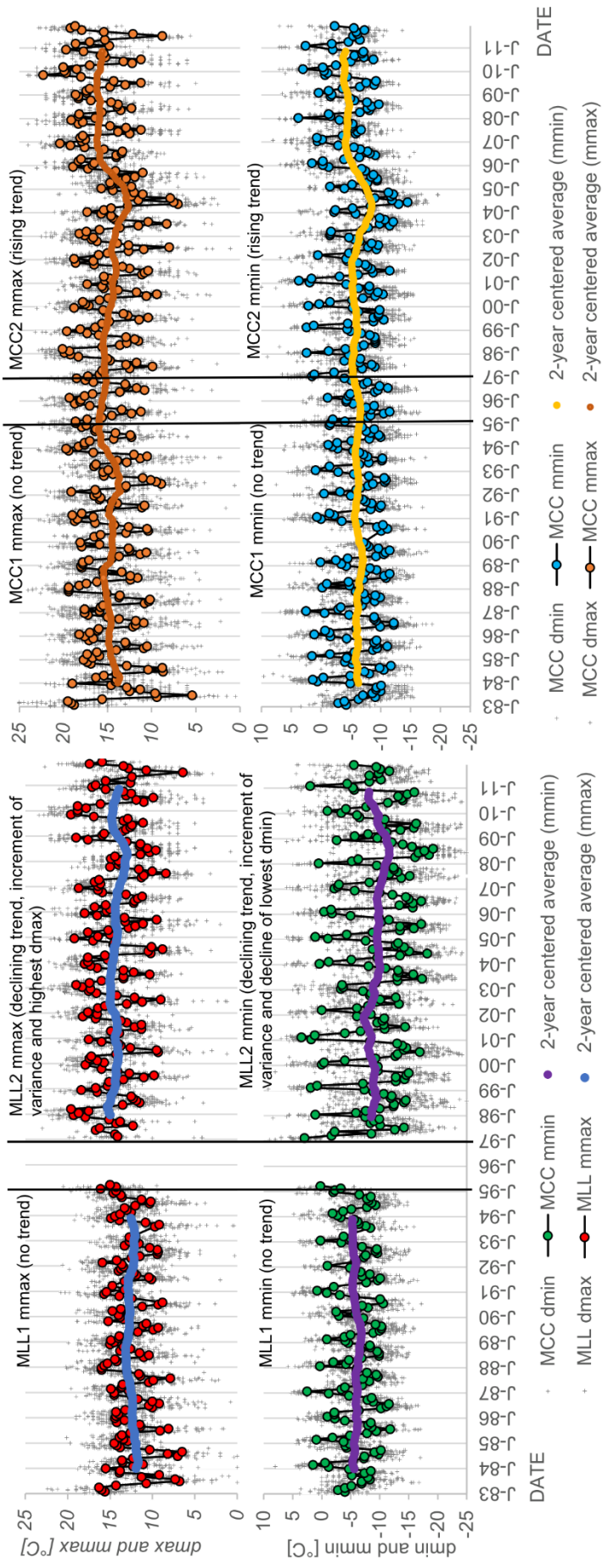

Figure 2.3 Daily (d) minimum and maximum and monthly (m) mean minimum and maximum temperatures at station MCC and MLL

At MCC, mean monthly maximum (mmax) temperatures oscillate between 8 and 20°C throughout a year. Mean monthly minimum (mmin) temperatures at MCC plot between 3 and -12°C. Very similar temperature ranges can be identified for time series MLL1 mmax and MLL1 mmin respectively. However, the 2-year average of MLL1 mmax tends to lie at ~2°C below the 2-year average of the time series MCC1 mmax.

High cross-correlation coefficients (0.7, at lag 0) for trend lines of MCC1 mmax and MLL1 mmax, as well as MCC1 mmin and MLL1 mmin, demonstrate that respective temperatures at both stations follow the same cycles of slight up and down turns between 1983 and 1995 (Figure 2.4). However, the same calculation for the period 1997-2012 (MCC2 and MLL2) reveals that the trend lines of both stations decouple. No positive cross-correlation can be verified for this period. This phenomenon can also be quantified by the modified Mann-Kendall trend test for autoregressive time series (after Yue and Wang 2004). While mean monthly temperatures for MCC1 and MLL1 do not follow any apparent trend (according to the modified Mann-Kendall test), mean monthly temperatures for time series MCC2 follow a slightly rising trend, and data of MLL2, in contrast, follow a declining trend (Table 2.1).

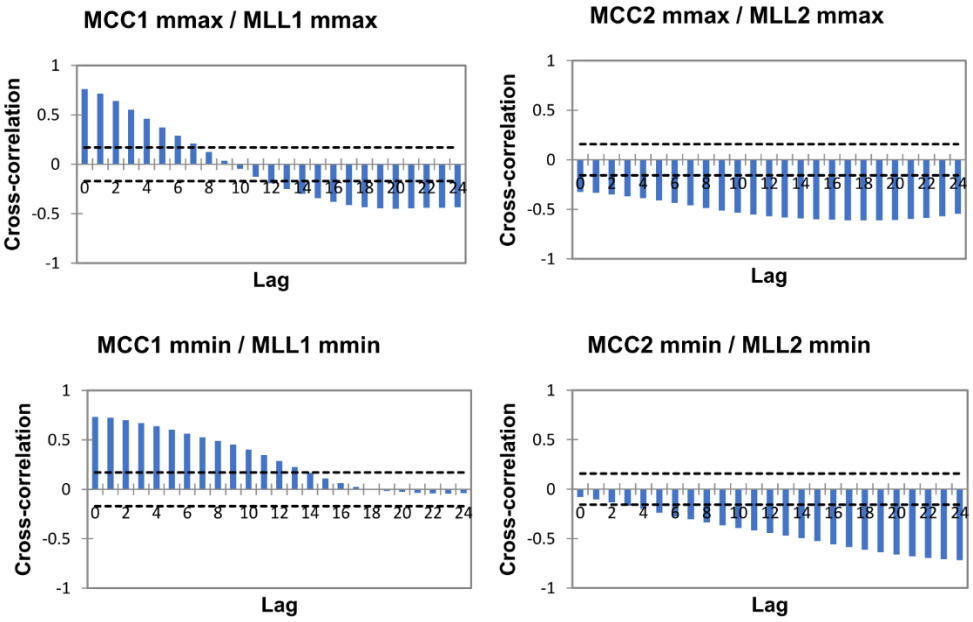

Figure 2.4 Cross-correlation calculations for 2-year centered average trend lines of mmax and mmin temperatures of stations MCC and MLL (dashed lines mark 95% confidence interval)

Table 2.2 Descriptive statistics and modified Mann-Kendall test calculations (for Figure 2.3)

	MCC1 dmax	**MCC2 dmax**	**MLL1 dmax**	**MLL2 dmax**	**MCC1 dmin**	**MCC2 dmin**	**MLL1 dmin**	**MLL2 dmin**
Descriptive statistics								
Minimum	-0.5	1.1	-2.8	-3.8	-18.6	-19.6	-17.2	-26.0
Maximum	25.5	24.9	22.4	23.8	9.6	13.0	14.8	12.8
1st Quartile	12.0	12.5	10.6	12.0	-10.0	-9.0	-9.0	-14.8
Median	15.0	15.4	12.8	14.6	-7.0	-6.0	-6.3	-9.7
3rd Quartile	17.8	18.0	14.8	17.0	-3.0	-2.0	-3.3	-4.2
Mean	14.8	15.0	12.5	14.4	-6.3	-5.4	-6.0	-9.3
Variance (*n*)	15.4	14.2	9.8	13.4	22.6	23.8	18.0	47.0
Std. dev. (*n*)	3.9	3.8	3.1	3.7	4.7	4.9	4.2	6.9
Modified Mann-Kendall test statistics, α = significance level, *p*-value is two-tailed								
Trend	No	Rising	No	Declining	No	Rising	No	Declining
Sen's slope	-	0.008	-	-0.006	-	0.01	-	-0.009
p-value (two-tailed)	0.196	0.022	0.953	<0.0001	0.709	0.013	0.665	0.003
α	0.05	0.05	0.05	0.05	0.05	0.05	0.05	0.05

Table 2.2 summarizes the descriptive statistics of all datasets. In particular, the strong increase of the variance between MLL1 and MLL2 daily minimum temperatures (dmin) is striking. It rises from 18.0 to 47.0. The increase of variance demonstrates that temperature up and downturns are less buffered. Also, the mean of series MLL2 dmin is 3°C lower than that of MLL1 dmin. In parallel, average daily maximum (dmax) temperatures at MLL rise by ~2°C. Differences between data from MCC1 and MCC2 are much more moderate and are in the range of expected natural variations.

2.4.3. Correlations between the Southern Oscillation Index and mmin temperature data from station MCC

Naturally occurring temperature fluctuations as well as precipitation variations in the Central Andes and northern Chile were earlier associated with the El Niño Southern Oscillation; in particular with the Southern Oscillation Index (SOI) (Houston 2006b; Lavado Casimiro et al. 2012; Cerveny et al. 1987).

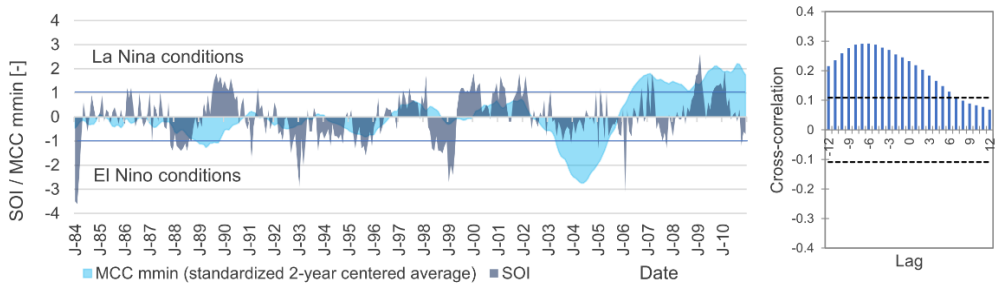

Figure 2.5 Correlation between MCC mmin temperatures (standardized only for visualization) and the SOI (dashed lines mark 95% confidence interval)

At reference station MCC it can be shown that the 2-year trend line of mmin temperatures correlates positively and statistically significantly with the SOI between 1984 and 2011 (Figure 2.5). This implies that during La Niña conditions, strong easterly trade winds favor warmer night conditions in the area of work.
A positive correlation between mmax temperatures of station MCC and the SOI cannot be established, which indicates that there are additional or other influencing factors. Mmin temperatures represent night temperatures and mmax temperatures reflect approximately midday temperatures. Effects associated with cloud cover, in particular, can affect dmax temperatures significantly, which could be a reason for the differing observations.

However, it is reasonable to assume that temperature time series at station MCC reflect natural temperature variations in the locality of the area of work. There are two reasons for this. (1) Cross-correlations between dmin and dmax temperatures at station MCC and MLL for the period 1983-1995 demonstrate a high, statistically significant correlation at lag 0 (section 2.4.2), which implies that both stations followed the same temperature trends during this time. (2) The 2-year trend line of mmin temperatures at station MCC correlates over a period of 29 years with the SOI, which is a major climate index for the Southern Pacific region (Trenberth 1984; Stenseth et al. 2003; Ropelewski and Halpert 1987).

2.4.4. Quantification of temperature changes at MLL with reference to station MCC

To assess structural breaks in the annual variance of dmin and dmax temperatures, two homogeneity test were applied (Pettitt's test and Buishand's test, Table 2.3). Both tests identify structural breaks for the annual variance time series at station MLL (Figure 2.6). These occurred approximately in the period 1994-1997 for dmin temperatures and in 1999-2001 for dmax (data gaps in 1995 and 1996).

At the same time, no structural break can be detected for the time series of station MCC. The detected shift in values of variance indicate a relatively fast (non-linear) and local system change that affected, particularly, extreme minimum and maximum air temperatures in the Laguna Lagunillas basin.

The here encountered effects on mmin temperatures were stronger than on mmax temperatures (variance rose by 160% for mmin compared to 35% for mmax).

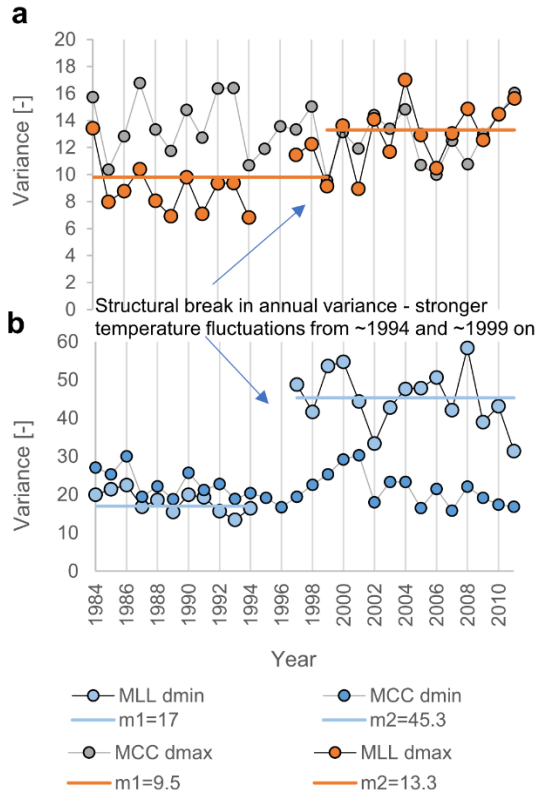

Figure 2.6 Annual variance of **(a)** dmax and **(b)** dmin temperatures at MCC and MLL with change points as calculated by Pettitt's test (m=mean). Structural breaks occur in the years ~1994 and ~1999 at station MLL. The variance time series of station MCC exhibit no structural break for the whole observation period.

Table 2.3 Results of homogeneity tests (for Figure 2.6 and Figure 2.7b). t = change point (year), α = significance level. The p-value is two-tailed

Parameter	**Pettitt's test**	**Buishand's test**
Variance MLL dmax (Figure 2.6)		
t	1999	2001
p-value	0.010	0.006
α	0.05	0.05
Variance MLL dmin (Figure 2.6)		
t	1994	1994
p-value	< 0.0001	< 0.0001
α	0.05	0.05
Variance MCC dmin (Figure 2.6)		
t	-	-
p-value	0.255	0.208
α	0.05	0.05
Variance MCC dmax (Figure 2.6)		
t	-	-
p-value	0.621	0.135
α	0.05	0.05
Monthly max (mmax) summer temperatures (Figure 2.7b)		
t	1995	1995
p-value	< 0.0001	< 0.0001
α	0.05	0.05

Figure 2.7a depicts the variations of average mmin temperatures during austral summer (December-February) and winter (June-August) from 1984 to 2012. The annual temperature differences between station MLL and the reference station MCC were calculated. The temperature differences for both seasons demonstrate a declining trend since the beginning of water withdrawals in 1992 (according to the Mann-Kendall test, Table 2.4). While differences prior to 1992 fall into a range of ±1°C, the time series declines to values of up to -8°C in the following years. Local maxima for time series of station MCC and MLL seem to be associated with La Niña conditions (see section 2.4.2).

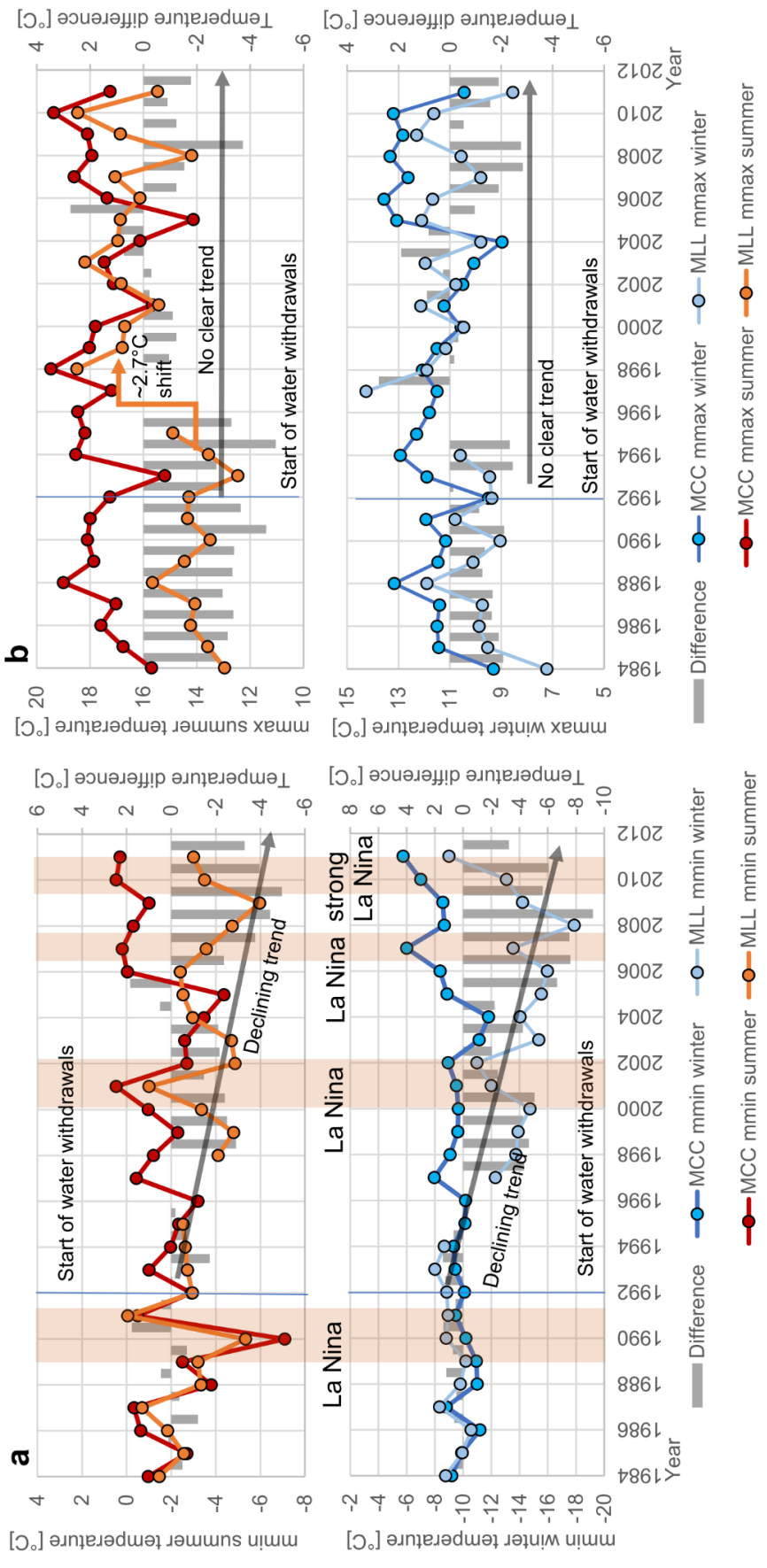

Figure 2.7 Comparisons of the development of **(a)** mmin temperatures and **(b)** mmax temperatures, at stations MLL and MCC for summer and winter periods (1984-2012)

Table 2.4 Results of Mann-Kendall trend tests (for Figure 2.7a, b). α = significance level. The *p*-value is two-tailed

Parameter	**Difference in summer**	**Difference in winter**
Monthly min (mmin) (Figure 2.7a)		
Trend	Declining	Declining
Sen's slope	-0.187	-0.385
p-value	0.012	0.005
α	0.05	0.05
Monthly max (mmax) (Figure 2.7b)		
Trend	No	No
Sen's slope	-	-
p-value	0.132	0.124
α	0.05	0.05

In conclusion, mmin temperatures in winter have been lowered by about 3–8°C compared to expected natural conditions as approximately represented by the reference station MCC. Additionally, the resulting yearly temperature differences show a declining trend. Likewise, mmin temperatures in summer fell by up to ~4°C with regard to the reference station and resulting temperature differences show concordantly a declining trend.

Figure 2.7b displays the development of average mmax temperatures for the summer and winter seasons at station MCC and MLL. From 1992 onward, the respective difference function shows no apparent trend for both seasons. The only remarkable observation is made for mmax temperatures of the summer season where around the year 1995 (data gap in 1996 and 1997) a shift of mmax temperatures by ~2.7°C occurs (slightly different change point to the structural break in the respective variance time series, Figure 2.6, Table 2.3).

2.4.5. Development of land-surface temperatures based on satellite imagery

Based on selected imagery of TIR data from Landsat 5 and ASTER measurements, a qualitative assessment of the development of eventual LST anomalies was carried out (see section 2.3.2).

Figure 2.8 displays the rescaled TIR data from the Landsat 5 satellite, masked by the extension of relevant sedimentary basins. The images were all taken around midday (local time). Orange colors represent higher land-surface temperatures

(LSTs), while white areas mark the lowest LSTs. Generally, low-temperature anomalies are associated with near-surface water resources. In section II (the southern part of the displayed area in Figure 2.8), the strongest temperature anomalies correspond consistently with the perennial stream network. In section I (the northern part, Figure 2.8), the strong anomalies are associated with the Lagunillas salt flat and the respective wetland area, where groundwater levels were shallower than 0.5 m bgl in 1991 (Figure 2.2). By Oct-1995, the anomaly in the eastern wetland area in section I had disappeared almost completely, which corresponds to a decline of the water table to below 2 m bgl. In parallel, the data visualizes the development of a heat anomaly in the central basin of the LL watershed (section I). TIR data values in images of November 1991 and 1993 are lower than values in October 1995 and 1997. This anomaly remains persistently during the coming years; Figure 2.9 depicts absolute surface temperatures based on ASTER data for Nov-2000, Nov-2004, Oct-2007 and Nov-2014.

The conversion of TIR-band anomalies into absolute temperatures reveals that diurnal LSTs during October and November plot between 23°C and 54°C, which is several degrees above air temperature (13-20°C) and is caused by a conversion of solar energy into heat energy in the upper section of the sedimentary layer (Alkhaier et al. 2012b). Land surfaces around station MLL are 10-20°C hotter than around the remaining wetland area (near-surface groundwater) because solar energy received by water humidity and saturated sediments (higher soil moisture) is, in great part, consumed by evaporation processes (Alkhaier et al. 2012b; Berg et al. 2014; Lakshmi et al. 2003). The extinction depth of the evaporative energy potential in the arid Andean environment is 2 m bgl (Houston 2006a). Consequently, the data demonstrate that surface water and near-surface groundwater cause negative anomalies in LSTs by up to 20°C. Cooler sediment bodies occurring in the northern section of the LL basin in Nov-2000 and Nov-2014 could indicate infiltrating recharge (probably mountain front recharge (Kikuchi and Ferré 2016)).

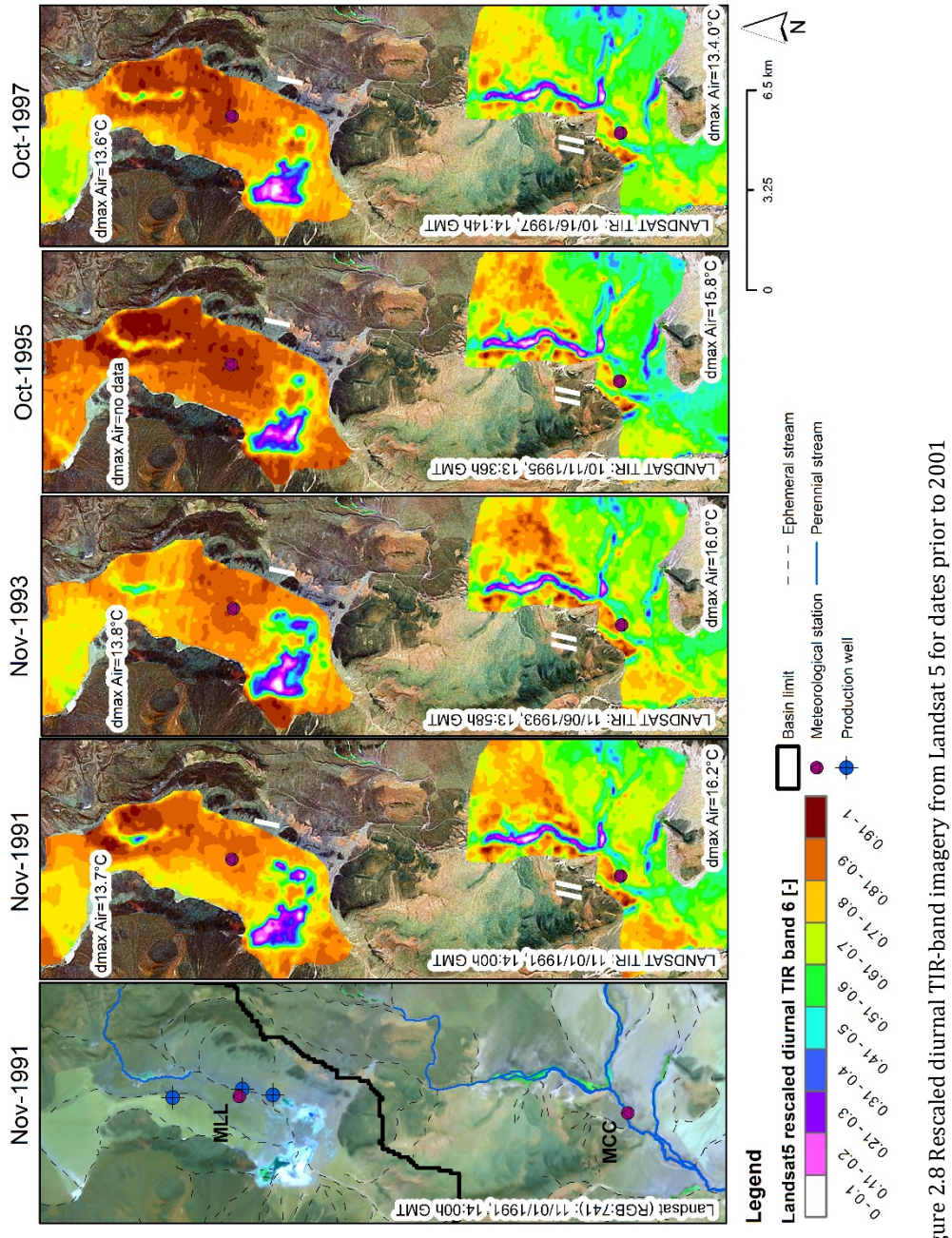

Figure 2.8 Rescaled diurnal TIR-band imagery from Landsat 5 for dates prior to 2001

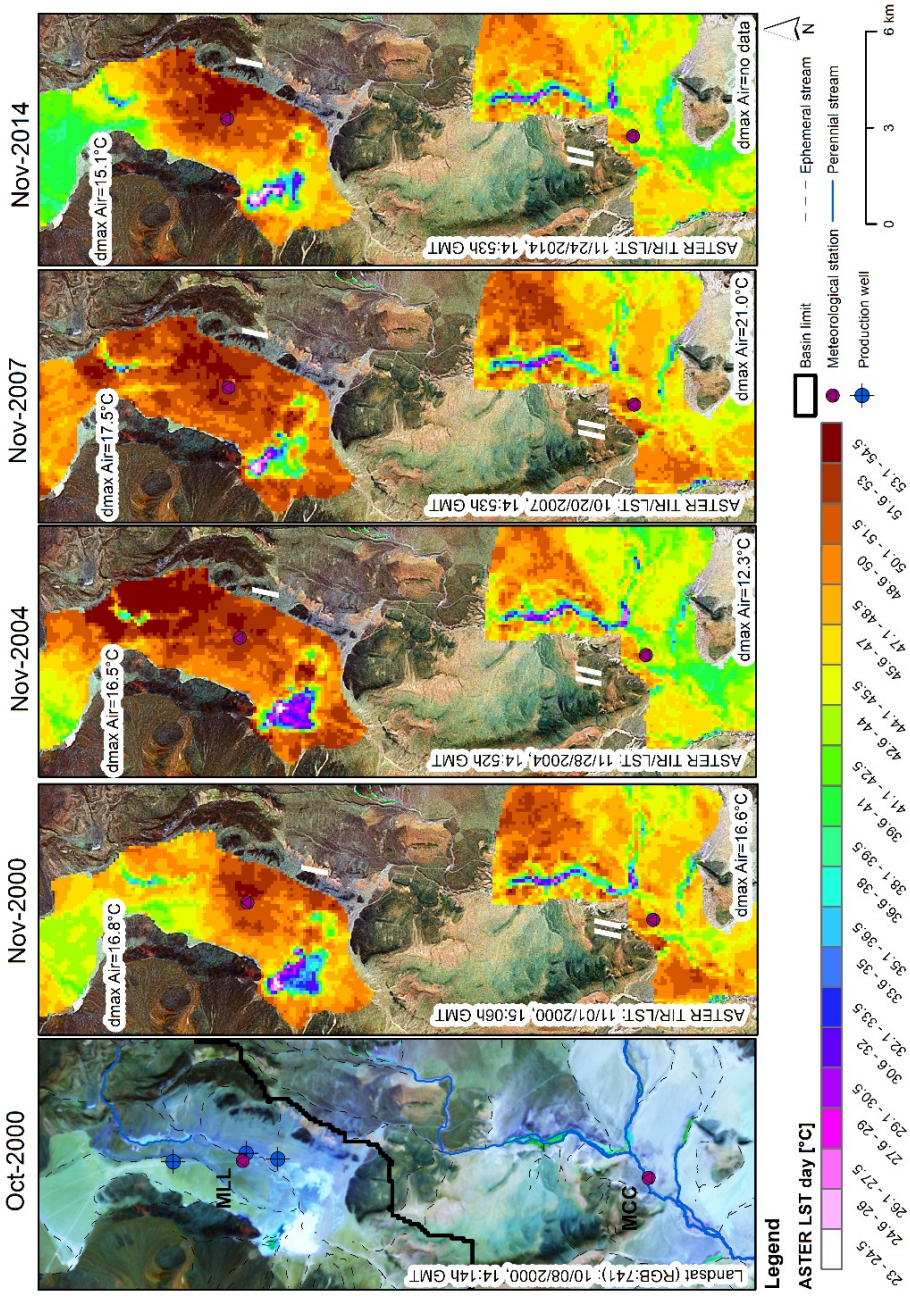

Figure 2.9 ASTER diurnal land-surface temperatures of October and November imagery (2000-2014)

Subsequently, night LSTs will be examined. Figure 2.10 visualizes land-surface temperatures of the early night (always ~03:17h GMT; the time difference to Santiago de Chile is -3h in austral summer and -5h in austral winter).
In response to a strong storm event in 2001, the Lagunillas salt flat area was still flooded in May 2002. Therefore, in the image of June 2002 a large positive heat anomaly is observed in the Salar area. Generally, winter LSTs plot between -24°C and 0°C. Throughout the years, it can be observed that LSTs close to the surface and near-surface groundwater are considerably warmer compared to areas with a deeper groundwater level (differences of up to 20°C) which implies that near-surface water resources function as a heat source during night in the area of work.

However, the imagery also demonstrates that there is a negative heat anomaly associated with the LL watershed around the respective meteorological station when compared to LST around station MCC. Note that in 2002 (earliest available image) the main climate changes with regard to mmin temperatures (night temperatures) did already occur. Independent of the year, LSTs in section II are 4-10°C higher than in section I. The relative difference of LST between sections I and II appears to increase slightly over time.

In Figure 2.11 the same anomaly is observed when comparing images of different seasons during the year 2008. In austral winter (Jul-2008), a widespread anomaly is displayed around section I (~6°C lower than in section II). But images of Jan-2008, Aug-2008 and Oct-2008 illustrate the phenomenon too.
The strongest negative anomalies that are associated with the dry salar areas, can be caused by the differing thermal properties of the associated surface salt-flat deposits compared to valley sediments (the porosity of surface salt-flat deposits can reach up to 50%) (Warren 2006). Another factor may be the total aquifer thickness which is lowest in the southern marginal area (southern section).

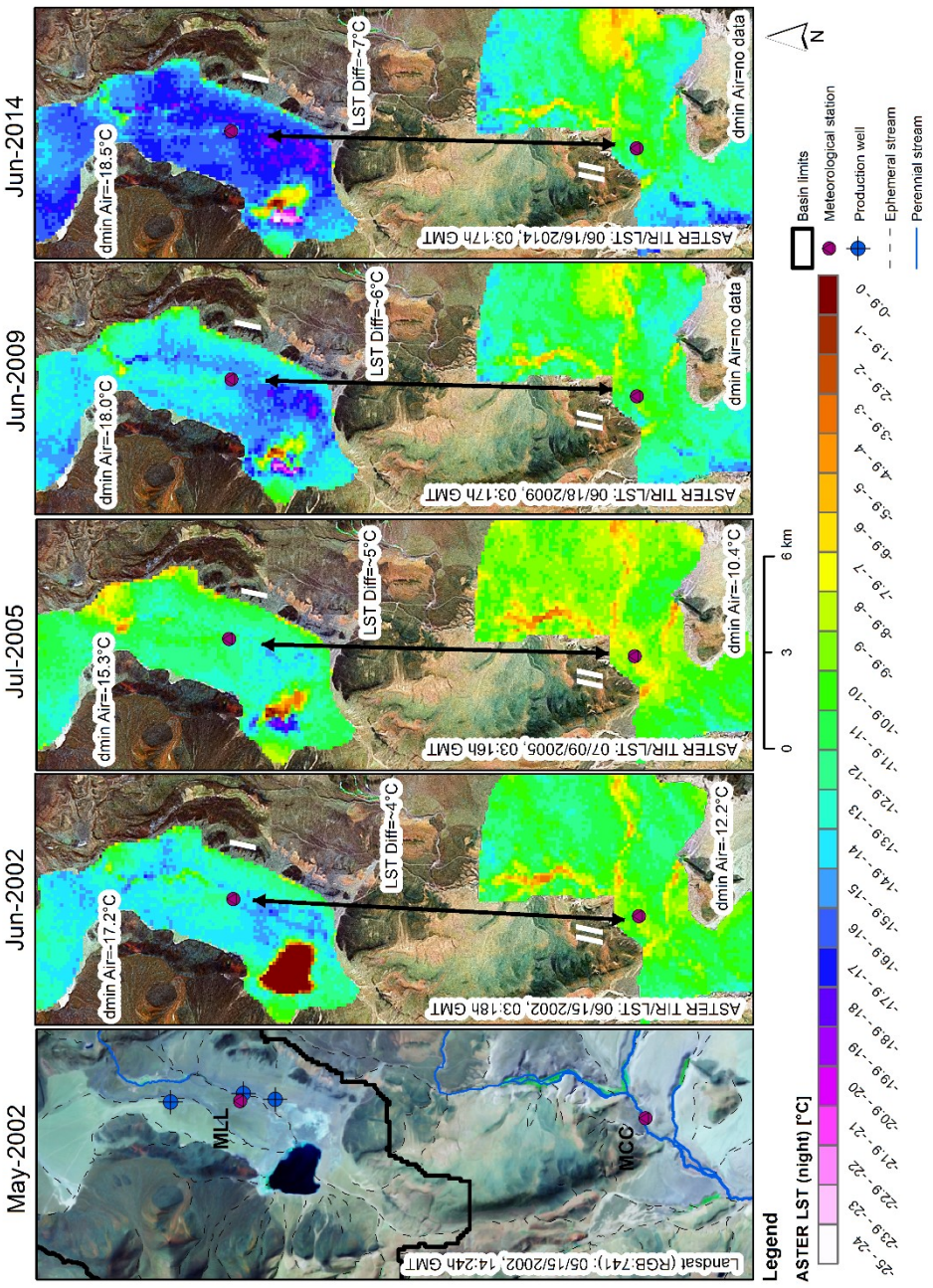

Figure 2.10 ASTER night land-surface temperatures (winter imagery 2002-2014)

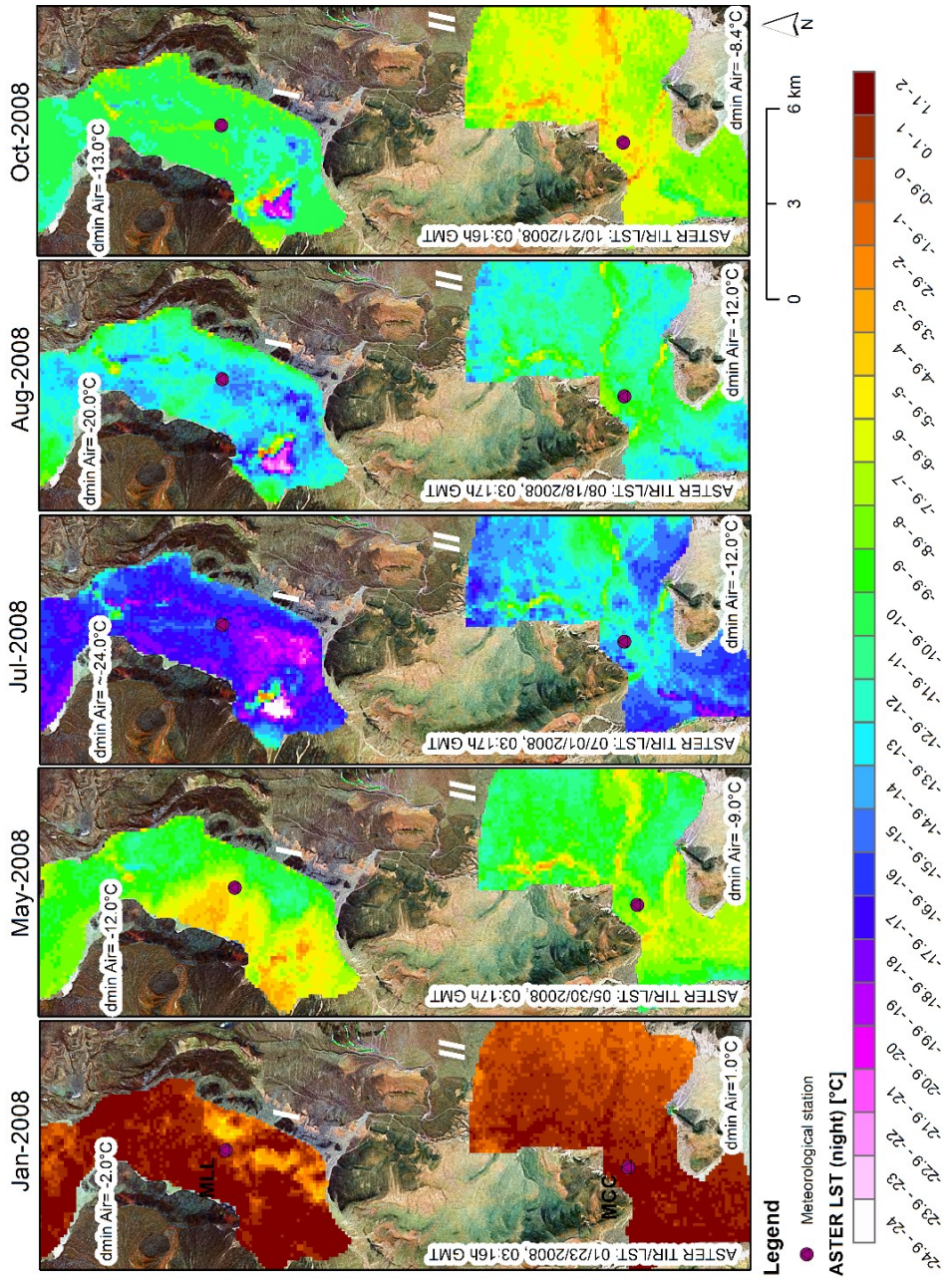

Figure 2.11 ASTER night land-surface temperatures for various months in 2008

2.5. Discussion

Together with an ongoing groundwater overexploitation in the LL basin, a change in air temperatures and anomalies in surface temperatures can be detected.
Since the beginning of water withdrawals, mmin winter temperatures (night temperatures) in the LL basin have fallen by 3-8°C compared with a reference station. Also, mmin temperatures during summer fell by 2-4°C (Figure 2.7). The respective time series show a declining trend between 1992 and 2012, although intermittent temperature upturns occur. These appear to be triggered by La Niña conditions and hence strong easterly trade winds (Figure 2.5 and Figure 2.7). Several non-linear effects have also been observed; mmax summer temperatures (day temperatures) rose relatively abruptly by 2.7°C on average around the years 1995-1997. During the same period, the variance of mmin temperatures and, later, mmax temperatures also shifted to a new mean (Figure 2.6).
In particular, the presence of different continuous trends and non-linear shifts concerning mmax and mmin temperatures of the winter and summer time series (Figure 2.6 and Figure 2.7) provides evidence that the recorded climatic change is not a product of an eventual consecutive error that was introduced after the data gap between 1995 and 1997. Likewise, the observed climatic changes can also not be attributed to a regional climate forcing affecting the locality, because a cross-correlation of the temperature time series with an uninfluenced nearby reference station demonstrates a decoupling of respective trend lines after the year 1997 (Figure 2.4, and section 2.4.4). This emphasises that there is a local factor superimposing natural climatic trends at station MLL. It is proposed that the continuously declining water table in the LL basin is the cause for this local climatic change.

Generally speaking, shallow groundwater is associated with wetter soil profiles due to the upward water and vapor fluxes (Alkhaier et al. 2012b). The effect of solar energy absorption by soil moisture and near-surface groundwater due to evaporation has been studied before and is known to have a regulating impact on both land-surface temperatures and maximum air temperatures in the lower atmosphere (Lakshmi et al. 2003; Whan et al. 2015; Berg et al. 2014; Alkhaier et al. 2012b; Alkhaier et al. 2012a). The observed increase of land-surface temperature around station MLL is probably induced by the lowering of the water table from less than 1 m bgl to depths below the evaporative energy

potential extinction depth (~2 m bgl) (Houston 2006a; Hernández-López et al. 2014). This goes, very likely, hand-in-hand with a decrease of the soil moisture in the top layers (Alkhaier et al. 2012b). The water table around station MLL fell below 2-3 m bgl in the period between 1995 and 1997. Hence the absorption of solar energy by evaporative processes ceased and instead causes a stronger up heating of respective surface sediments. This up heating, in turn, could have influenced temperatures of the lower atmosphere and would explain the abrupt rise of mmax summer temperatures by a mean of 2.7°C around the years 1995-1997. The abruptness could be explained by the high drawdown rates of 0.5-1 m/a. A collapse of the capillary rise process in the vadose zone, due to the ongoing rapid water-level decline, could be another influencing factor.

Related effects can play a role when it comes to mmin temperatures. It is known that the presence of shallow groundwater increases significantly the thermal conductivity of the saturated top sediment layers, which facilitates a higher heat transfer between the atmosphere and subsurface (Alkhaier et al. 2012b). Near-surface groundwater is by convection connected to a constant heat reservoir of 10°C (average groundwater temperature). During the day, near-surface groundwater could heat up above 10°C and cool slowly down during dusk, according to the temperature gradient with regard to the lower atmosphere. As soon as shallow-water temperature drops significantly below 10°C, the convection processes within the saturated sediment could provide a constant heat flux from the lower layers in the aquifer. This process could facilitate a significant heat exchange between the lower atmosphere and the shallow groundwater and give a possible explanation for processes that would buffer the extreme air temperature downturns during winter nights (from ~5°C down to ~-20°C). The total aquifer thickness can play an additional role in this process as well as an eventual influence of steep geothermal gradients (see section 2.2). Night LSTs indicate that in response to a groundwater level decline, night surface temperatures also decline. This is in accordance with findings of Alkhaier et al. (2012a) who reported for a shallow aquifer in Syria, where air temperatures dropped during the night to -5°C, that groundwater caused an up heating of night surface temperatures when found above ~4 m bgl. In the Andean environment, the temperature gradient between night air temperatures and the groundwater reservoir is even higher. In response to an ongoing water-level decline, the provided heat flux from the subsurface to the surface and hence to the lower

atmosphere is probably reduced continuously and hence mmin temperatures could fall lower.

However, while absolute mmin temperatures appear to follow a declining trend until 2012 (Figure 2.7) the respective variance time series (Figure 2.6) shows a non-linear shift. This could be explained by the disappearance of the up-heating effect during daytime of shallow groundwater by solar energy. Groundwater below 2 m bgl, which is much less thermally connected to the surface layers, will probably show a relatively constant temperature of ~10°C throughout a 24h-day, whereas near-surface groundwater experiences a notable up heating when surface temperatures rise above 30°C (also in winter). This is confirmed by Hernández-López et al. (2014) who carried out laboratory evaporation experiments with soil from the Salar del Huasco basin (variation of surface temperature: 40-50°C, spectrum of groundwater temperatures at 30-50 cm bgl: 22-30°C). Hence, shallow groundwater would function here again, on the one hand as a heat storage, and on the other as a thermal conductor.
Nevertheless, to gain a deeper understanding of the causes and different environmental feedbacks implied in the observed climatic change, further research is required. A climatic modelling on respecting interactions between the subsurface, surface and lower atmosphere could yield more detailed insights.
For now, the area affected by the described local climate change can only be estimated. It is assumed that the central valley of the Pampa Lagunillas around the wetland Lagunillas with elevations lower than 4050 m asl is the only area concerned, where shallow groundwater has prevailed and LST data consequently show changes or anomalies. This is an area of approximately 30 km^2.
According to the given data, the changes in temperature begin to set in around the years 1995-1999 and developed relatively fast, which is likely explained by the high water-level drawdown rates of 0.5 to 1 m/a (Figure 2.2). In particular, the dropping of near-surface groundwater levels below 2-3 m bgl appears to be a critical threshold.

There could be multiple consequences of this local climate change. Effects on the ecosystem such as plants, insects, birds, small reptiles and rodents, particularly around the concerned wetland, would need to be studied further. At the same time, impacts on meteorological parameters such as evaporation could be a consequence. Higher mmax temperatures in summer can lead to an increased

evaporation of the precipitation that falls almost exclusively during the summer months. Maximum temperatures are a major controlling factor when it comes to actual evaporation in the Andes of northern Chile (Houston 2006a).
The extreme climatic environment of the arid Andes seems to fortify feedbacks between hydrological and atmospheric parameters. The given case study is of interest also in terms of water management measures when planning, executing and monitoring groundwater production projects in similar environments. Water resources in arid Andean high-elevation aquifers are, so far, a mostly untouched and attractive resource in an otherwise water-scarce environment (PUC 2009). The great majority of respective closed Andean basins exhibit very similar geological and environmental characteristics (Risacher et al. 2003).

The presented data demonstrate for the first time that, apart from other negative environmental effects, a severe overexploitation in arid Altiplano basins can have a serious impact on the local climate. This is a point hardly considered so far. A first best-practice recommendation for ongoing and future projects could be to prevent water-level drawdowns below 2 m bgl in areas with near-surface groundwater.

2.6. Conclusions

The Laguna Lagunillas basin in the arid Andes of northern Chile is exposed to extreme climatic conditions with air temperature variations from 20°C to -25°C. Land surface temperatures can vary between -25°C (winter nights) to +50°C (summer days).
Since the beginning of water withdrawals from the shallow Pampa Lagunillas aquifer in ~1992, groundwater drawdown rates have varied between 0.5 and 1 m/a. As a consequence of the ongoing overexploitation and the linked retreat of the near-surface groundwater level, a local climate change can be observed.
In the concerned area, mean monthly minimum winter air temperatures follow from 1992 to 2012 a declining trend and dropped by approximately 3-8°C. Mean monthly minimum summer air temperatures fell by 2-4°C. At the same time, mean monthly maximum summer air temperatures shifted distinctly upwards between 1995 and 1997 by 2.7°C on average. The observed changes are accompanied by an increase of variance of the respective time series data. Air

temperature changes are in accordance with detected anomalies in land-surface temperature imagery.

A regional climatic forcing affecting the locality can be excluded as a reason for the observed variations due to a demonstrated decoupling of air temperature trends from an uninfluenced nearby reference station in the Salar del Huasco basin. In this context, it is shown that particularly variations of monthly minimum air temperatures in the area of work are normally in high correlation with variations of the Southern Oscillation Index (SOI).

In conjunction with a review of results of thematically related studies, it is proposed that two major factors caused the local climate change. One is related to a dropping of the water table below the evaporative energy potential extinction depth of ~2 m bgl in large areas of the basin. Solar energy that was earlier consumed by evaporative processes during daytime, contributes now to an up heating of the top sedimentary layer which in turn influences maximum air temperatures. At the same time, the removal of near-surface groundwater reduces the thermal conductivity of the upper sedimentary layer continuously, which consequently reduces the heat exchange between the aquifer (constant heat source of ~10°C) and the lower atmosphere. Hence night air temperature downturns down to ~-20°C are less effectively buffered. Nevertheless, further research is required to clarify the interactions between the subsurface and the lower atmosphere and to examine the processes involved, which exhibit continuous as well as non-linear characteristics.

In the extreme climatic environment of the arid Andes, feedbacks between hydrological and atmospheric parameters appear to be strongly fortified. The observed critical water-level drawdown of the near-surface groundwater in this case study is ~2-3 m bgl before non-linear climatic changes occur.

For future and existing water production projects in arid and semi-arid Andean Altiplano basins, it is recommended to take groundwater-climate interactions into account when executing environmental impact studies and monitoring. A best-practice recommendation for water withdrawals from high, arid Andean basins could be to prevent a water-level decline of near-surface groundwater levels below 2 m bgl.

2.7. Acknowledgment

This study was financed by CONICYT (National Commission for Science and Technology, Chile). The authors thank the Early Career Hydrogeologist Network of the International Association of Hydrogeologists and the GRAPHIC project of the UNESCO-IHP for promoting this article in the topical collection 'Groundwater and Climate Change'.

2.8. References

Alkhaier F, Su Z, Flerchinger GN (2012a) Reconnoitering the effect of shallow groundwater on land surface temperature and surface energy balance using MODIS and SEBS. Hydrol. Earth Syst. Sci. 16(7):1833–1844. doi: 10.5194/hess-16-1833-2012

Alkhaier F, Flerchinger GN, Su Z (2012b) Shallow groundwater effect on land surface temperature and surface energy balance under bare soil conditions: Modeling and description. Hydrol. Earth Syst. Sci. 16(7):1817–1831. doi: 10.5194/hess-16-1817-2012

Aravena D, Muñoz M, Morata D, Lahsen A, Parada MÁ, Dobson P (2016) Assessment of high enthalpy geothermal resources and promising areas of Chile. Geothermics 59:1–13. doi: 10.1016/j.geothermics.2015.09.001

Barsi JA, Schott JR, Palluconi FD, Hook SJ, Butler JJ (2005) Validation of a Web-Based Atmospheric Correction Tool for Single Thermal Band Instruments. Earth Observing Systems X:58820. doi: 10.1117/12.619990

Berg A, Lintner BR, Findell KL, Malyshev S, Loikith PC, Gentine P (2014) Impact of Soil Moisture–Atmosphere Interactions on Surface Temperature Distribution. J. Climate 27(21):7976–7993. doi: 10.1175/JCLI-D-13-00591.1

BHP Billiton (2015) BHP Billiton Chile Sustainability report 2014. http://www.bhpbilliton.com/~/media/bhp/documents/society/reports/2014/csr-eng150518sustainabilityreport2014bhpbillitonchileoperations.pdf. Accessed 17 May 2016

Boucher O, Myhre G, Myhre A (2004) Direct human influence of irrigation on atmospheric water vaporand climate. Climate Dynamics 22(6-7). doi: 10.1007/s00382-004-0402-4

Buishand TA (1982) Some methods for testing the homogeneity of rainfall records. Journal of Hydrology 58(1-2):11–27. doi: 10.1016/0022-1694(82)90066-X

Cerveny RS, Skeeter BR, Dewey KF (1987) A Preliminary Investigation of a Relationship between South American Snow Cover and the Southern Oscillation. Mon. Wea. Rev. 115(2):620–623. doi: 10.1175/1520-0493(1987)115<0620:APIOAR>2.0.CO;2

DGA (2015) Información Oficial Hidrometeorológica y de Calidad de Aguas en Línea - Oficial online information; hydrometeorology and water quality. http://snia.dga.cl/BNAConsultas/reportes. Accessed 20 December 2015

GFZ (2015) Access to GEOFON and EIDA Data Archives. http://eida.gfz-potsdam.de/webdc3/. Accessed 19 December 2015

Hernández-López MF, Gironás J, Braud I, Suárez F, Muñoz JF (2014) Assessment of evaporation and water fluxes in a column of dry saline soil subject to different water table levels. Hydrol. Process. 28(10):3655–3669. doi: 10.1002/hyp.9912

Herrera C, Custodio E, Chong G, Lamban LJ, Riquelme R, Wilke H, Jodar J, Urrutia J, Urqueta H, Sarmiento A, Gamboa C, Lictevout E (2016) Groundwater flow in a closed basin with a saline shallow lake in a volcanic area: Laguna Tuyajto, northern Chilean Altiplano of the Andes. Sci Total Environ 541:303–318. doi: 10.1016/j.scitotenv.2015.09.060

Houston J (2006a) Evaporation in the Atacama Desert: An empirical study of spatio-temporal variations and their causes. Journal of Hydrology 330(3-4):402–412. doi: 10.1016/j.jhydrol.2006.03.036

Houston J (2006b) Variability of precipitation in the Atacama Desert: its causes and hydrological impact. Int. J. Climatol. 26(15):2181–2198. doi: 10.1002/joc.1359

Jiménez-Muñoz JC, Sobrino JA (2003) A generalized single-channel method for retrieving land surface temperature from remote sensing data. J. Geophys. Res. 108(D22). doi: 10.1029/2003JD003480

Kendall MG, Gibbons JD (1990) Rank correlation methods, 5. ed. Oxford Univ. Press, New York

Kikuchi CP, Ferré TPA (2016) Analysis of subsurface temperature data to quantify groundwater recharge rates in a closed Altiplano basin, northern Chile. Hydrogeol J. doi: 10.1007/s10040-016-1472-1

Lakshmi V, Jackson TJ, Zehrfuhs D (2003) Soil moisture-temperature relationships: Results from two field experiments. Hydrol. Process. 17(15):3041–3057. doi: 10.1002/hyp.1275

Larraín S, Poo P (2010) Conflictos por el agua en Chile - Entre los derechos humanos y las reglas de mercado (Water conflicts in Chile - between human rights and the rules of the free market), 1a ed. [s.n], Santiago, Chile

Lavado Casimiro WS, Labat D, Ronchail J, Espinoza JC, Guyot JL (2012) Trends in rainfall and temperature in the Peruvian Amazon-Andes basin over the last 40 years (1965-2007). Hydrol. Process.:n/a-n/a. doi: 10.1002/hyp.9418

Lehmann E (2006) Nonparametrics: Statistical methods based on ranks, 1., rev. ed. Springer, New York NY

Lo M-H, Famiglietti JS (2013) Irrigation in California's Central Valley strengthens the southwestern U.S. water cycle. Geophys. Res. Lett. 40(2):301–306. doi: 10.1002/grl.50108

Maxwell RM, Kollet SJ (2008) Interdependence of groundwater dynamics and land-energy feedbacks under climate change. Nature Geosci 1(10):665–669. doi: 10.1038/ngeo315

Montgomery E, Rosko M (1996) Groundwater exploration and wellfield development in the Pampa Lagunillas y Pampa Lirima areas, Iquique, Chile - 1996. Revista Geológica de Chile 23(2). doi: 10.5027/andgeoV23n2-a03

NASA (2002) ASTER Surface Kinetic Temperature Product indications. https://asterweb.jpl.nasa.gov/content/03_data/01_Data_Products/release_surface_kinetic_temperatur.htm

NASA (2014) Atmospheric Correction Parameter Calculator. http://atmcorr.gsfc.nasa.gov/. Accessed 3 March 2015

NASA (2017) Advanced Spaceborne Thermal Emission and Reflection Radiometer (ASTER). https://asterweb.jpl.nasa.gov/. Accessed 7 March 2017

NASA LP DAAC (2017) ASTER Level 2 Surface Temperature Product retrieval. https://search.earthdata.nasa.gov/. Accessed 26 February 2017

ODEA (2016) Observatorio del Agua [Water resources observatory]. www.odea.cl. Accessed 7 December 2016

Pettitt AN (1979) A Non-Parametric Approach to the Change-Point Problem. Applied Statistics 28(2):126. doi: 10.2307/2346729

PUC (2009) Levantamiento Hidrogeológico para el Desarrollo de nuevas fuentes de Agua en áreas prioritarias de la zona norte de Chile, Regiones XV, I, II y III (Hydrogeological study for the development of new water resources in northern zones of Chile, regiones XV, I, II and III). documentos.dga.cl/REH5161v4.pdf. Accessed 13 May 2016

Reyes N, Vidal A (2011) Geothermal Exploration at Irruputuncu and Olca Volcanoes Pursuing a Sustainable Mining Development in Chile. GRC Transactions 35

Risacher F, Alonso H, Salazar C (2003) The origin of brines and salts in Chilean salars: a hydrochemical review. Earth-Science Reviews 63(3-4):249–293. doi: 10.1016/S0012-8252(03)00037-0

Ropelewski CF, Halpert MS (1987) Global and Regional Scale Precipitation Patterns Associated with the El Niño/Southern Oscillation. Mon. Wea. Rev. 115(8):1606–1626. doi: 10.1175/1520-0493(1987)115<1606:GARSPP>2.0.CO;2

Sanchez-Alfaro P, Sielfeld G, van Campen B, Dobson P, Fuentes V, Reed A, Palma-Behnke R, Morata D (2015) Geothermal barriers, policies and economics in Chile – Lessons for the Andes. Renewable and Sustainable Energy Reviews 51:1390–1401. doi: 10.1016/j.rser.2015.07.001

Scheihing KW, Moya CE, Tröger U (2017) Insights into Andean slope hydrology: Reservoir characteristics of the thermal Pica spring system, Pampa del Tamarugal, northern Chile. Hydrogeol J 119(2):33. doi: 10.1007/s10040-017-1533-0

SEA (2014) Informe Consolidado Nº 2 de Solicitud de Aclaraciones, Rectificaciones y/o Ampliaciones al Estudio de Impacto Ambiental del Proyecto "Proyecto Continuidad Operacional Cerro Colorado": 2nd consolidated report; request for clarification, recitification and/or amplification of the environmental impact study of the project 'Operational continuation project of Cerro Colorado'.http://infofirma.sea.gob.cl/DocumentosSEA/MostrarDocumento?docId=70/4c/3458d2195a9a0439fd12881b7b693532e730. Accessed 16 March 2017

Sernageomin (2003) Geological Map of Chile: digital version. 1:1,000,000. www.ipgp.fr/~dechabal/Geol-millon.pdf. Accessed 17 May 2016

Stenseth NC, Ottersen G, Hurrell JW, Mysterud A, Lima M, Chan K-S, Yoccoz NG, Adlandsvik B (2003) Review article. Studying climate effects on ecology through the use of climate indices: the North Atlantic Oscillation, El Nino Southern Oscillation and beyond. Proc Biol Sci 270(1529):2087–2096. doi: 10.1098/rspb.2003.2415

Tassi F, Aguilera F, Darrah T, Vaselli O, Capaccioni B, Poreda RJ, Delgado Huertas A (2010) Fluid geochemistry of hydrothermal systems in the Arica-Parinacota, Tarapacá and Antofagasta regions (northern Chile). Journal of Volcanology and Geothermal Research 192(1-2):1–15. doi: 10.1016/j.jvolgeores.2010.02.006

Trenberth KE (1984) Signal Versus Noise in the Southern Oscillation. Mon. Wea. Rev. 112(2):326–332. doi: 10.1175/1520-0493(1984)112<0326:SVNITS>2.0.CO;2

Uribe J, Muñoz JF, Gironás J, Oyarzún R, Aguirre E, Aravena R (2015) Assessing groundwater recharge in an Andean closed basin using isotopic characterization and a rainfall-runoff model: Salar del Huasco basin, Chile. Hydrogeol J. doi: 10.1007/s10040-015-1300-z

USGS (2017) Landsat data retrieval. http://glovis.usgs.gov/. Accessed 7 March 2017

Whan K, Zscheischler J, Orth R, Shongwe M, Rahimi M, Asare EO, Seneviratne SI (2015) Impact of soil moisture on extreme maximum temperatures in Europe. Weather and Climate Extremes 9:57–67. doi: 10.1016/j.wace.2015.05.001

Yáñez Fuenzalida N, Molina Otárola R (2008) La gran minería y los derechos indígenas en el norte de Chile [The big mining and the rights of indiginous people in northern Chile], 1. ed. Ciencias humanas. Estado y pueblos indígenas. LOM, Santiago

Yue S, Wang C (2004) The Mann-Kendall Test Modified by Effective Sample Size to Detect Trend in Serially Correlated Hydrological Series. Water Resources Management 18(3):201–218. doi: 10.1023/B:WARM.0000043140.61082.60

Zeng Y, Xie Z, Yu Y, Liu S, Wang L, Zou J, Qin P, Jia B (2016) Effects of anthropogenic water regulation and groundwater lateral flow on land processes. J. Adv. Model. Earth Syst. 8(3):1106–1131. doi: 10.1002/2016MS000646

Zeng Y, Xie Z, Zou J (2017) Hydrologic and Climatic Responses to Global Anthropogenic Groundwater Extraction. J. Climate 30(1):71–90. doi: 10.1175/JCLI-D-16-0209.1

Zou J, Xie Z, Yu Y, Zhan C, Sun Q (2014) Climatic responses to anthropogenic groundwater exploitation: A case study of the Haihe River Basin, Northern China. Clim Dyn 42(7-8):2125–2145. doi: 10.1007/s00382-013-1995-2

3. Insights into Andean slope hydrology: reservoir characteristics of the thermal Pica spring system, Pampa del Tamarugal, northern Chile

Konstantin W. Scheihing[a,*], Claudio E. Moya[b, c], Uwe Tröger[a]

[a] Department of Applied Geosciences, Hydrogeology Research Group, Technische Universität Berlin, Berlin 10587, Germany

[b] CONICYT Regional/CIDERH, Centro de Investigación y Desarrollo en Recursos Hídricos (R09I1001), Iquique, Chile

[c] Universidad Arturo Prat, Iquique, Chile

[*]corresponding author: kscheihing@gmx.de

Citation:

Scheihing KW, Moya CE, Tröger U (2017) Insights into Andean slope hydrology: Reservoir characteristics of the thermal Pica spring system, Pampa del Tamarugal, northern Chile. Hydrogeol J 119(2):33. doi: 10.1007/s10040-017-1533-0

Article history:

Received: 19 May 2016 / Accepted: 2 January 2017 / Published online: 1 March 2017

This is a postprint-version. The final publication is available at Springer via https://doi.org/10.1007/s10040-017-1533-0.

Abstract

The thermal Pica springs, at ~1400 m above sea level (asl) in the Pampa del Tamarugal (Chile), represent a low-saline spring system at the eastern margin of the hyper-arid Atacama Desert, where groundwater resources are scarce. This study investigates the hydrogeological and geothermal characteristics of their feed reservoir, fostered by the interpretation of a 20-km, east-west-heading reflection seismic line in the transition zone from the Andean Precordillera to the Pampa del Tamarugal. Additional hydrochemical, isotope and hydrologic time-series data support the integrated analysis. One of the main factors that enabled the development of the spring-related vertical fracture system at Pica, is a disruption zone in the Mesozoic Basement caused by intrusive formations. This destabilized the younger Oligocene units under the given tectonic stress conditions. Thus, the respective groundwater reservoir is made up of fractured Oligocene units of low to moderate permeability. Groundwater recharge takes place in the Precordillera at ~3800 m asl (no hydraulic connection to the Salar del Huasco basin). From there groundwater flow covers a height difference of ~3000 m with a maximum circulation depth of ~800-950 m, where the waters obtain their geothermal imprint. The maximal expected reservoir temperature, as confirmed by geothermometers, is ~55 °C. Corrected mean residence times of spring water and groundwater plot at 1200–4300 years BP and yield average interstitial velocities of 6.5–22 m/a. At the same time, the hydraulic head signal, as induced by recharge events in the Precordillera, is transmitted within 20–24 months over a distance of ~32 km towards the Andean foothills at Pica and Puquio Nunez.

3.1. Introduction

The town of Pica forms a flourishing oasis at the eastern margin of the Pampa del Tamarugal (PdT), in the hyper-arid Atacama Desert in northern Chile (Figure 3.1 and Figure 3.2)). At the foothills of the Andean Precordillera (~1400 m asl) thermally influenced and very low-saline water (~33 °C, ~320 µS/cm) is uprising and nourishing the Pica spring system and the related Pica aquifer (total spring discharge ~53 l/s) (Galli and Dingman R. 1965; Fritz et al. 1981; Magaritz et al. 1989).

Figure 3.1 South-west South America (the extent of the study area in Figure 3.2 is marked by a black rectangle)

Another related spring (much less abundant: 1 l/s) can be found 10 km south of Pica around Puquio Nunez (Galli and Dingman R. 1965). Here spring water shows an electrical conductivity of ~600 µS/cm but no apparent geothermal imprint. While groundwater resources in Pica are being primarily used for agricultural and domestic purposes the area around Puquio Nunez (PN) is practically deserted and groundwater is not being exploited significantly.

The origin of the low-saline spring- and groundwater was discussed in earlier studies. While it was clear that the groundwater would be related to an Andean recharge area due to its depleted contents of deuterium, different conceptual models were suggested (Fritz et al. 1981; Magaritz et al. 1989; Magaritz et al. 1990; Rojas et al. 2010; Jayne et al. 2016). On the one hand a recharge in the nearby Precordillera at Altos de Pica was proposed (Fritz et al. 1981). On the other hand, flow through deep fissures from the adjacent Altiplano watershed, the Salar del Huasco basin, towards Pica and the Pampa del Tamarugal is considered (Magaritz et al. 1989; Magaritz et al. 1990; Jica 1995). However, based on hydrochemical and water balance considerations in the Salar del Huasco basin a recent publication points out that the latter should be disregarded (Uribe et al. 2015). The results of the study reported here substantiate these findings.

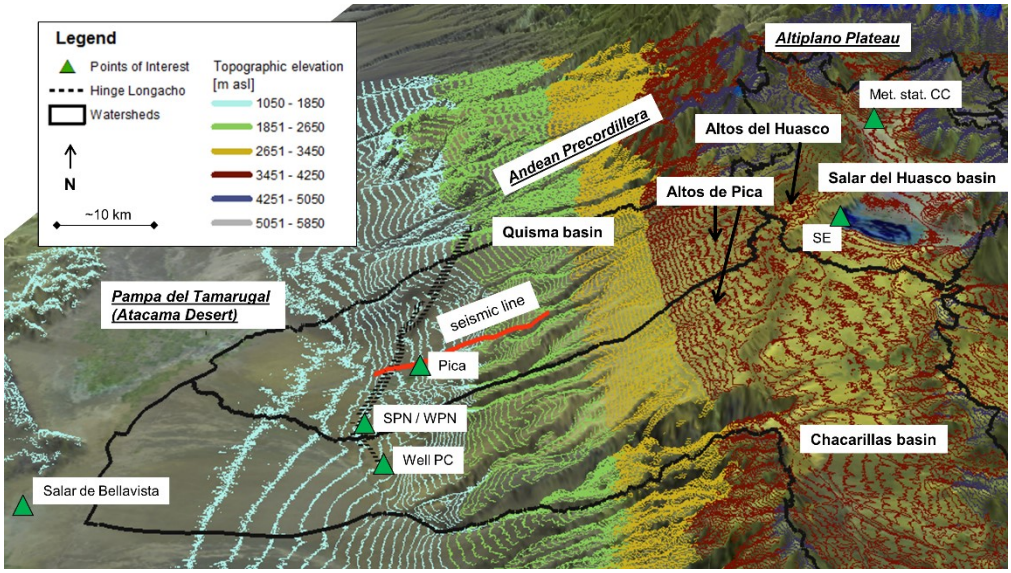

Figure 3.2 3D visualization of the study area (elevation model five times exaggerated)
(SPN = Puquio Nunez Spring, WPN = Puquio Nunez Well, PC = Chacarillas Well, SE = Ermitano Spring)

The main aim of this study is to gain detailed understanding of the hydrogeological and geothermal functioning of the Andean slope reservoir that aliments the Pica spring system. For the first time, seismic imagery is presented of a transition zone from Precordillera to Pampa del Tamarugal. A stratigraphic and tectonic analysis of the 20 km long and east-west heading reflection seismic line, allows mapping of groundwater guiding units and thus of the reservoir geometry, and sheds light upon how the spring system could evolve geologically. Together with a local record of the geothermal gradient and hydrochemical data, the reservoir temperature, mean groundwater residence times and average interstitial velocities can be determined. Furthermore, the statistical analysis of four relevant hydrologic time-series allows an assessment of the hydraulic delay of the slope system to recharge events. Thus, the study gives a rare insight into the hydrologic and hydrogeologic functioning of an Andean slope reservoir under arid climate conditions.

3.2. Geologic and climatic setting

The area of work is situated in northern Chile at ~20.5°S latitude close to the Bolivian border (Figure 3.1). The regional morphologic setting can be subdivided into 3 main geological units. These are the Pampa del Tamarugal (PdT) as part of

the so called Central Depression, followed east by the Precordillera, which forms the western flank of the Andean Altiplano Plateau (Figure 3.2). The latter builds up the third unit. The Altiplano lies at an altitude of about 4000 m asl while Pica and PN lie between 1200 and 1400 m asl.

The uplift of the Altiplano Plateau and the related evolution of its western flank began in the early Oligocene (~30 Ma) (Jordan et al. 2010; Schlunegger et al. 2010). These uplift processes led to short- (~1 km), long- (30-50 km) and very long (>50 km) wavelength monoclinal relief formations and induced a rock uplift of the entire forearc, as well as a westward tilting of the Atacama lithospheric block (Jordan et al. 2010). Arc volcanic processes accompanied the evolution of the Altiplano Plateau, which gave way to abundant ignimbrite formations in the Precordillera and Altiplano of the area of work (Blanco and Landino 2012).
The climate of the PdT has been primarily hyper-arid from 12±1 Ma onwards (Jordan et al. 2014). Today the amount of precipitation in areas below 2000 m asl is <5 mm/a and therefore no direct recharge from precipitation can be expected in these areas (Rojas and Dassargues 2007). Nevertheless, with increasing altitude also precipitation amounts increase continuously reaching an average of ~130 mm/a in the nearby Altiplano at ~4000 m asl (Lictevout et al. 2013; PUC 2009). In the broader area of work mainly ephemeral streams (Quebradas) guide runoff from the Precordillera and Altiplano towards the PdT.
Several studies were able to show that during the last 20 ka groundwater high stands in the Atacama Desert can be correlated with the Central Andean Pluvial Event (18–8 ka BP), during which exceptionally high precipitation amounts fell in the Altiplano (Gayo et al. 2012b; Gayo et al. 2012a; Betancourt 2000; Rech et al. 2002). Around Pica, mapped and age-dated ancient wetland assemblages indicate that a major groundwater recharge event took place between 12.5 and 8.8 ka BP (Blanco and Landino 2012; Blanco and Tomlinson 2013). Lithologically speaking from Jurassic to Quaternary the area of work is dominated by alternating strata of thick continental sedimentary rocks, such as conglomerates and sandstones, and minor horizons of felsic volcanic rocks (i.e. ignimbrites; Table 3.1). Cretaceous to Eocene plutonic rocks intrude sections of the Mesozoic basement (Blanco and Landino 2012).

Table 3.1 Overview to stratigraphic and lithologic units (modified after Blanco and Landino 2012)

Era	Period	Formation (Fm)		Lithology	Hydraulic properties	Thickness in seismic profile
Cenozoic	Quaternary	PlHa / Ha		Alluvial deposits		0-350 m
	Pliocene	MPg		Piedmont deposits, gravels and sands of alluvial origin	not discussed	
	Miocene	angular discordance				
		Mmd "El Diablo Fm"		Clastic unit of conglomerates and sandstones of alluvial origin	not discussed	
		Miih		Huasco Ignimbrite	generally aquitard, if not fractured and/or weathered like in the recharge area	~30 m
		angular discordance				
		OMap2a		Sandstones	unknown	0-200 m
		OMap2c		Poorly sorted conglomerates	unknown	
		Miit		Tambillo Ignimbrite	generally aquitard, if not fractured and/or weathered like in the recharge area	~30 m
	Oligocene	OMap1a		Poorly sorted sandstones	unknown	0-250 m
		OMap1c		Cemented conglomerates	permeable due to fracturing	
		angular discordance				
Mesozoic	Eocene		Intrusive formations			Not present
	Paleocene					
	Cretaceous	Ksce "Cerro Empexa Fm"		Unit of volcanic (andesite and ignimbrite) and continental clastic sedimentary rocks	aquitard, apart from eventually local developed fracture zones	?
		angular discordance				
	Jurassic	Jurassic Basement		Marine carbonatic clay- and siltstone	Regional aquitard	?

There are two lithologic profiles that are being used in this study to correlate reflection seismic data with geological field observations. Table 3.2 shows a lithologic profile of the Concova well (218 m below ground level (bgl)) situated at the eastern margin of Pica. In Table 3.3 the stratigraphy of a ~515 m outcrop is displayed. It is located 4 km south of the seismic line at an altitude of ~2200 m asl (locations displayed in Figure 3.2 and Figure 3.3).

Table 3.2 Lithologic profile and remarks for the Concova well WC (situated approximately 40m up-gradient from the similar named Concova spring, altitude 1430m asl; Figure 3.3) (data according to well report ND-0103-937)

Depth of bottom of lithological layer [m bgl]	**Lithological layer thickness [m]**	**Lithology**	**Unit**	**Well construction**	**Remarks according to well report**
46	46	Fine sands partly silty	Quaternary	Full casing	Resulting hydraulic head at ~38 m bgl
56	10	Sandstone	OMap2a/c	Open borehole	Dry
86	30	Ignimbrites	Miit		Dry
178	92	Clayey and silty conglomerates	OMap1c		First water guiding fractures at 115 m bgl, thickness ~6m (confined/leaky aquifer)
190	12	Volcanic rocks			Dry
218	End of drilling at 218 m bgl	Poorly sorted conglomerates			Water at 208 m, thickness ~2m (confined/leaky aquifer)

Table 3.3 Stratigraphy of an outcrop (UTM: 481366.49 m E, 7733504.04 m S, ~2200 m asl)

Depth of bottom of lithological layer [m bgl]	**Lithological layer thickness [m]**	**Unit**	**Remarks**
290	290	≤Middle Miocene	All units are dry
320	30	Miih	
515	195	OMap2a/c	
?	~30	Miit	

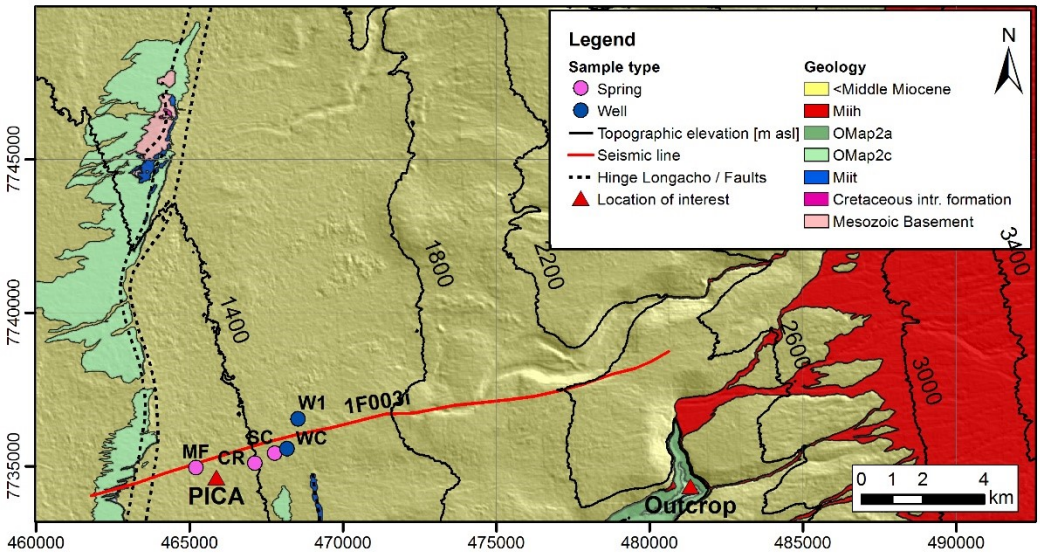

Figure 3.3 Geological map of the surroundings of seismic line 1F003i (outcrop lithology is reported in Table 3.3). Abbreviations: MF: Miraflores, CR: Cocha Resbaladero, SC: Concova Spring, WC: Concova Well, W1: Well 1

3.3. Methodology

3.3.1. Tectonic and geological interpretation of a 2D seismic line

A reflection seismic line is used to derive the local tectonic and stratigraphic setting in the transition zone between the Precordillera and the PdT. The seismic line 1f003i was given by Empresa Nacional de Petróleo, Chile (ENAP), to the Centro de Investigación y Desarrollo en Recursos Hídricos (CIDERH). The seismic data are presented in segy-format, processed and time-to-depth converted. The data originate from an internal survey carried out during 1986. Data of the same dataset have been published by Nester (2008). Nester used the data to evaluate the broader geologic and tectonic development of the PdT basin. However, the seismic data used here are so far unpublished.

Processing steps

All processing and geological interpretation was done with a full academic license of the DGB OpendTect software suite. To enhance the mapping of geologic

units, seismic data were analyzed by using an unsupervised neural network module, scanning for clusters consisting of the following data attributes: Q-factor, Energy, Laplace, Amplitude variance, Amplitude average, Frequency, Similarity, Polar dip, Curvature and others. Best results for horizon tracking were achieved by the application of the steering algorithm in combination with the related dip-steered median filter. Fault detection has been carried out manually supported by a supervised neural network module, which helped in an iterative process to identify fault zones of increased fault likelihood. The supervised neural network was trained with the following fault sensitive criteria: S/N Ratio, Stability of Steering, Average Frequency, Signal, Noise, TWT, Curvature and Similarity.

Correlation of seismic sequences with regional and local geology

Nester (2008) established a useful seismic reflection characterization of the dataset and related it to lithologic and stratigraphic units. In this study, the same reflector characterization is used. However, it is adjusted to conditions at the transition from the PdT to the Precordillera and updated by the new stratigraphic unit nomenclature introduced by recently published geological maps (Table 3.4). Intrusive formations in the Mesozoic Basement where derived by the detection of attribute discontinuities within the unit. For lithologic correlation, a stratigraphic profile of a deep well (WC well, Table 3.2) and surface outcrops of relevant strata are being used (). Additionally, recently published geological maps by SERNAGEOMIN helped to relate surface and subsurface geology (Blanco and Tomlinson 2013; Blanco et al. 2012; Blanco and Landino 2012; Gardeweg and Sellés 2013). Stratigraphic matches between seismic imagery and the well profile or surface geology were of good accordance.

Table 3.4 Reflection characteristics associated with seismic sequences, seismic boundaries and corresponding stratigraphic units (modified after Nester, 2008). Sequence I, as defined by Nester 2008, is not present in the given seismic profile.

Seismic sequence	Reflection character	Sequence boundary	Interpreted unit	Age
V	Low to medium amplitudes, appears dominantly transparent	-	-	≤ Middle Miocene
-	Inclined reflection with medium to high reflectivity	d	Top Miih	
IV	Inclined reflection with medium to high reflectivity, occasionally interrupted	-	Miih	Early Miocene (~16.2 Ma)
-	Medium to high amplitude reflection with medium to high continuity	c	Top of OMap2a/c	
III	Low to medium amplitude, semi-continuous. Reflections generally parallel to sequence boundary 'b', with noticeable onlap onto 'b'	-	OMap2a/c	Early Miocene
-	~30 m thick high amplitude and high continuity reflection, reflectivity weakens towards east	b	Miit	Early Miocene (~19.8 Ma)
II	continuous reflections with high reflectivity at top, appears transparent towards bottom	-	OMap1a/c	Late Oligocene
-	Reflection with highly variable amplitude which dominantly appears transparent. Locally marking discordance to sequence '0'	a		
0	Highly variable, often medium amplitude, medium frequency, semi-continuous to continuous reflection. Reflections often appear chaotic to transparent.	-	Mesozoic "basement"	>~40 Ma

3.3.2. Hydrochemical analysis

Groundwater samples and geothermal gradient recording

The in-situ measurement of the fluid temperature over depth was recorded at Chacarillas well (PC; Figure 3.2) by a temperature probe head connected to a 500-m-winch. The well is an outlying observation well and not affected by water production. All chemical and isotopic data were given by Compañía Minera Doña Inés de Collahuasi (CMDIC) to CIDERH. These data originate from a company internal study (CMDIC 2012).

Mean groundwater residence-times correction based on the ^{14}C isotope

For determining the relevant chemical processes that alter the carbon chemistry (and hence the ^{14}C concentration) of given water samples, a graphical methodology is applied (Han et al. 2012). Following well defined guidelines, the interpretation of three carbon related plots ($\delta^{13}C$ against 1/[DIC], ^{14}C against 1/[DIC] and ^{14}C against $\delta^{13}C$) allows making a substantiated decision on choosing an accurate correction model (Han et al. 2012; Han and Plummer 2016). In the given case, all relevant water samples show a pH of ~8 (Table 3.5). This means that the reciprocal of [DIC] is equivalent to the reciprocal of [HCO_3], which was applied here (Clark and Fritz 1999).

Table 3.5 Chemical groundwater composition and geothermometer-derived reservoir temperatures (Tr = Reservoir Temperature, gt. = geothermometer)

Parameter	**Site**					
	SC	**W1**	**CR**	**MF**	**SPN**	**SE**
Sample date	2/13/11	2/9/11	2/9/2011	2/9/2011	2/11/2011	5/12/2011
Altitude [m asl]	1435	1488	1387	1392	1190	3789
Type	Spring	Well	Spring	Spring	Spring	Spring
***T* [°C]**	31.9	32.7	32.2	31.4	25.0	14.4
Na-Li gt [°C]	48	56	50	52	-	-
Error Na-Li gt [°C]	± 12	± 12	± 12	± 12	-	-
Mg-Li gt [°C]	58	64	55	53	-	-
Crist. gt. [°C]	43	40	42	43	-	-
Chalc. gt. [°C]	62	59	61	62	-	-
Av. Tr [°C]	54	57	52	53	-	-
pH	8	8.3	8.1	8.4	8.8	8.4
Elec. cond. [µS/cm]	319	318	323	336	594	567
Ca [mg/l]	18.4	17.6	18.1	20.1	6.22	-
Mg [mg/l]	0.14	0.1	0.21	0.28	0.14	-
Na [mg/l]	43.6	41.3	45.6	44.7	118	-
K [mg/l]	<2	<2	<2	<2	3.8	-
Cl [mg/l]	35.7	23.4	30.6	35.7	74.4	-
SO_4 [mg/l]	35	36	39	85	80	-
HCO_3 [mg/l]	87.8	91.4	92.7	90.2	93.9	-
Li [mg/l]	0.025	0.028	0.027	0.028	-	-
SiO_2 [mg/l]	41	38	40	41	-	-

The graphical methodology allows identifying processes such as dissolution of carbonates, oxidation of fossil organic matter, methanogenesis, ion exchange and isotope exchange altering the carbon chemistry, carbonate precipitation, dedolomitization, weathering of silicates, loss of CO2 gas and/or the influence of other CO2 sources (such as volcanic) (Han et al. 2012).

Geological thermometers

Four approved geothermometers for low temperature reservoirs are applied; Mg-Li, Na-Li and the Si-thermometers for alpha-cristobalite and chalcedony.
The Mg-Li-thermometer is appropriate for sedimentary basins. It is defined as (Kharaka and Mariner 1989):

$$T = \frac{1000}{0.389\ (\pm 0.11) + \log\left(\frac{\mathrm{Na}}{\mathrm{Li}}\right)} - 273.15 \qquad \text{Eq. 3-1}$$

T is given in °C and Mg and Li concentrations in mg/l. A Na-Li-thermometer is best used for low-temperature reservoirs consisting of sedimentary- and volcanic-hosted reservoirs (Nicholson 2012). From the here applied geothermometer it is the only one for which error margins can be calculated (Verma et al. 2008). For waters with Cl concentrations <0.3 mol/kg (accomplished in the area of work) it is defined as follows (Fouillac and Michard 1981):

$$T = \frac{1000}{0.389\ (\pm 0.11) + \log\left(\frac{\mathrm{Na}}{\mathrm{Li}}\right)} - 273.15 \qquad \text{Eq. 3-2}$$

T is given in °C and Na and Li concentrations in mmol/l.

The two applied silica-thermometers for alpha-cristobalite (3) and chalcedony (4) are defined as (Fournier 1977):

$$T = \frac{1000}{4.78 - (\log SiO_2)} - 273.15 \qquad \text{Eq. 3-3}$$

$$T = \frac{1032}{4.69 - (\log SiO_2)} - 273.15 \qquad \text{Eq. 3-4}$$

T is given in °C and SiO2 concentrations in ppm. Alpha-cristobalite is a Si-variation that is present in felsic volcanic rocks and volcanic ashes (Deer et al. 2004; Damby et al. 2014). In the study area, silica rich volcanic rocks such as ignimbrites and rhyolites are abundant and build the parent rock material for most of sedimentary rocks younger than Cretaceous (Blanco and Tomlinson 2013). Because alpha-cristobalite shows a higher solubility than chalcedony, it should be the main source of solute silica when present. As a means of reference also the reservoir temperature according to equation 4 is calculated.

3.3.3. Interpretation of hydrological time series data

To correlate given hydrologic time series the following methodology is applied: Based on linear regression the cross correlation function between a predictor (first time series) and a predictand (second time series) is computed for various lags (one-tailed significance testing with a confidence limit of 95%) (Burn and Hag Elnur 2002; Lee and Lee 2000; McCuen 2003; USGS 2014). This method is commonly applied for the time dependent linear correlation of hydrologic time series data. Effectively it allows inferring the maximum positive correlation between two time series by calculating the cross correlation coefficient (Cc) along a preset number of lags (time steps). To calculate the cross correlation function both time series need to be presented in equal time steps (in this case monthly). This is why, for the respective procedure, the water level and discharge time series needed to be interpolated. For interpolation, an Akima Spline is applied (USGS 2014; Akima 1978). For the correlation of rainfall data and spring

discharge at SE additionally the SE time series is detrended (linear fit) to delete superimposing long-term trends. Another method applied is the cumulative rainfall departure (crd) which is a concept based on water-balance principles that quantifies relative precipitation patterns (Weber and Stewart 2004). The crd-concept was thoroughly discussed by Weber and Stewart (2004). Although its application is critical for periods of decades, in the given context, when looking at periods of 12-14 years, it is suitable (Weber and Stewart 2004).

Overall the procedure was to compare (1) the crd at meteorological station Collacagua (CC; Figure 3.2) with detrended spring discharge at spring SE, (2) crd with water levels at well WPN, (3) discharge at SE with water levels at WPN, and (4) spring discharge at SE with water levels at well WC.

Relevant datasets are needed in full year length. Time series for discharge amounts at SE are available for the period October 1998 to October 2012 (monthly to bimonthly measurements). Water level records at well WPN are available for the period 2001-2014 (measurements every 2-3 month). Rainfall data are presented for the periods 1999-2014 (monthly). Well WC was destroyed during an earthquake in July 2005 which is why representative data are only available for the period 2001 to 2005 (measurements every 2-3 month). The Concova observation well WC is situated approximately 40 m up-gradient (~1475 m asl) from the similar named Concova spring, at the far eastern margin of the town of Pica. Both, well water and spring water show a temperature of ~32 °C, an electrical conductivity of 320 µS/cm and a $\delta^{18}O$ values of -13 ‰ (Magaritz et al. 1989; Uribe et al. 2015). The well penetrates the confined fractured aquifer that feeds the geothermally influenced spring system of Pica. Stratigraphy and construction details are given in Table 3.2. Due to its location upstream the town of Pica, the influences of groundwater production on the water level in the well can be neglected.

The second well, WPN (~1190m asl), is situated 10 km south of Pica at Puquio Nunez. Apart from total depth (52 m bgl), the construction details of this well are unknown. However, it is likewise alimented by groundwater of the Precordilleran area (Fritz et al. 1981; Magaritz et al. 1989). As mentioned earlier, the area around Puquio Nunez is practically deserted. Influence of water production on the water table can be disregarded. All relevant data are public and were retrieved from the ODEA website (ODEA 2016).

3.4. Results

3.4.1. Analysis and Interpretation of a 2D reflection seismic profile

The reflection seismic line used in this study starts several kilometers east of Pica uphill and ends in Pica, above the hinge Flexura Longacho (Figure 3.2). The starting point is at an altitude of ~2400 m asl. Tectonic and stratigraphic interpretation allows identifying units that contribute to groundwater flow towards Pica.

Stratigraphically speaking the profile can be divided into six main units (Figure 3.4a, b). These are the Mesozoic basement, followed by unit 'OMap1a/c' representing the Oligocene, overlain by the Tambillo ignimbrite 'Miit'. Early Miocene units belong to the 'OMap2a/c' Formation, which in turn are overlain by the Huasco Ignimbrite 'Miih'. All subsequent strata are being classified as earlier than middle Miocene, i.e. '≤Middle Miocene'. The units that correspond to '≤Middle Miocene' contain the 'El Diablo' Formation 'Mmd', the piedmont deposits 'MPg', and Quaternary sediments termed 'PlHa' and 'Ha'. Related reflection characteristics used for interpretation are displayed in Table 3.4.

All units older than middle Miocene show significant faulting and/or folding due to the ongoing Altiplano Plateau uplift (~1200 m uplift since Neogene) (Jordan et al. 2010; Allmendinger et al. 1997). Faults are typically north-south striking and show both west-vergent and east-vergent normal and reverse faults, while reverse faults dominate (Nester 2008).

Noteworthy is also the huge hinge "Flexura Longacho" (Figure 3.2, Figure 3.4) which is of regional scale and extends over at least 60 km in the north-south direction through the whole area of work. At small sections along the hinge (i.e. Cerro Longacho) impermeable Mesozoic basement crops out while at other parts the bedrock dips deeper into the underground (Blanco and Tomlinson 2013; Blanco and Landino 2012; DGA 2013). In the following, Figure 3.4a and b are discussed, from east to west.

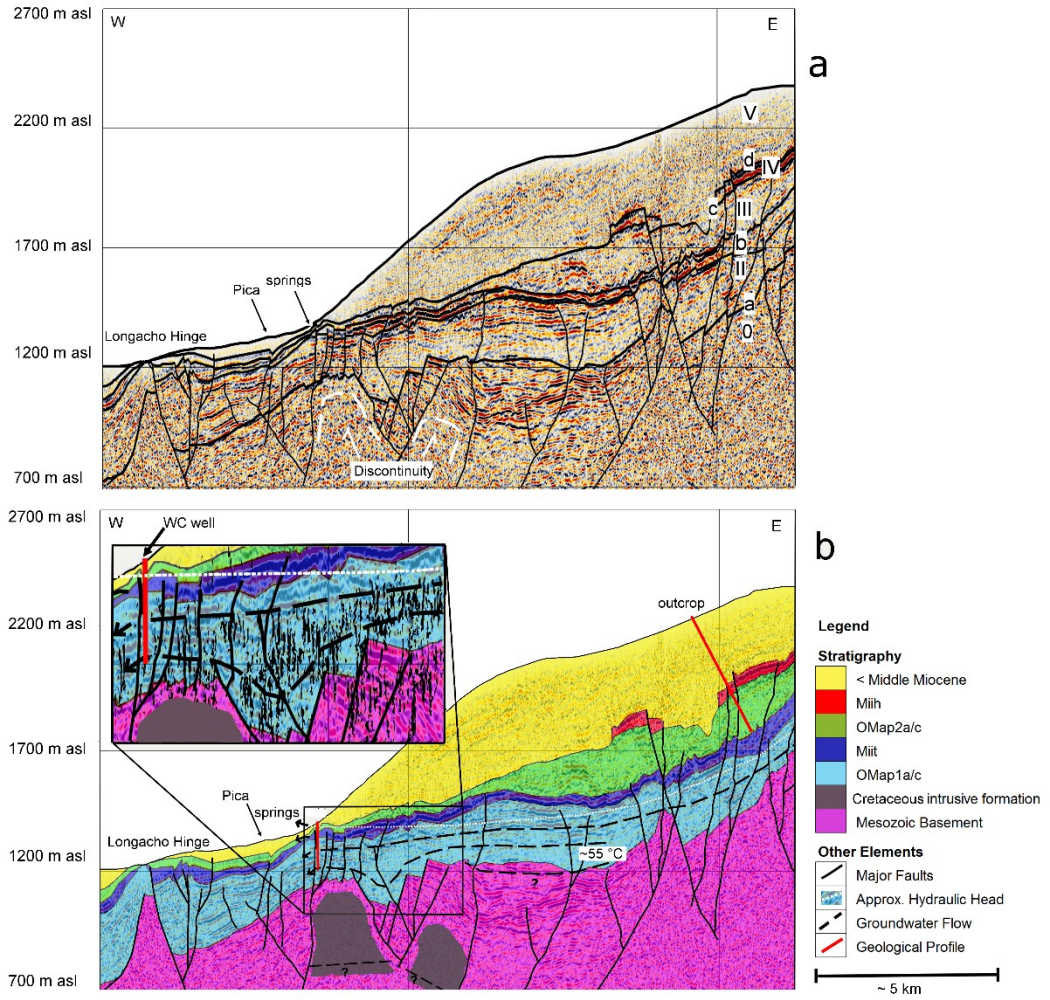

Figure 3.4 **(a)** Seismic line 1f003i with sequence boundary, reflector designation and major faults, **(b)** Interpreted seismic line 1f003i.

Groundwater flow will primarily occur in the well-fractured parts of the OMap1a/c Formation. Temperatures at the deepest infiltration point in the OMap1c Formation will reach approx. 55°C. The detail window in (b) shows computed fault likelihood >95% in black (Misclassification error ≤5%). The older member of OMap1a/c shows distinct zones of increased fracturing compared to surrounding formations and will form the main reservoir.

Mesozoic Basement

The Cretaceous Cerro Empexa Formation ('Ksce') builds generally the top of the Mesozoic basement (Table 3.1). It abuts upon the OMap1a/c formation by an angular unconformity in the mid-section of the profile (along sequence boundary a; Figure 3.4a). In parts, the 'Ksce' Formation might be eroded giving way to Jurassic units or Cretaceous intrusive rocks. Because 'Ksce' cannot be clearly differentiated in the seismic profile against older units, it is included in the layer Mesozoic basement in Figure 3.4b.

About 10 km north of Pica, the Mesozoic basement crops out at Cerro Longacho with the Jurassic Longacho Formation. Here the formation is penetrated by Cretaceous granitic intrusions (Figure 3.3; (Blanco and Landino 2012)). Discontinuities in the respective seismic data show that east of Pica, subsurface, also plutonic intrusions (of probably Late Cretaceous age) penetrate and deform parts of the Mesozoic Basement (Figure 3.4b). Similar intrusions are also exposed 50 km north of Pica at the Andean slope (Blanco and Landino 2012). Apart from locally fractured zones, the unit 'Ksce' can be considered to be an aquitard (Jayne et al. 2016). The Jurassic Basement forms a regional aquitard (marine claystone and siltstone; Table 3.1). The data show that fissures that would connect the area displayed with the Altiplano plateau would need to be several kilometers deep.

Formation OMap1a/c - Aquifer

Formation OMap1a/c grows in extent towards the midsection of the profile (starting east) until a maximum thickness of ~250 m and dips west of the hinge Longacho into the PdT basin.

OMap1a Formation is younger than 1c. It represents coarse to medium sandstones and is not present at outcrops around the Pica area (Blanco and Tomlinson 2013). Unit OMap1c consists of poorly sorted conglomerates which are cemented and partly intercalated by rhyolitic ignimbrites (Blanco and Tomlinson 2013). Seismic analysis shows that the unit is notably fractured in the transition zone from the PdT to the Precordillera. Apparently, this is due to the Altiplano Plateau uplift. Another crucial factor for fracturing in the area close to Pica, are intrusive formations that created massive faults and disruptions in sections of the Mesozoic basement while ascending. These faults seem to have contributed under former tectonic stress conditions to a reduced stability of the OMap1a/c formation and hence lead to partly diffuse, partly vertical fracturing, which makes spring discharge possible.

The unit OMap1a/c forms therefore the fractured aquifer that feeds spring water in Pica. Although south of Pica superficially exposed outcrops of this formation at higher altitudes (~1480 m asl) are dry, water will be present in the deeper second half of the unit and flow upwards along preferential pathways of connected fracture networks (see also section 3.4.6). Commonly, fractured aquifers are best developed at the midsection of fractured zones (Ahmed et al.

2011). Because of this, it is expected that exceptionally deep fractures will not contribute significantly to the overall groundwater flow.

At the altitude of the Concova well (1475 m asl), water is first reached at a depth of ~115 m bgl and later at ~208 m bgl (DGA 1997). Its hydraulic head lies here at an altitude of approx. 1437 m asl. A few hundred meters downslope, in Pica, this increased hydraulic head leads to spring discharge. The seismic data show that around Pica several vertical deep faults lead from OMap1c through formation Miit and partly to OMap2a/c. Springs in Pica typically discharge out of exposed and fractured sections of the sandstone member of OMap2a/c.

OMap1c Formation also forms the main geothermal reservoir. The deepest point of infiltration is reached at the midsection of the profile with an aquifer depth of about ~850 m bgl. At the deepest circulation depth, around 8 km from the eastern margin of the profile, the main heating up of groundwater will occur (Figure 3.4b).

Based on a supervised neural network (section 3.3.1) the fault likelihood in a search gate of 30-120 m is computed, to distinguish highly fractured zones from less fractured zones (Figure 3.4b). The computation allows us to delineate a highly fractured zone of the aquifer section to the east of Pica at a depth of 400-500 m bgl. It is possible that some groundwater circulates here to a maximal depth of ~500 m bgl.

Tambillo Ignimbrite and Huasco Ignimbrite

The Tambillo Ignimbrite (Miit) extends over the whole profile. Its average thickness is ~30 m. It shows a clear and accentuated sequence boundary reflection (sequence boundary b, Figure 3.4a) indicating no major erosion apart from the eastern margin from where it begins to rise steeply towards the Altos de Pica area. The less pronounced reflection is an indication for a higher grade of weathering and hence permeability. The top of Miit at the outcrop position (red line in Figure 3.4b, see also Table 3.3) is dry. Groundwater flow on top of this unit, from the Altos de Pica area towards Pica, can therefore be disregarded.

The Huasco Ignimbrite (Miih) starts at the eastern margin arriving from the Altos de Pica and Altos del Huasco recharge area where it is exposed (Figure 3.3). The formation thins out only 3 km west of the eastern margin where it seems to be somewhat eroded or broken apart. Similar formations can be observed at a

nearby ground opening of up to ~500 m at Quebrada Quisma (termed 'Outcrop' in Figure 3.3). Ephemeral flood erosion of weak Miocene epiclastic strata beneath the strong welded tuff is a promoted reason for this observation (Irwin et al. 2014). Another explanation could be groundwater sapping (Hoke et al. 2004).
At Altos the Pica, the Miih Formation is underlain by the Miit Formation which abuts the Ksce Formation (Blanco and Tomlinson 2013) (the formations OMap1a/c and OMap 2a/c die out on the way uphill). Highly weathered outcrops of the Miih ignimbrite at Altos de Pica show that these formations tend to break into banked and highly fractured units (fractures in cm-scale). At altitudes >3400 m temperatures usually fall during night below 0 °C and rise again during the day above freezing temperatures, which accelerates the weathering process favored by frost wedging. Thus, fractures in ignimbrites will facilitate water infiltration and allow groundwater to circulate downslope towards the OMap1a/c formation.

Formation OMap2a/c

Just like unit Miit, OMap2a/c extends over the whole profile. It almost dies out at the altitude of the Concova well and later crops out at the hinge Flexura Longacho. Maximum thickness is approx. 200 m. The formation is much less fractured than OMap1a/c and should demonstrate a lower permeability. Typically OMap2a consists of sandstones and conglomerates (Blanco and Tomlinson 2013).

3.4.2. Reservoir temperature estimation using geothermometers

Analysis of geothermally sensitive ions of four groundwater samples allowed calculations of the expected geothermal reservoir temperature (samples SC, W1, CR and MF; Figure 3.3 and Table 3.5). Because well sample W1 shows an almost identical chemical composition to the water from the springs CR, MF and SC (Table 3.5), it can be assumed that these groundwaters are not being significantly influenced by near surface reactions. Groundwater mixing with surface waters is also unlikely due to the proven absence of influence of modern waters (section

3.4.5). Four geothermometers for low-temperature reservoirs are being used, to estimate the reservoir temperature (see section 3.3.2).

Discharge temperatures at Pica lie between 31 and 34 °C. Applying the respective geothermometers to all four samples yields similar estimations for the reservoir temperature. While the Mg-Li-thermometer plots reservoir temperatures of 53-64 °C, the Na-Li-thermometer indicates temperatures of 48-56 (±12) °C. At the same time the alpha-cristobalite thermometer indicates temperatures of 40-43 °C and the chalcedony thermometer values of 59-62 °C. It is assumed that the alpha-cristobalite geothermometer is more reliable (chapter 'Geological thermometers'). At the same time, due to slow water cooling along the flow path (section 3.4.1), parts of the solute silica might already precipitate prior to discharge which can result in underestimation of the reservoir temperature based on the respective saturation index (SI) thermometer.

By calculating average reservoir temperatures for each sample from all applied geothermometers, the maximal reservoir temperature of the Pica springs is estimated. It lies between approx. 53 and 57 °C.

3.4.3. Local geothermal gradient

The Chacarillas well was utilized to infer the local thermal gradient by recording the well fluid temperature vs. depth (total well depth 880 m bgl, situated 20 km south of Pica at a similar altitude of 1280 m asl). The well penetrates only sedimentary rocks interbedded with minor strata of horizontally deposited volcanic rocks until reaching basement rocks at a depth of 880 m bgl (Karzulovic 1980). Because of equipment restrictions the maximum logging depth is 500 m bgl. Logging started with the water level of 65 m bgl at 29 °C and reached 42.6 °C at the end of logging at 500 m bgl (Figure 3.5). The measurement shows that the gradient steadily rises by ~3.1 °C per 100 m.

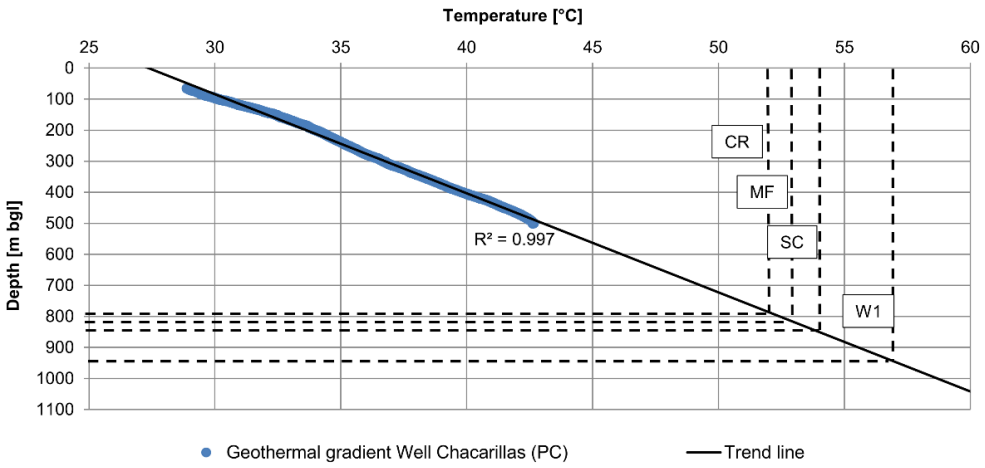

Figure 3.5 Geothermal gradient recorded at the Chacarillas well (PC) together with estimated reservoir temperatures from geothermometers

This is very close to the global average of 3 °C per 100 m and indicates that within the first 500 m bgl there is no evidence for an anomalous heat accumulation in the area.

Plotting the linear trend line of the gradient backward to the ground surface, results in a surface temperature of ~27.4 °C. Plotting it forward, towards a subsurface temperature of 53-57 °C (as predicted by geothermometers; section 3.4.2), results in a circulation depth of ~800-950 m bgl (Figure 3.5). However, due to the confined nature of the aquifer a slight heat accumulation in the slope reservoir cannot be excluded. Also, advective heat transport could alter the temperature gradient at that depth. Such effects would lead to an overestimation of the calculated maximal circulation depth, meaning that the true maximum circulation depth would more likely lie at the upper margin of the given interval.

3.4.5. Isotope hydrology

Stable und unstable isotopes

Isotope data are given in Figure 3.6 and Table 3.6. ^{14}C measurements of Pica waters uninfluenced by irrigation show percent modern carbon (pmC) values of 27-33 and tritium (^{3}H) values of ≤0.09 (±0.09) TU, which emphasizes that

groundwaters are chemically not influenced by modern rainfall. ^{3}H values of regional precipitation vary between 3 to 10 TU (Aravena et al. 1999).

The detected $\delta^{18}O$ values at the spring Ermitano (SE; Figure 3.2), which discharges from formation Miih at the western margin of the Salar del Huasco basin, is -12.4 ‰. In Pica, values between -13.0 ‰ and -13.4 ‰ were measured (Figure 3.6). According to the isotopic altitude effect documented by Uribe et al. (2015) (which is in accordance with Aravena et al. (1999)), the mean recharge altitude for Pica waters is ~3800 m asl. Deuterium excess (D_{ex}) is -1.2–0.5 ‰ for groundwater in Pica and 1.14 ‰ for SE, i.e. both cases within a similar range, which supports the concept of similar recharge conditions (recharge areas Altos de Pica and Altos del Huasco, Figure 3.2). At SE the ^{3}Hvalue is likewise ≤0.09 (±0.09) TU, which implies that there is no noteworthy presence of modern water in this spring discharge either.

Groundwater at PN shows a ^{14}C activity of 34 pmC, demonstrating a very similar value when compared to waters from the Pica area. Also ^{3}H counts equally, below 0.09 (±0.09) TU. Only $\delta^{18}O$ is slightly less depleted with -11.0 ‰, reflecting the topographically less pronounced altitude of the expected recharge area of in average ±3600m asl. $\delta^{13}C$ for waters in the Pica and PN area lies in a range of -7.7 to -11.7 ‰VPDB.

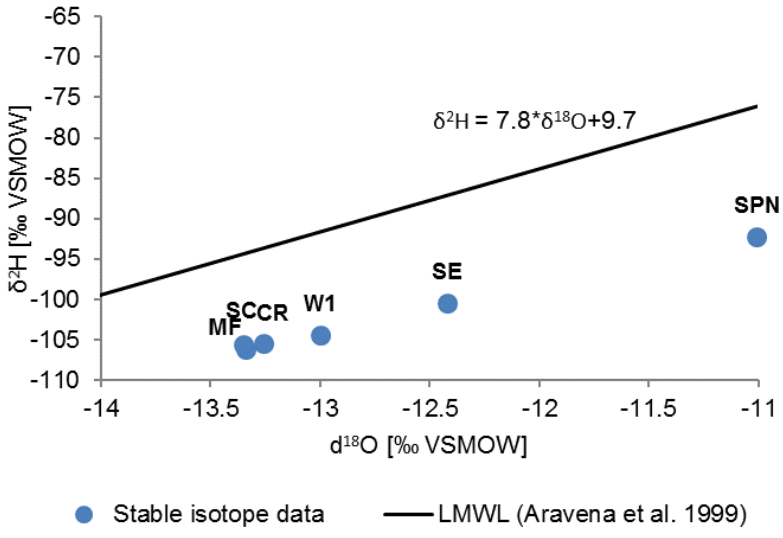

Figure 3.6 Stable isotope data plotted with the local meteoric water line (LMWL)

Table 3.6 Isotope data, mean residence times and resulting interstitial velocities (*VSMOW, **VPDB, RT= residence time, cRT = corrected residence time)

Parameter	**Site**					
	SE	SC	SPN	W1	CR	MF
δ^2H [‰*]	-100.5	-106.2	-92.3	-104.5	-105.4	-105.6
$\delta^{18}O$ [‰*]	-12.42	-13.34	-11.01	-13	-13.26	-13.35
D_{ex} [‰]	1.1	-0.5	4.2	0.5	-0.7	-1.2
^3H [TU]	≤0.09	-	≤0.09	≤0.09	-	≤0.09
^3H error	0.09	-	0.09	0.09	-	0.09
$\delta^{13}C$ [‰]**	-	-8.8	-11.7	-10.4	-9.6	-7.7
^{14}C [pmC]	-	29.05	33.9	27.23	32.05	27.67
pmC error	-	0.17	0.16	0.16	0.15	0.13
RT [a BP]	-	10219	8943	10754	9407	10620
rF&G cRT [a BP]						
-20‰ $\delta^{13}C$ soil gas CO_2	-	2757	4250	4913	2792	1905
-23‰ $\delta^{13}C$ soil gas CO_2	-	1512	3049	3657	1546	662
Av. cRT [a BP]	-	2135	3650	4285	2169	1284
Int. vel. [m/a]	-	13.1	8.8	6.5	12.9	21.8

Correction of mean groundwater residence times

In the Altos de Pica recharge area, ignimbrites are abundant, followed downstream by clastic sediments of primarily volcanic rocks, intercalated by rhyolite or tuffs and thick strata of poorly to good sorted conglomerates with clayey and silty portions. To gain insight into the processes that alter the carbon content of the respective groundwater during its evolution, a graphical methodology is applied (Han et al. 2012; Han and Plummer 2016). Three carbon related plots, of $\delta^{13}C$ against $1/[HCO_3]$ (Figure 3.7a), ^{14}C against $1/[HCO_3]$ (Figure 3.7b), and ^{14}C against $\delta^{13}C$ (Figure 3.7c) summarize the relevant carbon hydrochemistry and allow to infer hydrochemical processes that influence the ^{14}C value (Han et al. 2012). Hereafter, the framework by which the Figure 3.7 graphs were generated for the carbon system is explained.

In the area of work at sites with vegetation, $\delta^{13}C$ values of soil gas CO_2 are -18±2 ‰ (Fritz et al. 1981). Due to the higher humidity at the expected Precordilleran recharge area (Altos de Pica) the lower margin of this value is applied, namely -20 ‰. $\delta^{13}C$ of carbonate minerals is unknown but is usually close to 0 ‰ (Fritz et al. 1981; Clark and Fritz 1999).

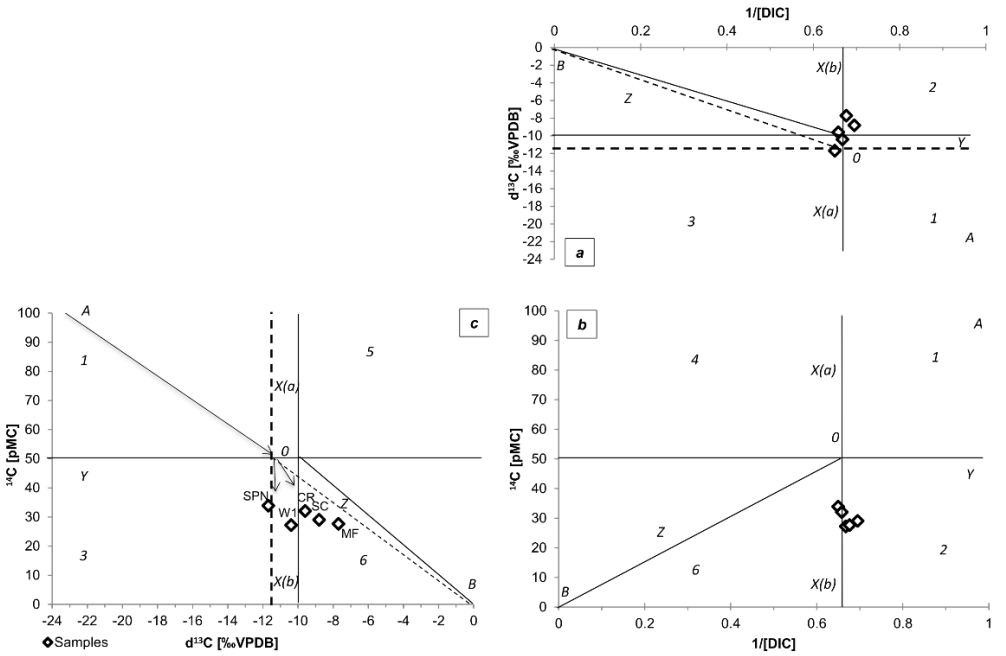

Figure 3.7 Graphical evaluation of carbon chemistry according to Han et al. (2012) (italic numbers mark plot sections): **(a)** samples plot around point *0* and line *X(b),* **(b)** samples plot along line *X(b),* **(c)** samples plot in section 6. Black arrows indicate the sample evolution for an initial value of $\delta^{13}C$ of soil gas CO_2 of -23 ‰

In general the plots can be read in the following way (Han et al. 2012): At point *A* the groundwater contains only CO_2 equilibrated with $\delta^{13}C$ of soil gas CO_2 (open system conditions). The point *0* (crossing point) marks the conditions under which biogenic (soil) CO_2 has reacted completely with rock carbonate under closed system conditions (calcite dissolution). At point *B*, the DIC in water is enriched in $\delta^{13}C$ by the $\delta^{13}C$ of carbonate rocks and/or has a very low ^{14}C activity. Samples that plot in Figure 3.7a around the point *0* and in Figure 3.7b and 7c along line *X(b)* underwent ^{14}C decay, because closed system conditions are reached and no further carbon was added or removed from the water and the ^{14}C activity reduced below 50 pmC. Samples that plot along line *X(b)* in Figure 3.7a and 7b and along line *Z* in Figure 3.7c, experience an isotope exchange between water and rock carbonate. This is because no carbon is added to the system but $\delta^{13}C$ is enriching. Therefore, the ^{14}C content is altered. In Figure 3.7 the position of samples from Pica mark a mixture of the three mentioned processes (calcite dissolution, isotope exchange and ^{14}C decay).

However, sample SPN demonstrates relatively depleted $\delta^{13}C$ contents (-11.7 ‰). In Figure 3.7c the sample plots left of the continuous line *X(b)* which marks, as defined, half of the determined initial $\delta^{13}C$ of soil gas CO_2 (-10 ‰). This would

imply that the sample is exposed to open system conditions (Han and Plummer 2016). Due to the known general aquifer geometry, this is very unlikely. A more suitable explanation is that the initial $\delta^{13}C$ of soil gas CO_2 is underestimated and would rather lie in a range of round about -23 ‰ $\delta^{13}C$ (resulting configuration changes marked in Figure 3.7 by dashed lines). This value is (like also -20 ‰) in accordance with CAM-plants that typically occur in semi-arid environments (Clark and Fritz 1999). SPN would then experience the same chemical processes as samples from Pica despite isotope exchange.

Based on the graphical analysis, other carbon altering processes, such as additional CO_2 sources, can be disregarded (Han et al. 2012), especially when considering the overall geological setting. In conclusion, the initial $\delta^{13}C$ of soil gas CO_2 lies most probably in a range between -20 and -23 ‰. For the given samples and the given processes observed (calcite dissolution under closed system conditions, isotope exchange and ^{14}C decay) there is only one ^{14}C single-sample-based correction model that accounts fully for the effects induced. This is the revised Fontes & Garnier (rF&G) model (Fontes and Garnier 1979; Han and Plummer 2013; Han and Plummer 2016). Subsequently the rF&G model is used for correcting mean groundwater residence times within the margins of -20 to -23 ‰ $\delta^{13}C$ soil gas CO_2.

Uncorrected residence times plot between 8900 and 10800 a BP (Tab 5). The averages of corrected mean groundwater residence times (cRT) for the spring related Pica samples CR and SC are in both cases ~2150 a BP (Tab 4). The well related sample W1, from the respective aquifer section, shows a cRT of ~4280 a BP. cRT at SPN accounts for ~3650 a BP. The youngest water was sampled at spring MF with ~1284 a BP.

3.4.6. Hydraulic properties

Average interstitial velocities and hydraulic conductivity estimation

Under the assumption that the corrected residence times are accurate, waters recharged at Altos de Pica (linear distance from an altitude of 3800m asl to Pica: ~28km; linear distance from 3600m asl to PN: ~32km; section 3.4.5), would exhibit an average interstitial velocity of ~6 to 22 m/a (Table 3.6). The average

interstitial velocities of groundwater that is sampled from the spring system at Pica with relatively high discharge (spring discharge at PN ~1l/s compared to ~53l/s at Pica), is notably higher than that of samples W1 and PN (12-22 m/a compared to 6.5 m/a and 8.8 m/a). This is an indication for the presence of preferential pathways along more conductive fracture networks related to the spring system.

Based on these findings and Darcy's Law, an estimate of the mean hydraulic conductivity (*K*) for the relevant slope reservoir can be made. When considering a hydraulic gradient *i* of ~0.08 (from topographical height difference between Altos de Pica and Pica or PN) and a common value for the effective porosity of fractured rocks of 2-4% (Singhal and Gupta 2010), the resulting mean hydraulic conductivity of water guiding units in the slope reservoir would be circa 2E-7 to 5E-8 m/s. These orders of magnitude of K are at the lower margin of literature values for fractured and fissured rock and represent a low to moderate permeability (Singhal and Gupta 2010).

Hydraulic response of the spring related aquifer system to recharge events

Carrying out a time series analysis in the area of work is a delicate undertaking due to some constraints:

(1) Best available precipitation data are given by station Collacagua (CC, ~4010 m asl) which lies 40 km north-east of the expected recharge areas Altos de Pica and Altos del Huasco. Hence absolute measured rainfall amounts will vary from those at the actual recharge area. Nevertheless, relative precipitation patterns, in particular marked regional storm events with high and dense precipitation, will be represented correctly by the given meteorological station.

(2) It is necessary to compare water tables at well WC and WPN (at Pica and Puquio Nunez) as well as spring discharge from SE (Salar del Huasco basin). Hydraulic heads close to spring discharge (WC and SE) tend to decline more rapid than at locations with no or negligible leakage (WPN).

(3) In the recharge area's fractured and weathered ignimbrites are abundant. Infiltration rates of fractured rock surfaces can vary locally, depending upon topography and intensity of fractures (Singhal and Gupta 2010). It was shown also that in welded tuffs, infiltration rates depend on rainfall intensity and duration, particularly in semi-arid climates, because swelling of clayey portions

can lead to a widening of fissures and therefore increase infiltration rates (Salve et al. 2008).

However, statistically significant correlations between the different given time series can be determined. First the raw data and the resulting processed data that serves for cross correlation will be presented. Figure 3.8 displays absolute rainfall amounts at station CC with the resulting crd. The crd will be used for cross correlation with spring discharge at SE and water levels at WPN. Spring SE discharges out of the fractured ignimbrite formation Miih that covers the whole Altos del Huasco and Altos de Pica recharge area. Figure 3.9 shows the discharge amounts of spring SE together with the resulting detrended time series. The measured unprocessed values plot correctly along the interpolated time series (section 3.4.6). In Figure 3.10 the water level fluctuation at well WPN and WC is presented together with the respective interpolated time series. Note the synchronous and equal net water level rise of ~30 cm during the year 2002 at well WPN and WC.

Consequently, the cross correlation of the different datasets will be discussed. The cross correlation between times series SE and CC crd yields maximum positive cross correlation coefficients (Cc) for lags of 0-1 month (Figure 3.11a and b). They exceed the 95 % confidence interval which implies that the calculated correlation is statistically significant.

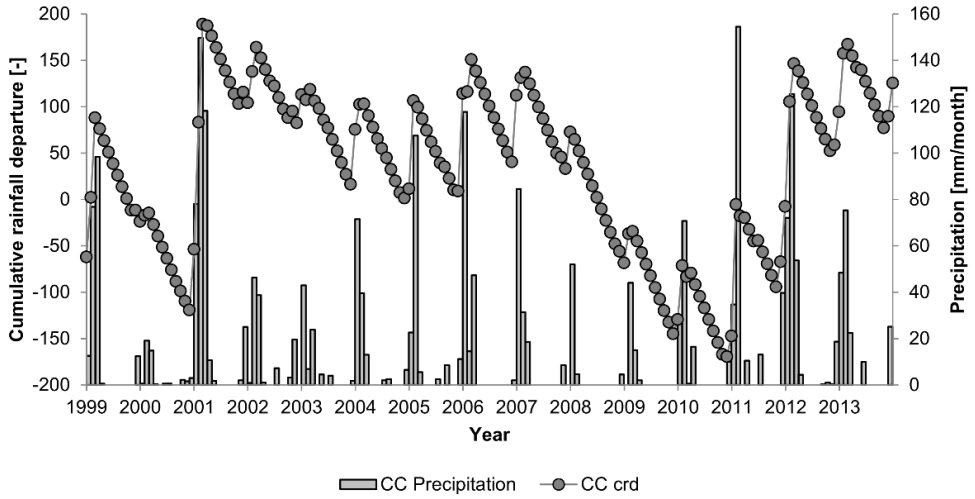

Figure 3.8 Rainfall at station Collacagua (CC) and resulting monthly cumulative rainfall departure (1999-2014)

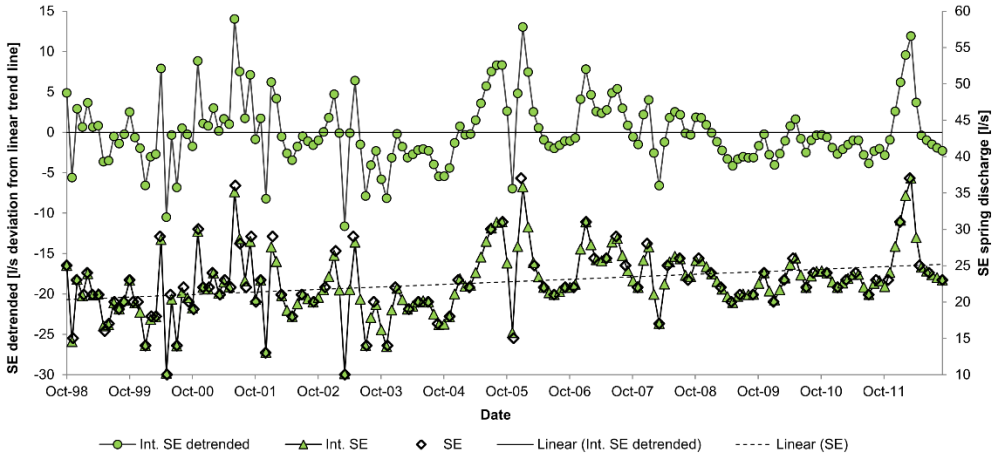

Figure 3.9 Spring discharge at SE with the resulting interpolated and detrended time series (October 1998 to October 2012).

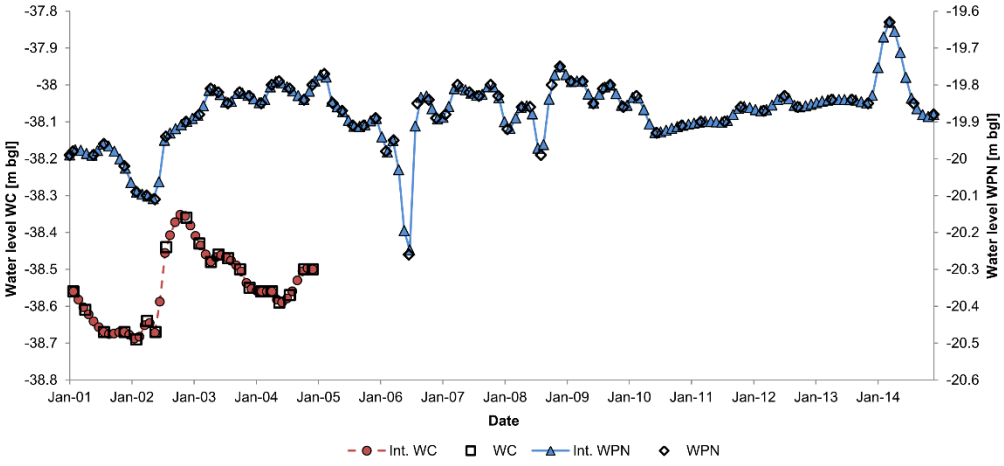

Figure 3.10 Water level fluctuation at well WPN and WC (2001-2015 and 2001-2005 respectively). Note the synchronous net water-level rise of ~30 cm during year 2002 at well WPN and WC

Arrows in Figure 3.11a mark the correlation of relative maxima and minima. The 6-month moving average helps to identify visually the similar trends in both time series. The result emphasizes that spring discharge at spring SE, and therefore the hydraulic pressure in the respective aquifer section, responds to rainfall in the catchment area generally within two months. Discharging waters at spring SE shows no relevant tritium contents (section 3.4.5), which implies that the recorded response cannot be induced by the physical arrival of rainwater but must be a pressure response of the hydraulic system. The measured lag will be therefore the time span in which infiltrated water reaches the hydraulic system.

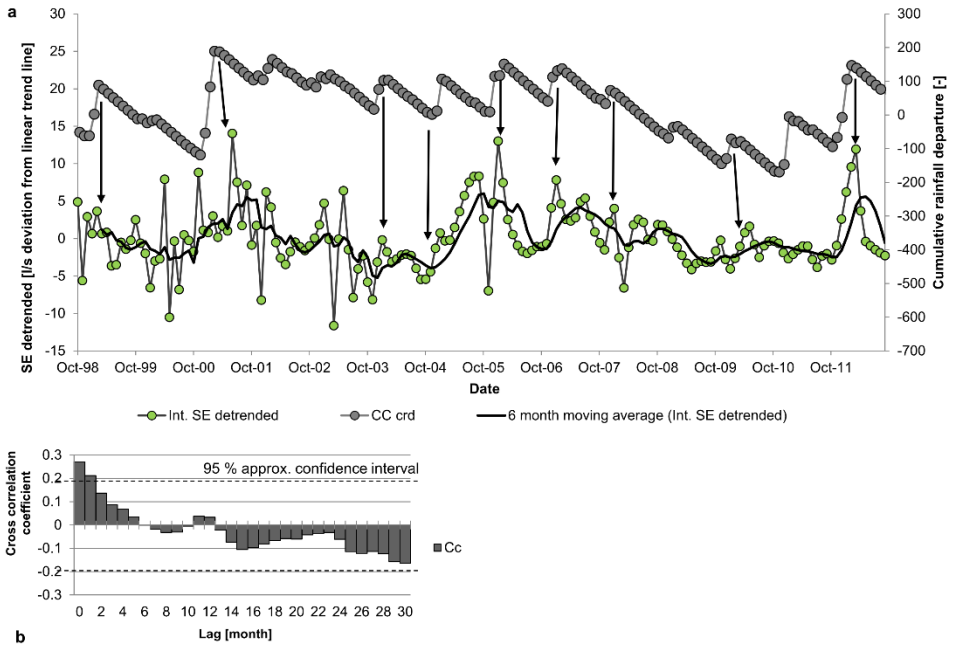

Figure 3.11 **(a)** Cross correlation between the detrended time series at SE and CC cumulative rainfall departure (crd), **(b)** resulting cross correlation coefficients (black arrows mark lags of 0-1 month)

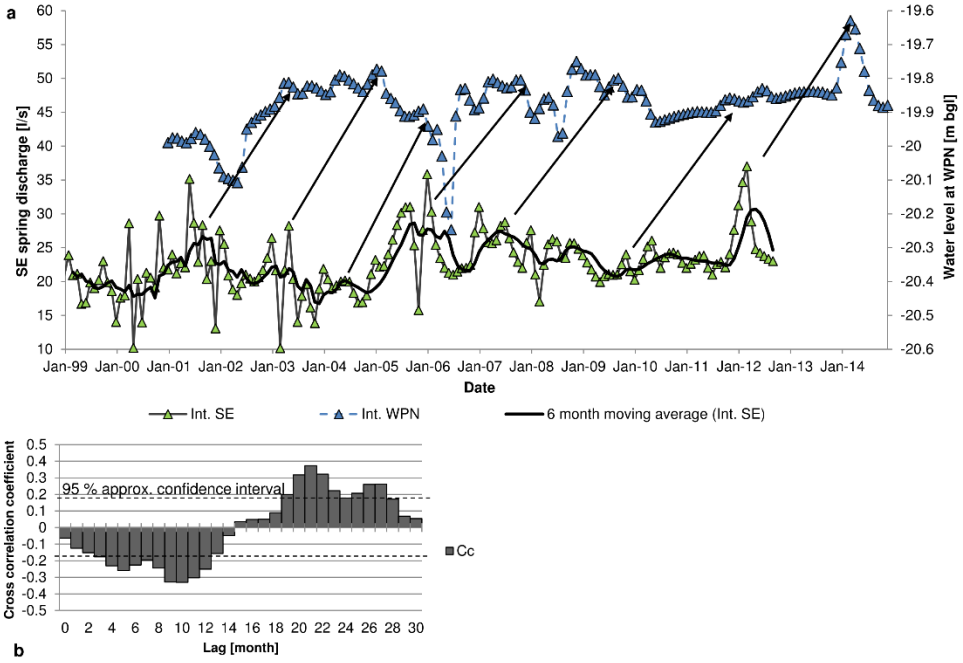

Figure 3.12 **(a)** Cross correlation between the spring discharge SE and water levels at WPN, **(b)** resulting cross correlation coefficients (black arrows mark lags of 20-22 month)

The discharge record at SE will therefore appropriately reflect the hydraulic head in the respective aquifer-forming units as a function of infiltrating water that reaches the hydraulic system at Altos del Huasco and Altos de Pica (Figure 3.2).

Figure 3.12 a shows the cross correlation between spring discharge at SE and water levels at WPN. The maximum positive correlation is computed for lags of 20-22 months (Figure 3.12b), where Cc reaches values of 0.32-0.37. The data give evidence that there is a statistically significant correlation between groundwater levels at the Andean foothills measured at well WPN and the spring discharge at the western margin of the Salar del Huasco basin. The same is true for the correlation between well WC and discharge at SE. Here, the cross correlation function yields a maximum positive correlation of 0.3-0.38 (above 95% confidence interval) at a lag of 23-24 months. This data can be confirmed by calculating the correlation between WPN and CC crd. The maximum positive correlation plots between months 19-22 with a Cc of 0.2-0.22 (above 95% confidence interval). When computing the cross correlation between the detrended WPN and CC crd, Cc even achieves a maximum of 0.45 (at a lag of 21 months).

The discussed data (Table 3.7) therefore strongly suggests that the hydraulic head changes (pressure changes) induced by rainwater recharged through the fractured ignimbrites (Miih), that are present at Altos de Pica and Altos del Huasco, are communicated rapidly within the whole slope reservoir. The discharge data at SE implies that recharging rainwater reaches the hydraulic system within 2 months. The pressure signal of the same recharge event is then communicated within a time span of, on average, 20-24 months to the Andean foothills at Pica and PN.

Table 3.7 Summary of cross correlation calculations

Time series	**C_c (maximum positive correlation)**	**Lag [months]**	**Exceeding 95% confidence interval**
CC crd and detrended SE	0.21-0.27	0, 1	yes
SE and WPN	0.31-0.37	20, 21, 22	yes
SE and WC	0.30-0.38	23, 24	yes
CC crd and WPN (detrended)	0.20-0.22, (0.45)	20, 21, 22, (21)	yes

Note that the observed hydraulic head signal at WPN and WC cannot be caused by the physical arrival of either recent or earlier infiltrated waters. The respective water shows no tritium content and earlier signals of infiltrated waters would certainly not arrive synchronously, with the same level increment at well WC and WPN (Figure 3.10). The statistical analysis demonstrates that a hydraulic head transmission with a constant delay is observed (lag 20-24 months). The described phenomena can only be explained by a short term hydraulic pressure response at the Andean foothills to recharge events at Altos de Pica/Altos del Huasco.

3.5. Discussion

The presented results confirm each other in a complimentary manner and thereby foster a comprehensive hydrogeological understanding of the discussed slope system. The conceptual model can be summarized in 5 points. (1) Recharge takes place at Altos de Pica (~3800 m asl) and is guided westwards downslope into the fractured parts of the OMap1a/c formation. (2) The maximal circulation depth is <950 m bgl. (3) The maximum reservoir temperature is ~53-57 °C. (4) The residence time of groundwater at the respective Andean foothills is circa 1300-4300 a BP. And (5) there is a short-term (20-24 months) transmission of hydraulic heads between the Precordilleran recharge area and the Andean foothills at Pica and PN.

Point (1) is crucial, knowing that originally it was considered by some authors that a leakage of the Salar del Huasco basin through deep fissures could have contributed notably to the spring discharge at the Andean foothills or alimented the PdT-Aquifer (Magaritz et al. 1989; Magaritz et al. 1990; Jica 1995; Jayne et al. 2016). Findings of this study substantiate the argumentation of Uribe et al. (2015) that this idea should be disregarded. There are mainly two reasons for that. First, the short-term hydraulic response of water levels at Pica and PN to recharge events at Altos de Pica gives robust evidence that a deep Altiplano reservoir is not leaking out towards the Pampa del Tamarugal. The hydraulic signal induced thereby, would very likely superimpose the hydraulic recharge signal from Altos de Pica. Secondly, the geothermal assessment in this study clearly indicates that waters are not exposed to very high reservoir temperatures (53-57 °C). When compared with the local geothermal gradient the maximal

circulation depth of the water should not exceed 950 m bgl. Waters that would leak out of the Salar del Huasco basin (or other high Andean basins) would need to circulate much deeper to cross the Precordilleran mountain ridge and would show a significantly higher salinity (Uribe et al. 2015). A maximum infiltration depth of >2 km, as recently suggested by a 2D-model from Jayne et al. (2016), is too deep for the thermal waters discharging at Pica.

The insights of this study inferred from geothermometers and the record of the geothermal gradient are also in accordance with the interpretation of the seismic imagery. The mapped fractured aquifer of the OMap1a/c Formation lies in the expected maximum infiltration depth of ~850 m bgl. It remains unknown whether there is a heat accumulation in the delineated reservoir due to advective heat transport and the confined nature of the aquifer. In this case, the maximum circulation depth (<950 m bgl) would be somewhat overestimated.

While the theoretical 2D-model set up by Jayne et al. (2016) points out some relevant observations, it is missing the new insights from this study. It does not take into account fracture flow which is, as indicated by seismic data, the main flow facilitator in the respective slope reservoir. Jayne et al. (2016) underestimated hydraulic conductivites of the aquifer-forming units by several orders of magnitude (~1E-11 to 1E-13 m/s compared to 2E-7 to 5E-8 m/s from this study; section 3.4.6). Apart from that, the model generalizes over a scale of 50 km where hydrogeologically highly heterogenic systems prevail (stable isotope samples from very distinct recharge areas are being compared (Fritz et al. 1981)). The used transect geology for the 2D-model is only fairly well constrained and relies on strong simplifications (Jayne et al. 2016). Overall, results derived from the model by Jayne et al. (2016) that make predictions about the area of work need to be treated very carefully.

Widening the scope again, it is important to consider the social background that stimulates the discussion about the hydraulic connection between the Salar del Huasco basin and Pica or the Pampa del Tamarugal. Particularly local inhabitants fear that a legal permission for water withdrawals from the Salar del Huasco basin could cause long-term water shortage in Pica. Although it is shown that a hydraulic connection between both systems is highly unlikely, it is also demonstrated that both watersheds share adjacent recharge areas that are joined by the same geologic formation. A massive overexploitation of water resoures in the Salar del Huasco basin (as has happened to the north, in the adjacent Laguna Lagunillas basin (Larraín and Poo 2010)) could cause a shift of

the subsurface water divide in the Altos de Pica / Altos del Huasco recharge area towards the west. The recharge area for waters at the Andean foothills could thereby be indirectly reduced and total recharge amounts that reach Pica could be decreased.

However, in general the geothermal framework of the slope reservoir is surely of no further commercial interest when compared to other potential geothermal energy sites in the Chilean Andes (Sanchez-Alfaro et al. 2015). Overall the reservoir temperature is too low and no strong positive heat anomaly can be expected in the area (volcanic activities are limited to the Altiplano Plateau).

The corrected mean residence times and interstitial velocities for groundwater (6-22 m/a) are in a reasonable magnitude when compared with the estimated hydraulic conductivities by Darcy's Law. 2E-7 to 5E-8 m/s is in accordance with K-values expected for fractured rock formations (Singhal and Gupta 2010).

A quite surprising fact may be the short-term transmission of hydraulic heads within the slope reservoir along more than 30 km. The computed Cc of >0.3 for cross correlations between SE and WPN as well as SE and WC indicate statistically significant correlations between different hydrologic time series related to the recharge area Altos de Pica / Altos del Huasco. The magnitude of the cross correlation coefficient is relatively good and overall satisfactory when taking into the account the naturally given constraints, such as the more rapid decline of spring discharge compared to water levels in wells, and factors that cause a deviation in the linearity of the hydraulic signal transmission (varying infiltration velocity and spatial dependence of recharge amounts through fractured rock surfaces; section 3.4.6.). A maximum positive correlation can be confirmed for a lag of 20-24 months when comparing the different datasets with water levels at the Andean foothills. Recharge signals in time series data caused by distinct recharge events, as a response to heavy rainfall events, can be identified and confirmed also visually for the determined lag window (black arrows in Figure 3.11 and Figure 3.12).

Yet there was little attention given to the possibility of a short-term hydraulic head transmission from Precordilleran recharge areas when revising water table fluctuations along the Andean foothills of the Pampa del Tamarugal. However, it is demonstrated that in this case it is possible (it might be the case at other similar sites too) and that the effective influence of Andean Precordilleran recharge on groundwater in the eastern Pampa del Tamarugal occurs within a very short time frame (contrary to the suggestion of Jayne et al. 2016). It implies that there is a

constantly active and connected hydraulic head leading from Altos de Pica to Pica and PN. In turn constructions to enhance recharge along Altos de Pica would have a soon perceptible impact on water levels at the eastern margin of the Pampa del Tamarugal in the area of work. Indirectly, a managed artificial recharge scheme for the respective area could be realized this way. Hydrologic models of the Salar del Huasco basin estimate recharge amounts of ~20 mm/a for the Altos del Huasco section (adjacent to Altos de Pica), while precipitation is on average at ~130 mm/a (Uribe et al. 2015; Acosta and Custodio 2008).

It is expected that waters from the Altos de Pica area are passing Pica and PN and continue to flow with the hydraulic gradient of the PdT-Aquifer southwest towards Salar de Bellavista (Figure 3.2). However, this hypothesis still needs to be proven.

3.6. Conclusions

The present study forms a comprehensive investigation into the functional hydrology of an Andean slope system under the integrated application of geophysical, hydrochemical and statistical methods. Several conclusions can be drawn.

Seismic data indicate that the development of the Pica spring system was facilitated by a disruption zone as induced by Cretaceous intrusions that penetrated the Mesozoic basement. It is suggested that in the long term this led to a decreased stability of overlaying Oligocene units (OMap1a/c) under the former stress conditions and enabled the development of the observed huge vertical fracture system (~200 m) at Pica.

The complementary information yielded from hydrochemical and hydrologic time-series data allow the conclusion that low-saline groundwater and spring water occurring along the Andean foothills are being recharged at the Precordilleran mountain ridge Altos de Pica and are not related to a leakage of the adjacent Salar del Huasco basin (as formerly suspected). By applying a statistical cross correlation between cumulative rainfall departures in the Altiplano, as well as spring discharge to the western margin of the Salar del Huasco basin and groundwater levels in Pica and Puquio Nunez, a statistically significant positive correlation between all datasets can be detected. It is demonstrated that hydraulic head changes at Pica and Puquio Nunez (1300 m

asl) are caused by recharge events at Altos de Pica and Altos del Huasco (~3800 m asl). The respective hydraulic head signals arrive with a lag of ~20-24 months. Apart from that, the maximal reservoir temperature for thermal waters in Pica was estimated to lie between 53 and 57 °C. According to the constantly rising recorded geothermal gradient of 3.1 °C/100 m, the maximum circulation depth of respective waters cannot exceed ~950 m bgl. This excludes a possible hydraulic connection through deep fissures between the Salar del Huasco basin and Pica. These findings are supported by the interpreted seismic data that allow a congruent mapping of the respective reservoir depth and unit, and the implicated flow path from Altos de Pica towards Pica. The resulting conceptual model explains the geothermal imprint well.

Based on the knowledge of the flow path, the calculated corrected mean residence times of 1300-4300 a BP allow to infer average interstitial velocities of ~6-22 m/a for groundwater in the slope reservoir. Overall the reservoir will therefore show a low to moderate hydraulic conductivity of ~2E-7 to 5E-8 m/s. In question is the further flow direction of groundwater that passes Pica and Puquio Nunez. Proof of groundwater flow into the Pampa del Tamarugal aquifer, from the Precordillera, still needs to be acquired. Confirmed amounts of recharge at Altos de Pica, and hence the provided recharge into the Atacma Desert, is another open issue.

3.7. Acknowledgment

This study is the result of cooperation between the Department of Hydrogeology of the Technical University of Berlin (Germany) and CIDERH, Iquique (Chile). The authors thank CIDERH for funding the field work and Compañía Minera Doña Inés de Collahuasi for the hydrochemical data. The authors express their gratitude also to ENAP, Empresa Nacional de Petróleo, Chile, for supplying seismic data. Apart from that, the study would not have been possible without funds from CONICYT (Comisión Nacional de Investigación Científica y Tecnológica, Chile).

3.8. References

Ahmed S, Jayakumar R, Salih A (2011) Groundwater dynamics in hard rock aquifers: Sustainable management and optimal monitoring network design, Book on demand. Springer, Dordrecht

Akima H (1978) A Method of Bivariate Interpolation and Smooth Surface Fitting for Irregularly Distributed Data Points. ACM Trans. Math. Softw. 4(2):148–159. doi: 10.1145/355780.355786

Allmendinger R, Jordan T, Kay S, Isacks BL (1997) The Evolution of the Altiplano-Puna Plateau of the Central Andes. Earth and Planetary Sciences. doi: 10.1146/annurev.earth.25.1.139

Betancourt JL (2000) A 22,000-Year Record of Monsoonal Precipitation from Northern Chile's Atacama Desert. Science 289(5484):1542–1546. doi: 10.1126/science.289.5484.1542

Blanco N, Landino M (2012) Carta Mamiña - Región de Tarapacá (Geological map Mamiña - Tarapacá Region). map scale 1:100.000. Sernageomin, Santiago, Chile

Blanco N, Tomlinson AJ (2013) Carta Guatacondo - Región de Tarapacá (Geological map Guatacondo - Tarapacá Region). map scale 1:100.000, 156th edn. Sernageomin, Santiago

Burn DH, Hag Elnur MA (2002) Detection of hydrologic trends and variability. Journal of Hydrology 255(1-4):107–122. doi: 10.1016/S0022-1694(01)00514-5

Clark ID, Fritz P (1999) Environmental isotopes in hydrogeology, [2. print., corr.]. Lewis Publ, Boca Raton

Damby DE, Llewellin EW, Horwell CJ, Williamson BJ, Najorka J, Cressey G, Carpenter M (2014) The α-β phase transition in volcanic cristobalite. J Appl Crystallogr 47(Pt 4):1205–1215. doi: 10.1107/S160057671401070X

Deer WA, Howie RA, Zussman J (2004) Framework silicates: silica minerals, feldspathoids and the zeolites, 2. ed. Rock-forming minerals, / W. A. Deer; R. A. Howie; J. Zussman ; Vol. 4,B. Geological Society, London

DGA (2013) Levantamiento de Información Geofísico en la Región de Tarapacá (Geophysical study of the region Tarapacá). Con potencial consultores LTDA. documentos.dga.cl/SUB5485v1.pdf. Accessed 13 May 2016

Fontes J-C, Garnier J-M (1979) Determination of the initial 14 C activity of the total dissolved carbon: A review of the existing models and a new approach. Water Resour. Res. 15(2):399–413. doi: 10.1029/WR015i002p00399

Fouillac C, Michard G (1981) Sodium/Lithium in water applied to geothermometry of geothermal reservoirs. Geothermics(10.1):55–70

Fournier RO (1977) Chemical geothermometers and mixing models for geothermal systems. Geothermics 5(1-4):41–50. doi: 10.1016/0375-6505(77)90007-4

Fritz P, Suzuki O, Silva C, Salati E (1981) Isotope hydrology of groundwaters in the Pampa del Tamarugal, Chile. Journal of Hydrology 53(1-2):161–184. doi: 10.1016/0022-1694(81)90043-3

Galli C, Dingman R. (1965) Geology and Ground-Water Resources of the Pica Area Tarapaca Province, Chile. https://pubs.er.usgs.gov/publication/b1189. Accessed 13 May 2016

Gardeweg M, Sellés D (2013) Geología del àrea Collacagua-Rinconada - Región de Tarapacá (Geology of the area Collacagua-Rinconanda - Tarapacá Region). map scale 1:100.000, 148th edn. Sernageomin, Santiago

Gayo EM, Latorre C, Santoro CM, Maldonado A, Pol-Holz R de (2012a) Hydroclimate variability in the low-elevation Atacama Desert over the last 2500 yr. Clim. Past 8(1):287–306. doi: 10.5194/cp-8-287-2012

Gayo EM, Latorre C, Jordan TE, Nester PL, Estay SA, Ojeda KF, Santoro CM (2012b) Late Quaternary hydrological and ecological changes in the hyperarid core of the northern Atacama Desert (~21°S). Earth-Science Reviews 113(3-4):120–140. doi: 10.1016/j.earscirev.2012.04.003

Han L-F, Plummer LN (2013) Revision of Fontes & Garnier's model for the initial 14C content of dissolved inorganic carbon used in groundwater dating. Chemical Geology 351:105–114. doi: 10.1016/j.chemgeo.2013.05.011

Han L-F, Plummer LN, Aggarwal P (2012) A graphical method to evaluate predominant geochemical processes occurring in groundwater systems for radiocarbon dating. Chemical Geology 318-319:88–112. doi: 10.1016/j.chemgeo.2012.05.004

Han LF, Plummer LN (2016) A review of single-sample-based models and other approaches for radiocarbon dating of dissolved inorganic carbon in groundwater. Earth-Science Reviews 152:119–142. doi: 10.1016/j.earscirev.2015.11.004

Hoke GD, Isacks BL, Jordan TE, Yu JS (2004) Groundwater-sapping origin for the giant quebradas of northern Chile. Geol 32(7):605. doi: 10.1130/G20601.1

Irwin RP, Tooth S, Craddock RA, Howard AD, Latour AB de (2014) Origin and development of theater-headed valleys in the Atacama Desert, northern Chile: Morphological analogs to martian valley networks. Icarus 243:296–310. doi: 10.1016/j.icarus.2014.08.012

Jayne RS, Pollyea RM, Dodd JP, Olson EJ, Swanson SK (2016) Spatial and temporal constraints on regional-scale groundwater flow in the Pampa del Tamarugal Basin, Atacama Desert, Chile. Hydrogeol J. doi: 10.1007/s10040-016-1454-3

Jica (1995) The study on the development of water resources in Northern Chile. http://sad.dga.cl/. Accessed 13 May 2016

Jordan TE, Nester PL, Blanco N, Hoke GD, Dávila F, Tomlinson AJ (2010) Uplift of the Altiplano-Puna plateau: A view from the west. Tectonics 29(5):n/a. doi: 10.1029/2010TC002661

Jordan TE, Kirk-Lawlor NE, Blanco NP, Rech JA, Cosentino NJ (2014) Landscape modification in response to repeated onset of hyperarid paleoclimate states since 14 Ma, Atacama Desert, Chile. Geological Society of America Bulletin 126(7-8):1016–1046. doi: 10.1130/B30978.1

Karzulovic J (1980) Informe hidrogeológico del sondaje profundo de Chacarilla Cuenca artesiana de Pica (Hydrogeological report on the deep probing in the artesian Chacarillas basin of Pica). http://sad.dga.cl/. Accessed 13 May 2016

Kharaka YK, Mariner RH (1989) Chemical Geothermometers and Their Application to Formation Waters from Sedimentary Basins. In: Naeser ND, McCulloh TH (eds) Thermal History of Sedimentary Basins. Springer New York, New York, NY, pp 99–117

Larraín S, Poo P (2010) Conflictos por el agua en Chile - Entre los derechos humanos y las reglas de mercado (Water conflicts in Chile - between human rights and the rules of the free market), 1a ed. [s.n], Santiago, Chile

Lee J-Y, Lee K-K (2000) Use of hydrologic time series data for identification of recharge mechanism in a fractured bedrock aquifer system. Journal of Hydrology 229(3-4):190–201. doi: 10.1016/S0022-1694(00)00158-X

Lictevout E, Maas C, Córdoba D, Herrera V, Payano R (2013) Recursos Hídricos Región de Tarapacá - Diagnóstico y Sistematización de Información (Water resources in the region Tarapacá - Diagnosis and systematisation of existing information). Universidad Arturo Prat, Iquique, Iquique

Magaritz M, Aravena R, Peña H, Suzuki O, Grilli A (1989) Water chemistry and isotope study of streams and springs in northern Chile. Journal of Hydrology 108:323–341. doi: 10.1016/0022-1694(89)90292-8

Magaritz M, Aravena R, Peña H, Suzuki O, Grilli A (1990) Source of Ground Water in the Deserts of Northern Chile: Evidence of Deep Circulation of Ground Water from the Andes. Groundwater(4). doi: 10.1111/j.1745-6584.1990.tb01706.x

McCuen RH (2003) Modeling hydrologic change: Statistical methods. Lewis Publishers, Boca Raton, Fla

Nester PL (2008) Basin and Paleoclimate Evolution of the Pampa del Tamarugal Forearc Valley, Atacama Desert, Northern Chile. https://ecommons.cornell.edu/bitstream/handle/1813/10484/Nester2008.pdf?sequence=1&isAllowed=y. Accessed 5 May 2017

Nicholson K (2012) Geothermal fluids: Chemistry and exploration techniques. Springer, Berlin

ODEA (2016) Observatorio del Agua [Water resources observatory]. www.odea.cl. Accessed 7 December 2016

PUC (2009) Levantamiento Hidrogeológico para el Desarrollo de nuevas fuentes de Agua en áreas prioritarias de la zona norte de Chile, Regiones XV, I, II y III (Hydrogeological study for the development of new water resources in northern zones of Chile, regiones XV, I, II and III). documentos.dga.cl/REH5161v4.pdf. Accessed 13 May 2016

Rech JA, Quade J, Betancourt JL (2002) Late Quaternary paleohydrology of the central Atacama Desert (lat 22°–24°S), Chile. Geological Society of America Bulletin 114(3):334–348. doi: 10.1130/0016-7606(2002)114<0334:LQPOTC>2.0.CO;2

Rojas R, Dassargues A (2007) Groundwater flow modelling of the regional aquifer of the Pampa del Tamarugal, northern Chile. Hydrogeol J 15(3):537–551. doi: 10.1007/s10040-006-0084-6

Rojas R, Batelaan O, Feyen L, Dassargues A (2010) Assessment of conceptual model uncertainty for the regional aquifer Pampa del Tamarugal – North Chile. Hydrol. Earth Syst. Sci. 14(2):171–192. doi: 10.5194/hess-14-171-2010

Salve R, Ghezzehei TA, Jones R (2008) Infiltration into fractured bedrock. Water Resour. Res. 44(1):n/a-n/a. doi: 10.1029/2006WR005701

Sanchez-Alfaro P, Sielfeld G, van Campen B, Dobson P, Fuentes V, Reed A, Palma-Behnke R, Morata D (2015) Geothermal barriers, policies and economics in Chile – Lessons for the Andes. Renewable and Sustainable Energy Reviews 51:1390–1401. doi: 10.1016/j.rser.2015.07.001

Schlunegger F, Kober F, Zeilinger G, Rotz R von (2010) Sedimentology-based reconstructions of paleoclimate changes in the Central Andes in response to the uplift of the Andes, Arica region between 19 and 21°S latitude, northern Chile. Int J Earth Sci (Geol Rundsch) 99(S1):123–137. doi: 10.1007/s00531-010-0572-8

Singhal B, Gupta RP (2010) Applied Hydrogeology of Fractured Rocks: Second Edition. Springer Science+Business Media B.V, Dordrecht

Uribe J, Muñoz JF, Gironás J, Oyarzún R, Aguirre E, Aravena R (2015) Assessing groundwater recharge in an Andean closed basin using isotopic characterization and a rainfall-runoff model: Salar del Huasco basin, Chile. Hydrogeol J. doi: 10.1007/s10040-015-1300-z

USGS (2014) Hydroclimate Manual: Hydrologic and Climatic Analysis Toolkit. http://pubs.usgs.gov/tm/tm4a9/pdf/tm4-a9.pdf. Accessed 15 August 2016

Verma SP, Pandarinath K, Santoyo E (2008) SolGeo: A new computer program for solute geothermometers and its application to Mexican geothermal fields. Geothermics 37(6):597–621. doi: 10.1016/j.geothermics.2008.07.004

Weber K, Stewart M (2004) A Critical Analysis of the Cumulative Rainfall Departure Concept. Groundwater 42(6):935–938

4. Reassessing hydrological processes that control stable isotope tracers in groundwater of the Atacama Desert (northern Chile)

Konstantin W. Scheihing[a,*], Claudio E. Moya[b,c,d], Ulrich Struck[e,f], Elisabeth Lictevout[b,g], Uwe Tröger[a]

[a] Department of Applied Geosciences, Hydrogeology Research Group, Technische Universität Berlin, 10587 Berlin, Germany

[b] CONICYT Regional/CIDERH, Centro de Investigación y Desarrollo en Recursos Hídricos (R09I1001), 1100565 Iquique, Chile

[c] Universidad Arturo Prat, 1110939 Iquique, Chile

[d] Golder Associates S.A., 7550055 Santiago, Chile

[e] Museum für Naturkunde, Leibniz-Institut für Evolutions- und Biodiversitätsforschung, 10115 Berlin, Germany

[f] Department of Geosciences, Freie Universität Berlin, 12249 Berlin, Germany

[g] Facultad de Ciencias Forestales, Universidad de Concepción, 4070374 Concepción, Chile

[*]corresponding author: kscheihing@gmx.de

Citation:

Scheihing K, Moya C, Struck U, Lictevout E, Tröger U (2018) Reassessing Hydrological Processes That Control Stable Isotope Tracers in Groundwater of the Atacama Desert (Northern Chile). Hydrology 5:3. doi: 10.3390/hydrology5010003

Article history:

Received: 20 November 2017 / Accepted: 21 December 2017 / Published: 26 December 2017

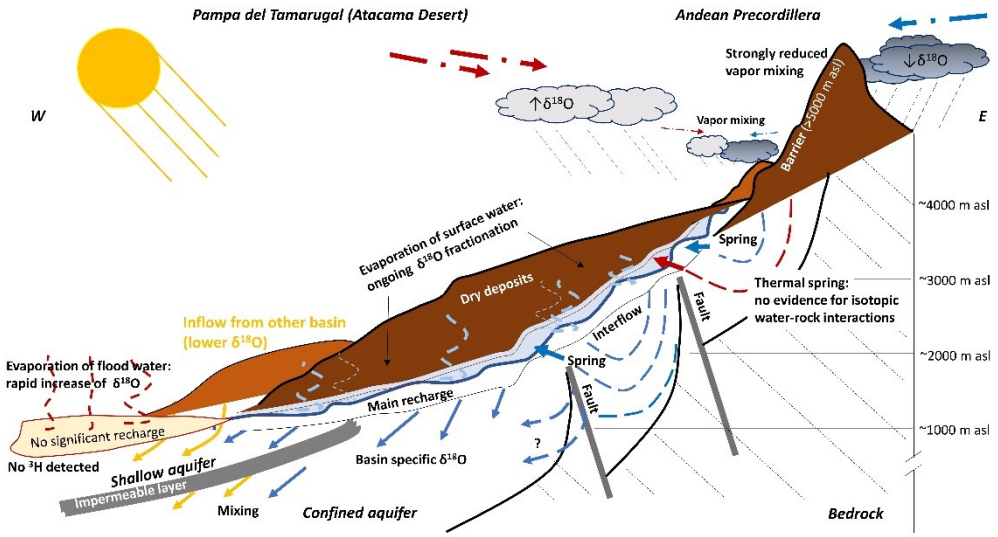

Figure 4.1 Graphical abstract

Abstract

A collection of 514 stable isotope water samples from the Atacama Desert is being reassessed geostatistically. The evaluation reveals that adjacent Andean catchments can exhibit distinct $\delta^{18}O$ and $\delta^{2}H$ value ranges in meteoric waters, despite similar sample altitudes of up to 4000 m above sea level (asl). It is proposed that the individual topographic features of each catchment at the western Andean Precordillera either inhibit or facilitate vapor mixing processes of easterly and westerly air masses with different isotopic compositions. This process likely causes catchment-specific isotope value ranges in precipitations (between −7‰ and −19‰ $\delta^{18}O$) that are being consistently reflected in the isotope values of groundwater and surface waters of these catchments. Further, due to evaporation-driven isotopic fractionation and subsurface water mixing, isotope samples of the regional Pampa del Tamarugal Aquifer plot collectively parallel to the local meteoric water line. Besides, there is no evidence for hydrothermal isotopic water-rock interactions. Overall, the observed catchment-dependent isotope characteristics allow for using $\delta^{18}O$ and $\delta^{2}H$ as tracers to delineate regionally distinct groundwater compartments and associated recharge areas. In this context, $\delta^{18}O$, $\delta^{2}H$ and ^{3}H data of shallow groundwater at three alluvial fans challenge the established idea of recharge from alluvial fans after flash floods.

4.1. Introduction

In the hyper-arid environment of the Atacama Desert in northern Chile, the regional Pampa del Tamarugal (PdT) Aquifer forms a strategic and vital source of groundwater, being the largest recognized aquifer in northern Chile (Jica 1995; Chávez et al. 2016). Its resources are used in the mining industry, for agricultural purposes or human consumption (Chávez et al. 2016). Remarkable for groundwater resources of the PdT Aquifer is the wide range of $\delta^{18}O$ values that span from −13‰ to −6‰ (Fritz et al. 1981; Magaritz et al. 1989; Aravena 1995; Salazar et al. 1998). To explain this observation different conceptual hydrogeological models were proposed for the study area, among others a deep interbasin fracture flow of groundwater from the Andes to the Atacama Desert (Fritz et al. 1981; Magaritz et al. 1989; Magaritz et al. 1990; Rojas et al. 2010; Uribe et al. 2015; Jayne et al. 2016; Scheihing et al. 2017). The encountered conceptual uncertainties impede the development of a sound hydrogeological model of the PdT Aquifer to support long-term groundwater management measures (Rojas et al. 2010). Recharge areas and groundwater inflow are not sufficiently understood (Rojas et al. 2010). At the same time, a reliable hydrogeological model is urgently needed to support water management because current groundwater production amounts from the PdT Aquifer account for ~4000 L/s (instantaneous) and groundwater resources are being persistently overexploited as in many other regions of northern Chile (Valdés-Pineda et al. 2014; Chávez et al. 2016; Scheihing and Tröger 2017).

Stable isotopes in water of oxygen (^{16}O and ^{18}O) and hydrogen (^{1}H and ^{2}H) are typically inert and conservative in mixing relationships and used as a tracer to investigate hydrogeological and hydrological processes including groundwater recharge and groundwater–surface-water interaction (Clark and Fritz 1999; Kendall 2006). Accordingly, the deuterium excess (D_{ex}) parameter of water samples can be used to detect relative evaporative enrichment effects particularly in arid regions (Clark and Fritz 1999). In this regard, the isotopic composition of precipitation is the initial isotopic signal of derived meteoric waters (surface, vadose zone or groundwater). The subsequent change of their isotopic composition by either evaporation, mixing or interaction with the lithosphere can be utilized to trace these processes (Clark and Fritz 1999).

Based on a geostatistical and chemical assessment of a dataset of 514 stable isotope measurements, which includes data of previous publications as well as

unpublished data, the presented study aims at deriving new insights into hydrological processes that control the stable isotope chemistry from the arid Andes to the PdT. It is demonstrated that a consistent understanding of the regions stable isotope hydrology, in conjunction with ^{3}H data, allows for clarifying some of the encountered conceptual hydrogeological uncertainties.
The findings yield a new explanation for the long-lived question why stable isotope values from the PdT Aquifer cluster parallel to the local meteoric water line (LMWL) and make it possible to differentiate different recharge areas. The results have general implications for the isotope hydrology of Atacama basins and challenge the established idea of a substantial alluvial fan recharge by occasional flooding events in the open desert.

4.2. Study area

The PdT is a nonmarine, intramassive forearc basin enclosed by the Precordillera of the central Andes to the east and the Chilean Coastal Cordillera to the west (Figure 4.2a,b). It is situated between altitudes of ~900–1800 m asl and forms a part of the Atacama Desert. The PdT evolved together with the Altiplano Plateau uplift from the Oligocene to present over a time span of about 30 Ma (Jordan and Nester 2012). The sedimentary fill of the PdT is of a lens-like shape and reaches ~1000–1700 m thickness (Nester 2008). It consists of horizontally deposited nonmarine Oligocene to modern clastic sediments intercalated with extrusive volcanic deposits (e.g., ignimbrites). The aquifer of the PdT is formed by the Middle Miocene to Quaternary sediment fill with a maximum depth of ~300 m bgl (Rojas and Dassargues 2007; Rojas et al. 2010). The PdT Aquifer exhibits various strata with a total thickness of 25–150 m (Jica 1995; Rojas and Dassargues 2007). A longitudinal cross-section of the aquifer was elaborated by Rojas et al. (2010). Mean corrected groundwater residence times in the PdT Aquifer likely reach a few thousand years (Fritz et al. 1981; Scheihing et al. 2017). In the study area, the overall tectonic setting of the basin is characterized by N-S, NNE-SSW and NNW-SSE striking west-vergent and east-vergent (basically blind) reverse faults (Nester 2008). One of the major faults is the ~65 km north-south striking Longacho Hinge, passing the localities Pica and Puquio de Nunez (Nester 2008; Blanco and Tomlinson 2013).

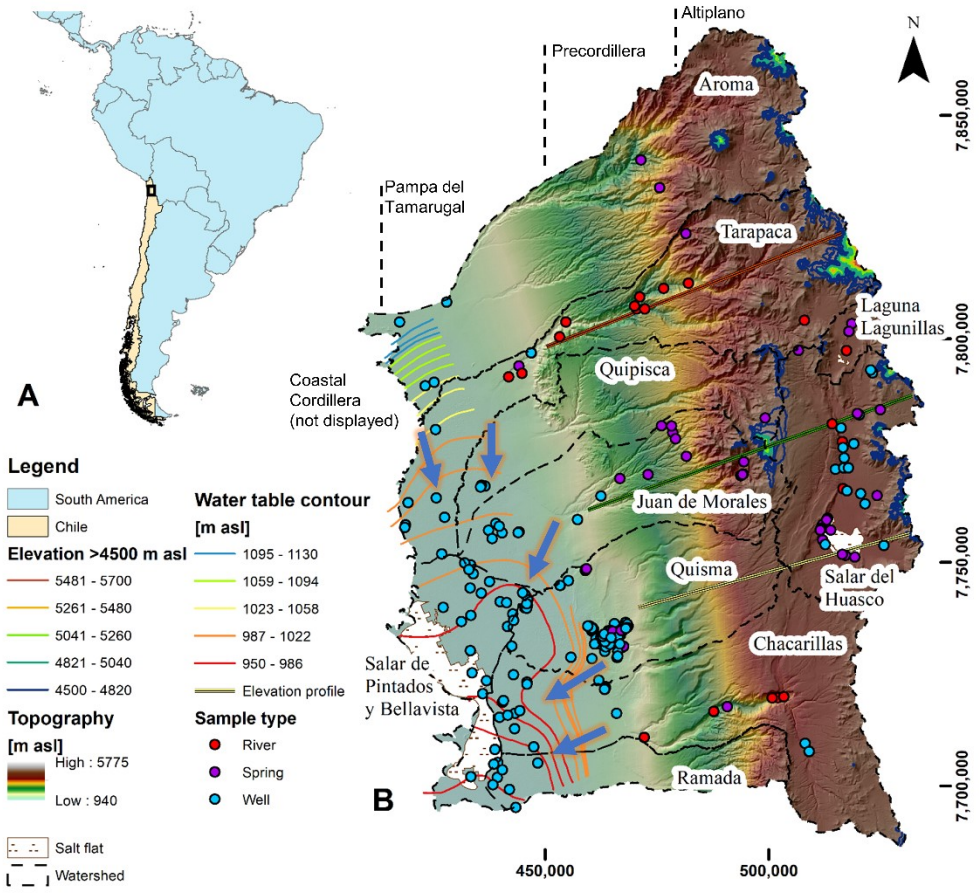

Figure 4.2 (**a**) View on South America (black rectangle represents the extent of Figure 4.2b), (**b**) Topographical map of the study area and sample types (elevation profiles are discussed in section 4.5.2). Water table contour lines indicate the regional groundwater flow regime of the PdT Aquifer and are based on Jica (1995). Arrows indicate resulting groundwater flow directions. Not all springs in the region are displayed.

East-west discharging ephemeral stream networks flow through narrow ravines (Quebradas) downslope from parts of the Altiplano and Precordillera to the relatively flat sedimentary basin of the PdT. Catchments in the area correspond to the Quebradas (from north to south) Aroma, Tarapacá, Quipisca, Juan de Morales, Quisma, Chacarillas and Ramada (Figure 4.2b).

Occasional storm events in the Andean Cordillera result in flash-floods of varying intensity which can reach the alluvial fans that spread into the PdT (return period ~4 years) (Houston 2002, 2006b). Along the Andean Precordillera, several springs can be found (Figure 4.2b) of which the most prominent are the thermal Pica springs (at the Pica Oasis) located at ~1300 m asl (Galli and Dingman R. 1965; Scheihing et al. 2017).

The general groundwater flow direction of the PdT Aquifer is south-south-west (Figure 4.2b) (Aravena 1995; Jica 1995; Rojas and Dassargues 2007; Chávez et al. 2016). Groundwater emerges to the surface at the basins western margin

where the magmatic rocks of the Coastal Cordillera constitute an impermeable barrier (Jordan and Nester 2012).

These emerging groundwaters can be found near-surface at salt flats in the PdT, from where they are evaporated (Pintados- and Bellavista-Salar, Figure 4.2b) (Nester 2008; Jordan and Nester 2012).

A characteristic of stable isotope data from the PdT Aquifer is that $\delta^{18}O$-^{2}H-values of groundwater plot parallel to the local meteoric water line and $\delta^{18}O$ ranges from −13‰ to −6‰ (Fritz et al. 1981; Magaritz et al. 1989; Aravena 1995; Aravena et al. 1999). Overall, there are two empirical local evaporation lines (LEL) established for the study area. One LEL was derived from water samples of an unsaturated soil profile at the river outlet of the Huatacondo River in the PdT (20 km south of the Ramada basin). In this case, the LEL showed a slope of ~4 (Aravena et al. 1989). A second LEL was derived based on data from the local salt flats (Aravena 1995). Again, a slope of ~4 was detected.

Potential evaporation in the PdT during austral summer months when more than 80% of yearly precipitation falls (Houston 2006c), is ~250 to ~350 mm/month (DGA 2017). Precipitations of more than 20 mm/a fall only above ~2500 m asl (Houston 2006c). Vapor masses that contribute to precipitation in the Andes can originate from east, north-east and west-north-west (most significant sources: Amazon basin and Atlantic Ocean) (Aravena et al. 1999; Vuille and Werner 2005; Herrera et al. 2017). However, the PdT itself which is situated in the Andean rain shadow did probably not experience notable amounts of precipitation in the Late Quaternary (Gayo et al. 2012b; Jordan et al. 2014). Nevertheless, the Altiplano area went through stages of significant variations in precipitation amounts during the last 20 ka (Central Andean Pluvial Event) (Placzek et al. 2006; Quade et al. 2008; Placzek et al. 2009). Wetter stages in the Altiplano indirectly influenced water availability in the PdT, mainly triggered by stream discharge from the Quebradas into the basin (Gayo et al. 2012b; Jordan et al. 2014). At 21° S latitude pluvial phases in the Altiplano can be correlated with the dating of ancient riparian vegetation in the PdT for periods between 17.6–14.2 ka BP, 12.1–11.4 ka BP and 2.5–2 ka BP (Gayo et al. 2012a; Gayo et al. 2012b). These periods mark likely prominent regional groundwater recharge events (Gayo et al. 2012b).

4.3. Data and methods

4.3.1. Groundwater sampling

Prior to groundwater sampling, a temperature log of the well fluid was recorded with a temperature probe head. Subsequently, depth-specific groundwater sampling was carried out using a Robertson Geologging Gas Sampler. The gas sampler contains a sealed sample chamber with a moveable piston and motor-actuated valve that is led down into the well with a partial vacuum inside to retrieve uncontaminated samples of well fluids at specific depths. In order not to disturb the natural flow conditions in the well, the speed of the probe heads was regulated not to exceed 5 m/min. All other groundwater samples (from earlier studies) represent a mixture of water over the entire wells screened profile due to pumping. Wells in the PdT are typically 50–200 m bgl deep with a water level typically at 20–70 m bgl.

4.3.2. Isotope sample analysis

For this study, stable isotope ratios of oxygen ($^{18}O/^{16}O$) and hydrogen ($^{2}H/^{1}H$) in H_2O in water samples were measured with a PICARRO L1102-i isotope analyzer. The L1102-i is based on the WS-CRDS (wavelength-scanned cavity ring down spectroscopy) technique (Gupta et al. 2009). Measurements were calibrated by the application of linear regression of the analyses of IAEA calibration material VSMOW, VSLAP and GISP. The stable isotope ratios of oxygen and hydrogen are expressed in the conventional delta notation ($\delta^{18}O$, $\delta^{2}H$) in per mil (‰) versus VSMOW (Coplen 2011). The reproducibility of replicate measurements is better than 0.1‰ for oxygen and 0.5‰ for hydrogen.

Stable isotopes from previously published studies were typically analyzed by mass spectrometry. Samples from studies published before the year 2000 give stable isotope ratios of oxygen and hydrogen in delta notation ($\delta^{18}O$, $\delta^{2}H$) in per mil (‰) versus SMOW. However, the reference standards SMOW and VSMOW are defined as equivalent to each other (Lin et al. 2010).

In this study, tritium data of four shallow wells at alluvial fans are presented. The data originates from an internal investigation of the mining company Compañía

Minera Doña Inés de Collahuasi (CMDIC) (Santiago, Chile) (CMDIC 2012). Tritium (^{3}H) measurements were carried out by Gas Proportional Counting at the Rosenstiel Laboratory of the University of Miami, which provides analytical errors of ±0.09 TU (tritium units).

The deuterium excess (D_{ex}) parameter of a water sample is calculated according to the following equation (Clark and Fritz 1999):

$$D_{ex} = \delta^{2}H - 8 \times \delta^{18}O \qquad \text{Eq. 4-1}$$

4.3.3. Isotope data

Earlier published studies include papers and reports about the isotopic content in precipitation, river water, and spring- and groundwater (Table 4.1, Figure 4.2b). The data is available attached to this thesis (section 6.3).

A geostatistical evaluation was conducted on the isotope data from spring, river and groundwater, together with unpublished data from an internal study of the mining company Compañía Minera Doña Inés de Collahuasi (CMDIC 2012) and data collected in this study. The report by Salazar et al. (1998) includes all isotope data collected by the Chilean water directorate (DGA) that were published by Magaritz et al. (1989), Aravena and Suzuki (1990) and Aravena (1995). The precision of the GPS-coordinates of the data is restricted by the accuracy of the GPS-instruments of each report or study but was found to be of good to sufficient accurateness for a regional scale assessment. Samples of surface water from the salt flats Salar de Pintados and Bellavista and Salar del Huasco—strongly affected by evaporation—were excluded from the dataset because they would distort the assessment of regional groundwater conditions.

In the dataset, there are 53 weighted precipitation samples from the region, 94 meteoric water samples from the Salar del Huasco basin and the Laguna Lagunillas basin (Altiplano) and 367 surface, spring and groundwater samples for the PdT. There are 26 samples from the Salar del Huasco basin for which no georeferenced coordinates were available (check data in section 6.3).

Table 4.1 Summary of stable isotope data of groundwater, spring and river water in the study region from different reports and studies (1964–2015).

Sample source	Sampling campaign dates	Covered catchments	Amount of samples	Sample types
(Aravena and Suzuki 1990)	April–May 1981 and April–May 1984	Tarapacá	13	River water
(CMDIC 2012)	February 2011, May 2011, August 2011	Quisma, Aroma, Chacarillas, Juan de Morales, Tarapacá, Salar del Huasco	36	Well, spring and river water
(Fritz et al. 1981)	January 1974, May 1975	Quisma, Aroma, Chacarillas, Juan de Morales, Tarapacá, Salar del Huasco	47	Well, spring and river water
(López et al. 2014)	October 2012, January–February 2014	Quisma, Aroma, Chacarillas, Juan de Morales, Tarapacá, Salar de Pintados and Bellavista, Salar del Huasco	92	Well and spring water
(PUC 2009)	September 2008	Salar del Huasco	17	Well and spring water
(Salazar et al. 1998)	May 1964, September 1967, October 1972, May 1973, July 1973, November 1973, January 1974, April–May 1974, December 1974, April 1975, November–December 1975, March 1979, April 1981, March–May 1982, January–May 1983, November 1983, January–May 1984, November–December 1984, March 1985, January 1987, February 1988, August 1996, January 1997, November 1997	Quisma, Aroma, Chacarillas, Juan de Morales, Tarapacá, Salar de Pintados and Bellavista, Salar del Huasco	209	Well, spring and river water
This study	August 2014, October–November 2015	Quisma, Aroma, Juan de Morales, Tarapacá, Chacarillas, Salar del Huasco	15 (of which 9 are depth-specific)	Well and spring water
(Uribe et al. 2015)	December 2009, January 2011	Juan de Morales, Quisma, Quipisca, Chacarillas, Salar del Huasco	32	Well, river and spring water

Isotopic values of weighted precipitations represent average values per meteorological station and rainfall season (austral summer or winter of respective years). Precipitations were sampled in summer 1973–1974, summer 1974–1975, summer and winter 1984, summer 1985–1986, winter 2010, summer 2009–2010 and summer 2010–2011.

In the PdT dataset, 170 samples are concentrated around the Pica area, where dozens to hundreds of wells can be found and several sample campaigns were

carried out. The remaining 196 samples are distributed across the PdT over an area of ~9000 km^2, including the slope of the Andean Precordillera.

4.3.4. Geostatistical interpolation

The δ^2H and $\delta^{18}O$ data was processed by the geostatistical kriging method by the ArcGIS geostatistical analyst (Kitanidis 1997). Kriging allows for deriving spatial interpolation models of georeferenced point data and helps thereby to identify spatial trends in the data distribution (Kitanidis 1997). To find the most accurate model for the investigated cases an iterative, semi-automated procedure was followed, including data trend analysis, trend removal, semi-variogram modeling, automated model optimization and anisotropy correction. Models that are presented in this study represent those models that performed best when tested by cross-validation, with the lowest root mean square error (RMSE) and average standard deviation (ASD). Both chosen models (δ^2H and $\delta^{18}O$) apply the nugget effect which allows kriging to deviate from exact measured values for yielding a lower RMSE and ASD globally (Kitanidis 1997). Allowing the nugget effect was necessary primarily because for some sample locations several measurements were available that deviated slightly from each other. This deviation was either due to sampling at different dates, different sample types (e.g., river and groundwater) or, for example, due to samples from areas that are locally affected by reinfiltrated irrigation water, which is influenced by additional evaporation (section 4.4.1). The chosen models are therefore optimized for a regional trend assessment. However, all generated candidate models demonstrated similar regional trends. Model parameters of the chosen kriging models can be found online (https://doi.org/10.3390/hydrology5010003). The final models were masked by the extension of the Tarapacá, Quipisca, Juan de Morales, Quisma, Chacarillas, Salar del Huasco and Laguna Lagunillas basin for enhanced visualization.

Trendlines of stable isotope data were derived by linear regression. Statistical visualization of data was done by Tukey box plots (Frigge et al. 1989).

4.3.5. Mathematical calculation of the intersection of the local meteoric water line and a given local evaporation line

To calculate the point of intersection of a specific local evaporation line—with a known slope of approximately four (section 4.2) and containing a sample point *S*—and the local meteoric water line (Aravena et al. 1999), the following equations are needed:

$$\text{LMWL: } \delta^2H_p = 7.8 \times \delta^{18}O_p + 9 \qquad \text{Eq. 4-2}$$

$$\text{LEL: } n_s = \delta^2H_s - 4 \times \delta^{18}O_s \qquad \text{Eq. 4-3}$$

δ^2H_p and $\delta^{18}O_p$ are the isotopic values of regional precipitations, δ^2H_s and $\delta^{18}O_s$ are the isotopic values of a given meteoric water sample *S* and n_s is the respective y-intercept of the specific local evaporation line. For calculating the intersection point (δ^2H_i and $\delta^{18}O_i$) where the deuterium value of the specific local evaporation line is equal to the coordinates δ^2H_p and $\delta^{18}O_p$, the following equation is finally entertained:

$$\delta^{18}O_i = (n_s - 9.7) / 3.8. \qquad \text{Eq. 4-4}$$

The resulting value $\delta^{18}O_i$ is the initial $\delta^{18}O$ value in precipitation from which the isotopic composition of sample *S* evolved by evaporation-driven fractionation. Eq. 4-4 will be fed with data of the kriging models for $\delta^{18}O$ and δ^2H to yield a spatial distribution of the initial isotopic composition of meteoric waters in the study area.

4.4. Results

4.4.1. Geostatistical assessment of stable isotope data from the Andean Altiplano to the PdT Aquifer

The kriging method is applied to assess spatial trends in the georeferenced δ^2H and $\delta^{18}O$ datasets that include for both parameters 435 single measurements (Figure 4.3, section 4.3.4) (26 samples from the Salar del Huasco basin were not included due to a lack of coordinates). The presented interpolation models are those that exhibit the lowest RMSE and ASD.

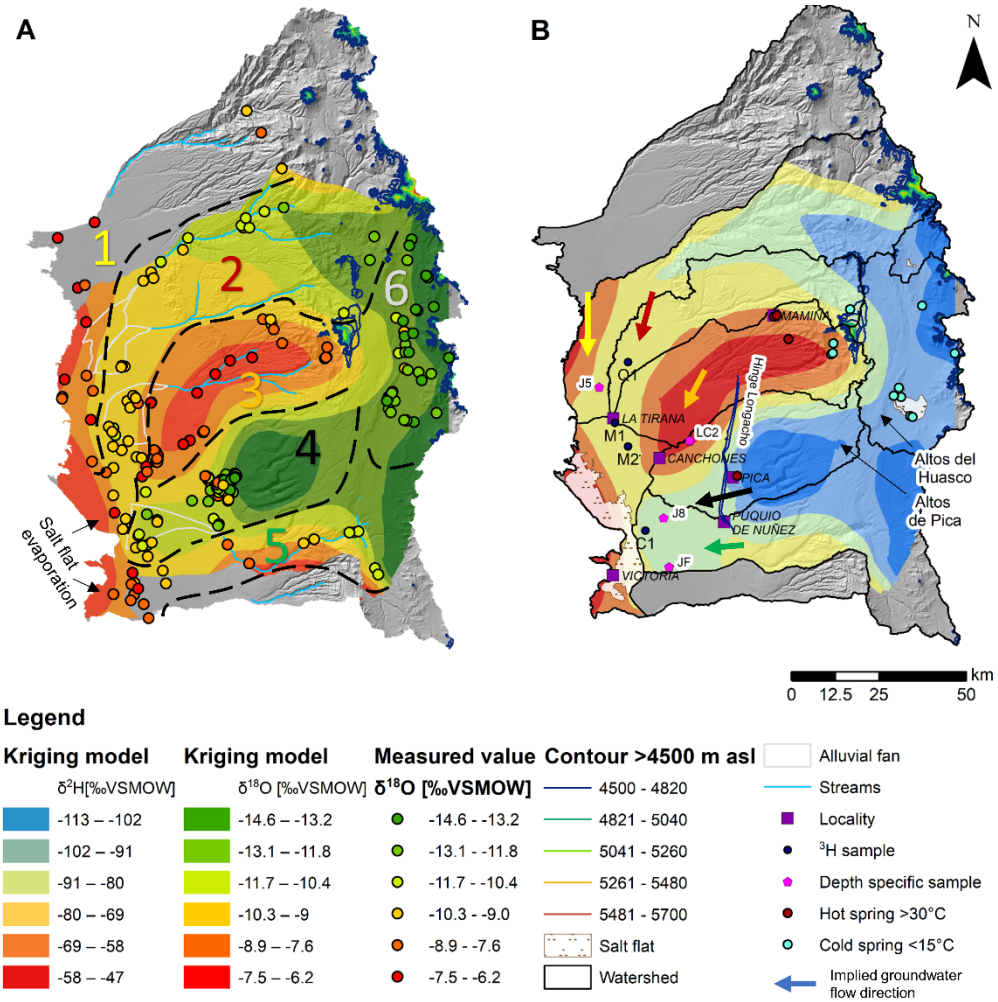

Figure 4.3 (**a**) Kriging model based on $\delta^{18}O$ values in river, ground and spring water and yielded meteoric water compartments 1–6 (limits marked by dashed lines), (**b**) Kriging model based on δ^2H data of river, ground and spring water and implied groundwater flow directions. Note that the extension of the alluvial fans at CP 3 and CP 5 is not corresponding with the respective groundwater flow direction (Figure 4.2b).

The derived δ^2H model exhibits an RMSE of 6.82‰ and an ASD of 5.92‰. The $\delta^{18}O$ model exhibits an RMSE of 0.89‰ and an ASD of 0.80‰. Reports on the model configuration and respective cross-validation plots can be found online (https://doi.org/10.3390/hydrology5010003).

The interpolation yields a clear spatial correlation that is almost identical for both parameters. Distinct meteoric water compartments (CP) within the study area are being visualized that exhibit different isotope value characteristics and correspond to the topographic watersheds in the region (Figure 4.3a,b). The statistical attributes of samples within the different compartments are summarized in Figure 4.4a,b.

CP 1 (18 samples) represents western marginal samples where the first and third quartiles of δ^2H values cover a range of −69–60‰ and for $\delta^{18}O$ values plot between −8.7 and −7.5. The water of CP 1 appears to originate from the Aroma basin.

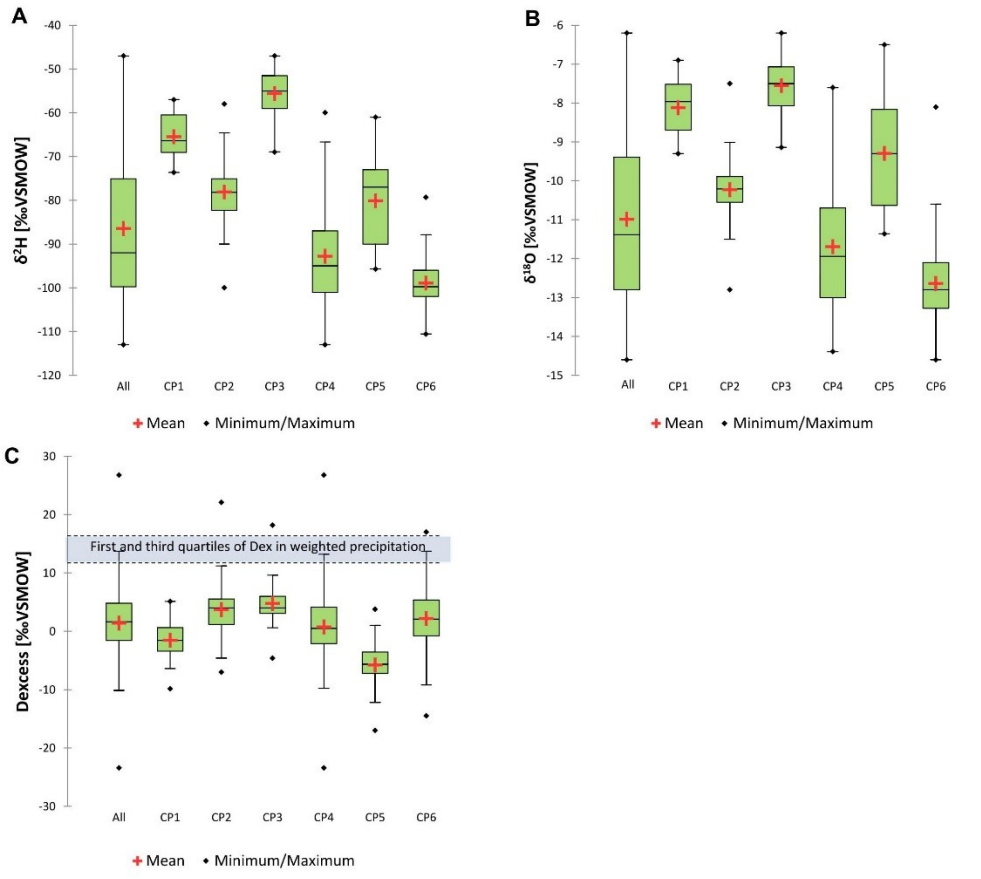

Figure 4.4 (**a**) Box plot of δ^2H data by compartment, (**b**) Box plots of $\delta^{18}O$ data by compartment, (**c**) Box plot of D_{ex} values by compartment, lower values are an indication for a higher isotope fractionation by evaporation (higher evaporative loss) (no significant difference in D_{ex} values of precipitations of north-western and east-north-eastern air masses).

CP 2 (48 samples) is associated with the drainage area of the Quebradas Tarapacá and Quipisca. δ^2H data range dominantly between −82‰ and −75‰ but decrease with higher altitudes. The first and third quartile of $\delta^{18}O$ values ranges from −10.5‰ to −9.9‰. Due to a lack of samples from the Quipisca basin, the Quipisca basin cannot be isotopically distinguished from the Tarapacá basin. Therefore, both basins are summarized into one compartment (CP 2).

CP 3 (54 samples) forms a distinct plume of higher δ^2H and $\delta^{18}O$ values which is physically related to the Juan de Morales River. This group marks δ^2H values in majority higher than −57‰. Its lower bound is formed by the δ^2H value −69‰ and the $\delta^{18}O$ value −9‰.

CP 4 (223 samples) shows low δ^2H values with down to −113‰ and $\delta^{18}O$ values down to ∼−13.5. It is associated with the Quisma basin. Recently it was demonstrated that the corresponding groundwater is recharged at the Altos de Pica recharge area (Figure 4.3b) (Scheihing et al. 2017). A slight increase of δ^2H and $\delta^{18}O$ values can be found in some samples of the local and shallow Pica aquifer, which is influenced by reinfiltrated irrigation and spring water affected by evaporation, which causes an additional isotopic fractionation (Galli and Dingman R. 1965; Fritz et al. 1981; DGA 2013).

Data of CP 5 (24 samples) shows a first and third quartile of δ^2H values at −90‰ and −73‰. For $\delta^{18}O$ respective values are −10.6‰ and −8.1‰. It lies in the drainage area of the Quebradas Chacarillas and Ramada. Some groundwater samples of this compartment and catchment, which were taken in the Andean Altiplano, reach δ^2H values of up to −95‰. Also here an isotopic value increase with decreasing altitude can be observed.

CP 6 corresponds to the Altiplano basins Salar del Huasco and Laguna Lagunillas (91 samples of the Salar del Huasco basin and three from the Laguna Lagunillas basin). The first and third quartile of δ^2H values plot at −102‰ and −96‰ respectively. $\delta^{18}O$ values range dominantly between −13.3‰ and −12.1‰.

The catchment-dependent isotopic characteristics are also reflected in the respective D_{ex} values as illustrated by Tukey box plots (Figure 4.4c). Extreme values outside the lower and upper bound of the box plots can be considered outliers (Frigge et al. 1989) (green boxes cover the data range that plots within the first and third quartiles). While CP 1 and CP 5 exhibit relatively low D_{ex} values in majority between 1‰ and −7‰, CP 3 exhibits highest D_{ex} values with 2–4‰. The first and third quartile of D_{ex} data of all sample groups plot below the first and third quartile of D_{ex} values in regional precipitations (Figure 4.4c).

4.4.2. δ^2H-$\delta^{18}O$-charts of all stable isotope data

Charting all PdT samples together in one δ^2H-$\delta^{18}O$-plot confirms results of earlier studies that found that stable isotope data from the PdT plots parallel to the LMWL (Figure 4.5a) (section 4.2). The resulting trend line of all PdT samples shows a slope of 7.4 (R^2 = 0.89) which is almost equal to the slope of the established LMWL of 7.8 (Aravena et al. 1999).

In comparison to that, Figure 4.5b summarizes a collection of stable isotope data (91 samples) from the Salar del Huasco basin (spring, river and groundwater). The Salar del Huasco basin abuts on watersheds draining into the PdT (Figure 4.2b). Contrary to the trend line of samples of the PdT, the trend line of data from the Salar del Huasco basin exhibits a slope of 3.9 (R^2 = 0.61), which is in accordance with empirically established LELs for the study area (section 4.2).

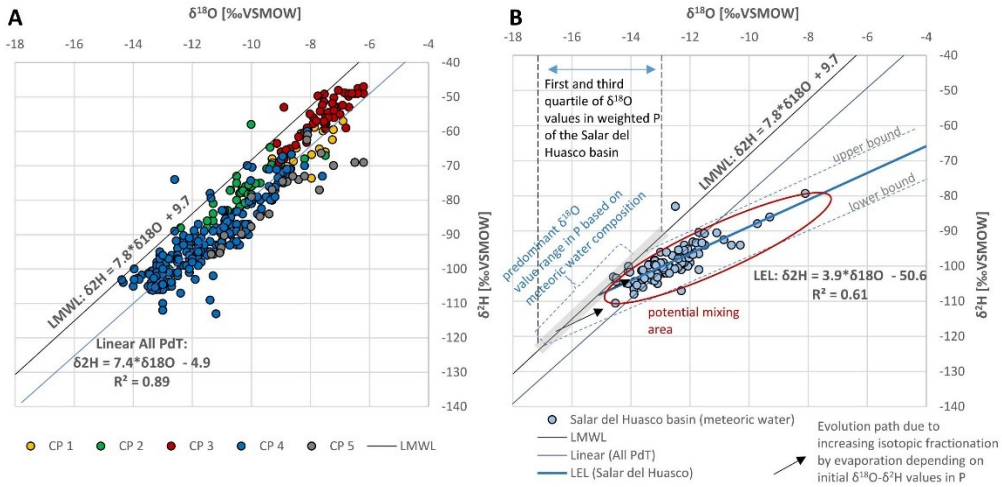

Figure 4.5 (**a**) $\delta^{18}O$ against δ^2H (all 367 samples of the PdT) and resulting trend line, (**b**) Collection of 94 river, groundwater and spring samples from the Salar del Huasco basin and resulting trend line (local evaporation line) (P = precipitation). The predominant $\delta^{18}O$ value range in P of the Salar del Huasco basin (~−17–14‰) is derived by the intersections of the lower and upper bound of the local evaporation line with the local meteoric water line (LMWL). The stable isotope value range in P for the Salar del Huasco basin varies due to amount, altitude and continental effects. The first and third quartiles of $\delta^{18}O$ data of weighted rainwater in the Salar del Huasco basin plots consistently at −17‰ and −13‰.

4.4.3. $\delta^{18}O$ against sample altitude for samples of compartments two, three and Five

Compartments two, three and five that correspond to the catchments Tarapacá/Quipisca, Juan de Morales and Chacarillas (section 4.4.1), provide enough Precordilleran slope samples to assess the relationship between $\delta^{18}O$ values and the sample altitude (Figure 4.6). As an apparent tendency, an increase of the $\delta^{18}O$ values with decreasing elevation can be observed for CP 5 and CP 2. CP 3 demonstrates no apparent increasing trend. However, available electrical conductivity data indicates generally an increase in salinity along the flow path with decreasing altitude. Isotope samples from the PdT Aquifer downstream of the respective compartments cluster typically around the upper end of the $\delta^{18}O$ values for each catchment. Nevertheless, the isotopic composition of groundwater below the alluvial fan of the Juan de Morales catchment does not correlate with the isotopic composition of its meteoric water upstream (Figure 4.3a and Figure 4.6c). Also, the isotopic values of groundwater below the alluvial fan of the Chacarillas river cannot be correlated with isotopically enriched flooding water at its alluvial fan but correspond to the isotopic composition of CP 4 and CP 5 upstream (further discussed in section 4.5.3). Floodwater was sampled on the day of flooding (data from Aravena et al. (1989)).

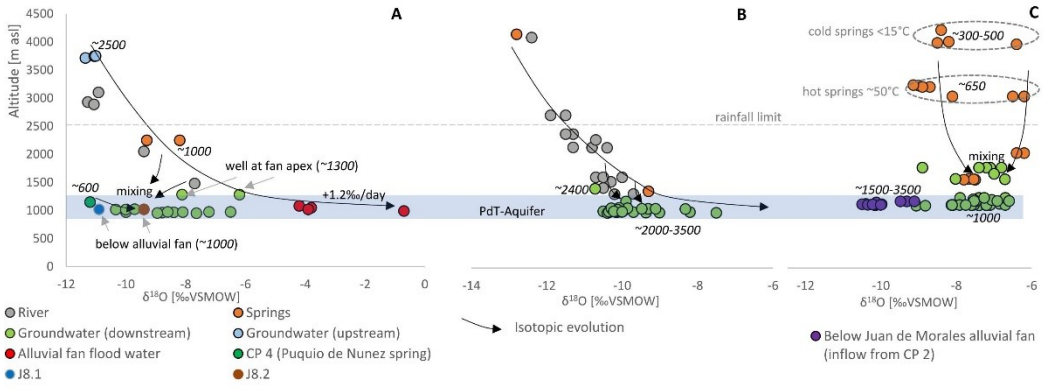

Figure 4.6 $\delta^{18}O$ against sample altitude (river, spring and groundwater) of different compartments (CP), (**a**) CP 5, Chacarillas basin, (**b**) CP 2, Tarapacá river, (**c**) CP 3, Juan de Morales river. Italic numbers indicate electrical conductivities of spring and groundwater in µS/cm.

4.4.4. Time series of stable isotope samples from spring sites between 1967 and 2014

The selected spring sites are the only ones in the study area that were sampled several times during the last 50 years. Figure 4.7 depicts the $\delta^{18}O$ values of the springs for different sampling campaigns from 1967 to 2014. The temporal resolution indicates that stable isotope values did not vary significantly over the last decades (average standard deviation for all springs: $\delta^{18}O_{asd}$ = 0.54‰, $\delta^{2}H_{asd}$ = 4.2‰). No strong long-term or seasonal variations can be observed. The spring site with the highest $\delta^{18}O$ variation are the Mamiña springs in CP 3.

4.4.5. Depth-specific stable isotope samples from the PdT Aquifer

Depth-specific stable isotope samples were taken at wells J5, LC2, J8 and JF during October 2015 (location displayed in Figure 4.3b, data presented inTable 4.2). Before sampling, temperature logs were recorded at the respective wells (Figure 4.8). While wells J5, J8 and JF are cased and exhibit screen sections (Jica 1995) well LC2 is an open borehole. The measurements at wells J5, JF and LC2 indicate that at the same locations stable isotope compositions of groundwater stayed almost constant over depth, with a tendency to slightly increase in salinity.

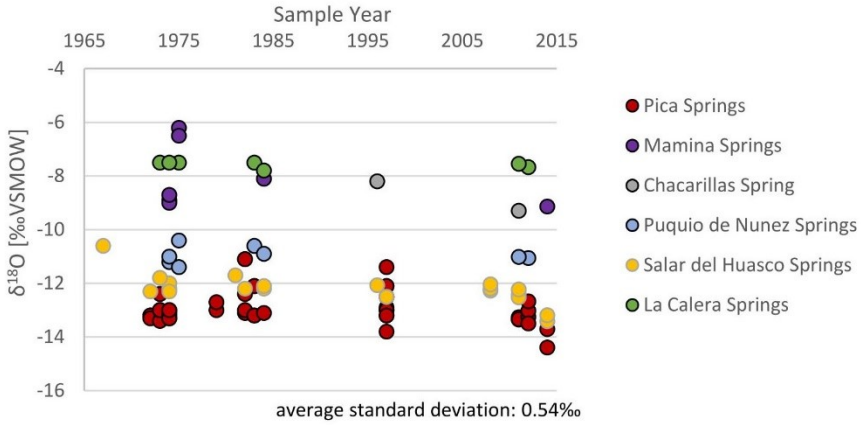

Figure 4.7 Time series of $\delta^{18}O$ measurements at different spring sites in the study area and average standard deviation in ‰VSMOW (1967–2014).

Table 4.2 Depth-specific samples taken for this study (locations displayed in Figure 4.3b).

Sample	**J5.1**	**J5.2**	**J5.3**	**J8.1**	**J8.2**	**JF.1**	**JF.2**	**LC2.1**	**LC2.2**
Date	October 2015	October 2015	October 2015	October 2015	October 2015	October 2015	October 2015	October 2015	October 2015
Sample depth [+]	36	150	262	60	170	68	158	85	255
Well elevation [-]		1029		1018		1017		1055	
Water level [+]		~32		~39		~55		~69	
Well depth [+]	300	300	300	210	210	224	224	270	270
Electrical conductivity (µS/cm)	3500	3660	3680	997	875	2450	2470	2380	2570
pH	8.7	9	9	8.3	8.5	8.1	7.8	8.2	8.1
δ2H *	−70.9	−70.1	−71.8	−80	−88	−87.7	−89.7	−57.8	−57.7
δ18O *	−8.7	−8.8	−8.9	−9.4	−10.9	−10	−10.3	−7.5	−7.5
Dex *	−1.5	0.3	−0.9	−5.2	−0.6	−7.6	−7	2	2.5

* [‰ VSMOW]; [+] [m bgl]; [-] [m asl].

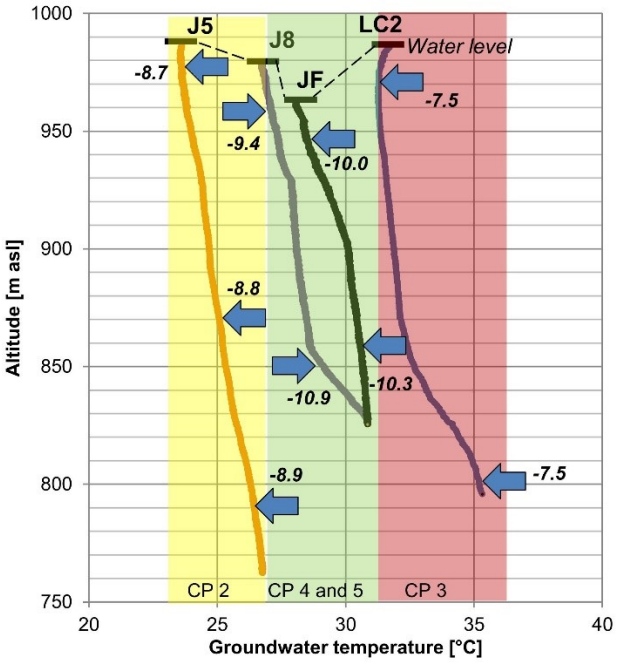

Figure 4.8 Temperature logs of wells J5, J8, JF and LC2 and depth of depth-specific stable isotope samples (blue arrows mark sample depth of depth-specific samples, italic numbers indicate measured $\delta^{18}O$ values).

Only at well J8 a marked difference between two sample depths can be identified. While the sample J8.2, taken at 170 m bgl, shows a $\delta^{18}O$ value of −10.9‰ with a conductivity of 875 µS/cm, the sample J8.1 (60 m bgl) demonstrates −9.3‰ $\delta^{18}O$ and 997 µS/cm. Also, the D_{ex} value differs by 4.6‰.

Besides, the temperature log indicates that in the case of wells J8 and LC2 a temperature gradient increase occurs at round about 860 m asl. At well J5 a continuous temperature increase is observed. At well JF the gradient appears to decrease slightly from ~900 m asl on. Noteworthy is the shift of the temperature profiles depending on the earlier delineated aquifer compartments (section 4.4.1).

4.4.6. ^{3}H samples from shallow alluvial fan groundwater in the PdT

^{3}H values of groundwater of four shallow wells situated at alluvial fans (af) show that no significant amounts of ^{3}H can be detected (Table 4.3 and Figure 4.3). A sample from the 54 m deep well C1 (water level at ~20 m bgl) at the western part of the Chacarillas fan in CP 4 shows no apparent tritium activity. Also, two samples of the Juan de Morales fan were taken that is situated in CP 2. The samples show tritium values ≤0.09 TU. A sample from the Quipisca alluvial fan (located in CP 2, Figure 4.3a) demonstrates likewise values of ≤0.09 TU.

Table 4.3 Isotope data of shallow groundwater at alluvial fans (alluvial fan = af, EC = electrical conductivity) (position of wells displayed in Figure 4.3b).

Sample	Q1	M1	M2	C1
Date	February 2011	February 2011	February 2011	February 2011
Area	Quipisca af	Juan de Morales af	Juan de Morales af	Chacarillas af
Well depth (m bgl)	Unknown (shallow)	20	24	54
EC (µS/cm)	1994	1681	2500	796
T (°C)	26.8	24.5	24.0	28.0
pH	8.52	7.55	7.74	8.42
^{3}H (TU)	≤0.09	≤0.09	≤0.09	≤0.09
$\delta^{18}O$ (‰VSMOW)	−10.8	−10.15	−9.98	−10.82
$\delta^{2}H$ (‰VSMOW)	−79.7	−81.3	−78.6	−86.3
D_{ex} (‰VSMOW)	0.94	−0.1	1.24	0.26
Source	(CMDIC 2012)	(CMDIC 2012)	(CMDIC 2012)	(CMDIC 2012)

4.5. Discussion

4.5.1. Hydrological processes controlling stable isotope tracers in the Salar del Huasco basin (Altiplano)

A significant hydrological process that alters stable isotope values of groundwater in arid regions is isotopic fractionation by evaporation that affects meteoric water before infiltrating into the underground (Clark and Fritz 1999; Kendall 2006). It causes the $\delta^{18}O$-$\delta^{2}H$ composition of groundwater to deviate from the trend of the LMWL—following a LEL and leads typically to an increase of the $\delta^{18}O$ value and hence a decrease of the D_{ex} value. Also, D_{ex} values in groundwater that are significantly lowered compared to D_{ex} values of regional precipitations indicate an isotopic fractionation by evaporation prior to recharge (Clark and Fritz 1999).

The effect of isotopic fractionation by evaporation can be observed well for data from the Salar del Huasco basin (Figure 4.5b). The trend line of respective samples exhibits a slope of 3.9 and is thereby in accordance with the slope of established empirical LEL in the region showing a value of ~4 (section 4.2). Hence, the general distribution of stable isotope data of spring, river and groundwater from the Salar del Huasco basin reflects the effect of an isotopic enrichment induced by evaporation of meteoric water prior to infiltration and is satisfyingly explained by this process. The dominance of isotopic fractionation by evaporation is confirmed by the lowered D_{ex} values of the dataset compared to values of regional (winter and summer) precipitations (Figure 4.4c, CP 6). However, Figure 4.5b also demonstrates a certain fuzziness of the data clustering in a corridor above and below the calculated local evaporation trend line, which is quantified by a moderately good regression coefficient (R^2) of 0.61. It is proposed that the cause of this fuzziness is the natural variation of the initial $\delta^{18}O$-$\delta^{2}H$ composition of precipitations that fall in the Salar del Huasco basin. These variations can be influenced by amount, altitude and continental effects, that are known to occur in the Andean Altiplano (Aravena et al. 1999; Uribe et al. 2015). Accordingly, the first and third quartile of $\delta^{18}O$ values of sixteen weighted rainwater samples of the Salar del Huasco basin plot between −17‰ and −13‰ (based on data of Fritz et al. (1981), Aravena et al. (1999) and Uribe et al. (2015)). In accord with that, the intersections of the estimated upper and lower bound of

the identified LEL with the LMWL mark a $\delta^{18}O$ value range between −17‰ and −14‰ (Figure 4.5b). That is because waters with isotope values along the upper and lower bounds must have evolved from rainwater departing from the LMWL along an evaporation line with a slope of ~4.

An additional effect that probably influences this isotope data are groundwater mixing processes occurring between the highest and the lowest isotope values in the respective aquifer (conservative mixing within red circle in Figure 4.5b). However, the most extreme isotope values that were used to delineate the predominant isotope value range of precipitations can be considered to be (almost) unaffected by mixing processes. That is because the datasets suggest that margin values represent the extreme ends of the investigated group and hence they cannot be the result of a substantial mixing. Therefore, mixing processes within the respective meteoric water compartment are negligible for estimating the predominant value range of feeding precipitations.

Another factor that must be taken into account when assessing stable isotope data in the Andean area are interactions with the lithosphere under hydrothermal conditions. Although previous isotopic studies in the Andean Altiplano suggest that isotopic exchange processes can occur in arid basins associated with hot springs (Cortecci et al. 2005; Herrera et al. 2016), isotopic interactions with the lithosphere cannot be observed for data from the Salar del Huasco basin. Such an effect would cause a limited set of samples —particularly of thermally influenced springs—to deviate from the evaporative trend observed for the basins meteoric water. This is not the case. Overall, the Salar del Huasco basin exhibits only slightly thermally influenced springs (~22–25 °C) but no hot springs (Uribe et al. 2015; Scheihing et al. 2017).

4.5.2. Hydrological processes controlling stable isotope tracers in the Pampa del Tamarugal and Andean Precordillera

Hydrothermal water-rock interactions

Jayne et al. (2016) discussed the possibility that isotopic anomalies encountered for waters close to the Juan de Morales basin (CP 3), might be caused by hydrothermal water-rock interactions. In fact, the Juan de Morales basin exhibits

some hot springs (water temperature ~50 °C) at altitudes around 2800 m asl (among others in Mamiña) (Figure 4.3b, Figure 4.6c and Figure 4.7). However, Uribe et al. (2015) sampled cold springs (<15 °C) in the Juan de Morales basin at elevations of ~4000 m asl (Figure 4.3b and Figure 4.6c). Despite the absence of a hydrothermal imprint on these cold springs, the respective waters show likewise relatively high $\delta^{18}O$ values that are in perfect accord with values measured at nearby hot springs. Hence, it is not likely that hydrothermal isotope exchange processes affect the isotopic composition of groundwater in CP 3 despite a possible circulation along deep faults into fractured segments. Also, thermal waters at Pica which circulate along disruption zones within the Andean slope to depths of ~900 m bgl (Scheihing et al. 2017), show no anomalous deviation in their isotopic composition from surrounding waters in CP 4 (Figure 4.3 and Figure 4.5). Overall there is, therefore, no evidence for the assumption that hydrothermal water-rock interactions affect the isotopic composition of groundwater west of the Andean Precordillera. Hence, there must be other effects involved that cause catchment-dependent isotopic value ranges.

Isotopic fractionation by evaporation of meteoric waters and initial isotopic composition of feeding rainwater

It is evident that spring- and groundwater from the PdT and Andean Precordillera must be strongly affected by an isotopic fractionation caused by evaporation. Apart from the high potential evaporation in the region (section 4.2), this is demonstrated by two facts. Firstly, D_{ex} values of meteoric waters west of the Andean Precordillera are consistently lower than in regional precipitations (Figure 4.4c). Secondly, there is evidence of a continuous $\delta_{18}O$ enrichment with decreasing altitude along at least two catchments in the region (). These two arguments allow for the conclusion that discharging spring and river water from Andean slope catchments is affected by isotopic fractionation caused by an ongoing evaporation on its way downstream and should evolve dominantly along an evaporation line as in the case of the Salar del Huasco basin (section 4.5.1).
When reviewing the different datasets of the spatial compartments of section 4.4.1 (Figure 4.3a and Figure 4.4), the isotopic data of CP 1–5 plot indeed in clusters similar to the data of the Salar del Huasco basin (Figure 4.5a,b). Analogous to the procedure applied to data from the Salar del Huasco basin—by

estimating an upper and lower bound for evaporation-driven fractionation—the predominant isotope value range of feeding precipitations of CP 1–5 can be estimated. Instead of following a graphical procedure as in the case of the Salar del Huasco basin (Figure 4.5b), the assessment can be carried out mathematically based on the data provided by the kriging models of $\delta^{18}O$ and $\delta^{2}H$ (Figure 4.3, section 4.3.5).

The assessment proposes that rainwater falling in the Juan de Morales basin exhibits predominantly $\delta^{18}O$ values between −11 and −7‰ (Figure 4.9a). On the contrary precipitations in CP 6 and CP 5 would exhibit dominantly $\delta^{18}O$ values from ~−17‰ to −13‰ (in accordance with the assessment in section 4.5.1) and in CP 4 from ~−19‰ to −13‰. The precipitations alimenting meteoric waters in CP 2 would show $\delta^{18}O$ values of dominantly ~−15 to −11‰. The respective signals lose in intensity downstream—below the rainfall limit of ~2500 m asl—where groundwater mixing processes become more significant and hence respective values are being averaged (Figure 4.9a).

Overall, the mentioned processes (catchment-dependent isotopic composition of rainwater, evaporation and eventual groundwater mixing) would cause the samples to shift from the LMWL collectively but at the same time deviate from the respective LEL.

Consequently, the reason for the different $\delta^{18}O$ value ranges in precipitations for different catchments will be discussed.

Catchment-dependent $\delta^{18}O$ value ranges of precipitations: topographic controls on air mass and vapor mixing

Previous authors speculated about the reasons why collectively examined $\delta^{18}O$-$\delta^{2}H$ samples from the PdT Aquifer show such a wide value range and plot parallel to the LMWL (Figure 4.5a).

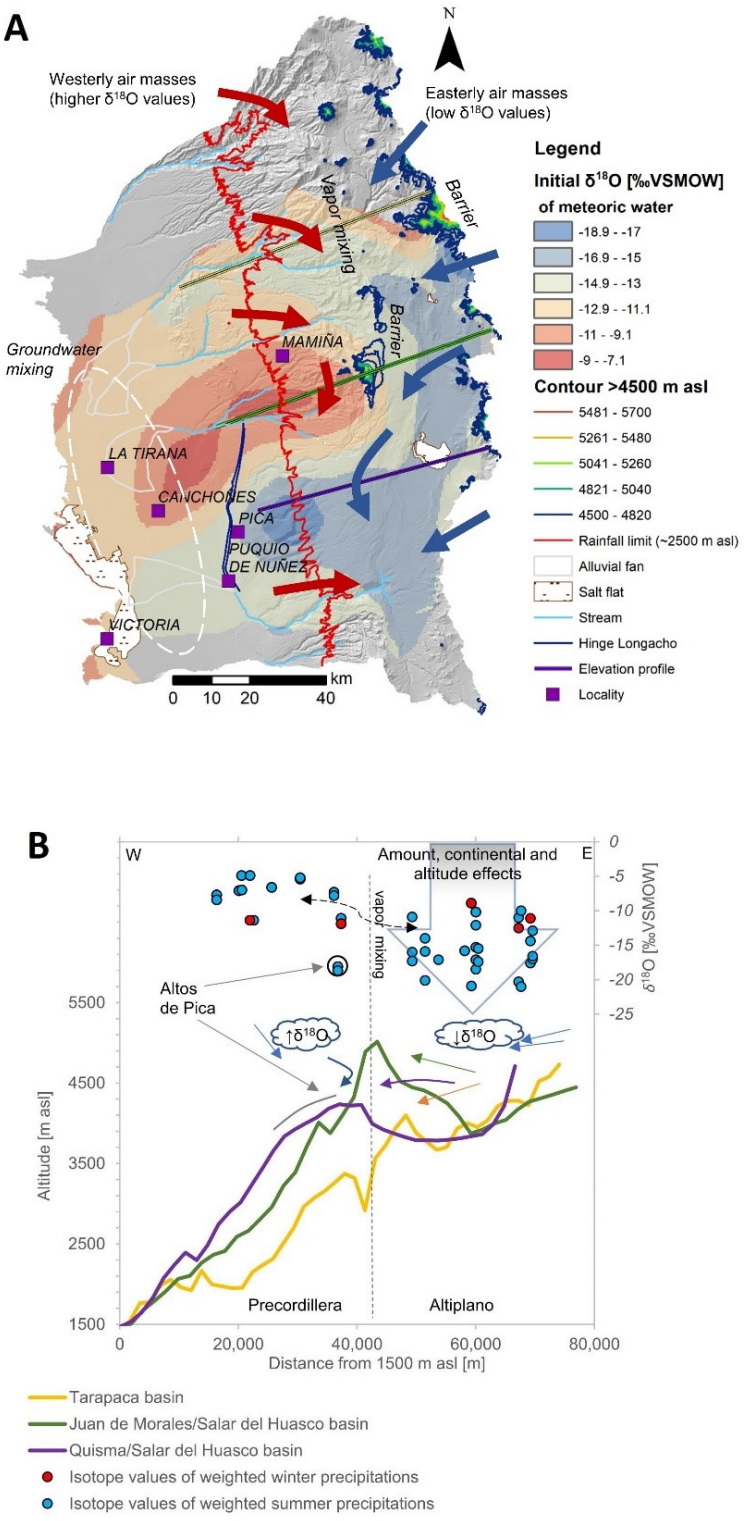

Figure 4.9 (**a**) Approximate initial $\delta^{18}O$ values of meteoric waters in the study area prior to evaporation-driven fractionation. The map is based on the interpolation data of the kriging models for $\delta^{18}O$ and $\delta^{2}H$ (Figure 4.3), arrows indicate suggested air mass contributions, (**b**) Schematic sketch of proposed topographic controls of isotope values in precipitations contributing to recharge in the PdT (isotope data of rain originates from Fritz et al. (1981), Uribe et al. (2015), and Aravena et al. (1999)).

Reasons proposed for this observation were different types of precipitation (snow and rain) or a change in climatic conditions (paleo-rain) (Magaritz et al. 1989; Aravena 1995; Aravena et al. 1999), as well as assumptions about recharge areas at different altitudes (altitude effect) (Aravena 1995). There are two arguments to disregard the hitherto proposed reasons.

The first argument is that data from the Salar del Huasco basin of the nearby Andean Altiplano consistently plot along an expected LEL (Figure 4.5b). Apparently, this water must have been recharged under the same climatic conditions as the water from the PdT Aquifer because it is known that pluvial phases in the Altiplano foster recharge in the PdT through discharging rivers (section 4.2). To assume that different types of precipitation or a variation in climatic conditions would have changed or affected the isotopic composition of rainfall in northern Chile, to be similar to waters from the PdT, is therefore not justified.

The second argument is that meanwhile it is known that altitude effects are limited to the Andean Altiplano. Such altitude effects develop with the elevation increase along the eastern Andean flank and are consequently linked to abundant summer rainfalls with mainly easterly and north-easterly vapor sources (originating from the Amazon basin and the Atlantic Ocean) (Aravena et al. 1999; Vuille and Werner 2005). Typical altitude effects do not apply to vapor masses rising along the western flank of the Andes with dominantly west-north-western vapor sources) (Aravena et al. 1999; Vuille and Werner 2005). Hence, different recharge altitudes cannot explain the spatially strongly varying isotope values in the PdT that exist up to sample altitudes above 4000 m asl

It is argued that the main reason for the observed variation of $\delta^{18}O$ and $\delta^{2}H$ values in the different compartments of the PdT Aquifer (Figure 4.3a) are predominant long-term stable isotope value ranges in precipitations that aliment the relevant recharge areas (as discussed in section 4.5.1 and section 4.5.2). These $\delta^{18}O$-$\delta^{2}H$ value ranges are likely controlled by topographic characteristics of the catchments in the transition zone from the Altiplano to the PdT that can show elevation differences of up to 1200 m (Figure 4.2b).

This is emphasized by Figure 4.9a that displays the distribution of the theoretical initial $\delta^{18}O$ value of meteoric waters prior to evaporation-driven fractionation, when neglecting eventual groundwater mixing processes (mixing occurs primarily in the PdT-Aquifer) (section 4.3.5). Anomalies in the initial $\delta^{18}O$ values of meteoric waters are associated with high topographic elevations (~above

5000 m asl) that form barriers against easterly air masses with depleted $\delta^{18}O$ values (Figure 4.9a). Further, Figure 4.9b depicts the contrast in $\delta^{18}O$ values in precipitations east and west of the Andean mountain range, which is caused by different vapor sources situated either east-northeast or west-northwest of the Andean mountain range. Similar observations of a rapid change in vapor isotope values when comparing windward and leeward sides of mountain ranges were also made, for example, in the Canadian Rocky Mountains and the Himalaya Mountains (Yonge et al. 1989; Clark and Fritz 1999; Hren et al. 2009).

In this understanding, the Juan de Morales basin exhibits a mountainous barrier against the windward side of easterly trade winds, with maximum elevations above 5000 m asl and so does the western limit of the Tarapacá basin. This condition probably leads to a rainout at their eastern margins, due to the adiabatically cooling of rising easterly air masses. Eventually crossing moistures could mix with predominantly north-western air masses and yield relatively elevated $\delta^{18}O$ values in precipitations of approximately ~−11 to −7‰ for CP 3 and −15 to −11‰ for CP 2 (Figure 4.9a, section 4.5.2).

Finally, it is crucial to understand why rainfall above the Quisma basin shows partially relatively depleted $\delta^{18}O$ values. Vapors that arrive from east-northeast on the mountainous barrier of the Juan de Morels basin will be depleted on its leeward side due to altitude and amount effects (rainout). Altitude effects are observed to occur in the Salar del Huasco basin with a $\delta^{18}O$ depletion of approximately −0.64‰/100 m (Uribe et al. 2015). These depleted vapor masses probably arrive occasionally with northeastern winds at the adjacent Altos de Pica mountain ridge of the Quisma basin and precipitate (Figure 4.3b and Figure 4.9a,b).

While altitude, amount and continental effects affecting regional precipitations in the study area were described before (Aravena et al. 1999; Vuille and Werner 2005; Terzer et al. 2013), the importance of local topographic features on the inhibition or facilitation of vapor mixing processes was disregarded so far when assessing stable isotopes of groundwater in the Atacama Desert.

Overall, it is this phenomenon of locally varying isotope value ranges in precipitations that allows for using stable isotopes in the PdT as a useful tracer for groundwater flow mapping. The influence of Andean topographic features on the movement of air masses and vapor mixing are very likely of relevance for similar basins of the Atacama Desert where basin-dependent pronounced topographic differences occur.

4.5.3. Kriging models, regional groundwater flow regime and identified recharge areas

The correlation structure that is being mapped by the kriging models (Figure 4.3a,b) is that of the spatial distribution of the isotopic composition of meteoric waters in the region. The respective RMSE and ASD of both models (δ^2H model: RMSE = 6.82‰, ASD = 5.92‰ and $\delta^{18}O$ model: RMSE = 0.89‰, ASD = 0.80‰) are relatively low and reasonable when considering that the dataset consists of different kinds of meteoric water (surface and groundwater) and includes samples of campaigns spanning over a period of ~50 years. Particularly spring sites were sampled several times during that period. $\delta^{18}O$ measurements at these springs show an ASD of 0.54‰ (Figure 4.7), which is quite close to the ASD of the respective kriging model (ASD of respective δ^2H values is 4.2‰). However, the low ASD of isotopic measurements at springs also demonstrates that the isotopic composition of groundwater at different localities is not exposed to prominent (seasonal) variations. That is reasonable when taking into account that groundwater in the Atacama Desert exhibits typically corrected residence times of a few thousand years (e.g., Pica springs and Puquio de Nunez spring (Fritz et al. 1981; Scheihing et al. 2017)). Long residence times damp signals of slightly varying seasonal variations due to mixing within the respective reservoir. Hence, extreme isotopic values—as associated with depleted rains during storm events—are smoothed out in the given spring data (as far as observed). Applying this insight to other groundwater measurements in the region implies that the observed isotopic conditions—as visualized by the kriging models—reflect long-term averaged conditions due to subsurface mixing within each compartment. However, based on the given dataset alone it is impossible to quantify or further distinguish these mixing processes.

The interpolations of δ^2H and $\delta^{18}O$ data confirm each other in their spatial extent, which allows for identifying six meteoric water compartments that are apparently physically related to different catchments in the study area (section 4.4.1, Figure 4.3a,b). Due to the catchment-dependent isotope value ranges (section 4.5.2) the spatial trends in δ^2H and $\delta^{18}O$ data can be used to trace the regional groundwater flow regime and indirectly derive conclusions about the recharge areas of respective waters. The fact that the geostatistically modeled spatial molding of CP 1–5 is in high accordance with the regional groundwater flow direction—as indicated by regional water table contour lines—further

substantiates the validity of the identified spatial trends (Figure 4.2b and Figure 4.3a,b). Besides, a preliminary comparison of electrical conductivity measurements for CP 2, 3 and 5 (Figure 4.6), also confirms the delineated groundwater flow regime by a continuous increase of the salinity along the flow path. Also, an earlier report on major ions of the central PdT Aquifer distinguished very similar aquifer compartments based on chemical groundwater types (Risacher et al. 1999).

Hence, groundwater in CP 1 likely originates from the Aroma basin, groundwater in CP 2 is recharged at the Tarapacá and Quipisca basins, and groundwater from CP 3 infiltrates in the Juan de Morales basin. Groundwater in CP 4 is recharged in the Quisma basin (in particular at the Altos de Pica area [10]), and groundwater associated with CP 5 percolates in the Chacarillas catchment. Finally, close to the western margin of the PdT where near-surface water prevails at salt flats, further evaporation processes probably cause waters to enrich isotopically increasingly as reflected by the respective kriging models (Figure 4.3). These enriched brines might affect groundwater close to salt flats isotopically by either density-driven recirculations or modern groundwater pumping from production wells (change of natural flow conditions).

A first preliminary observation of the distinct patterns in the distribution of δ^2H values in the PdT (based on less than 25 samples and without any quantitative method applied) was made by Fritz et al. (1981). Nevertheless, the results presented in the current study yield for the first-time a statistical assessment of the isotopic conditions based on an extensive stable isotope dataset.

Depth-specific samples indicate that the geostatistical trend of isotope values in the region is consistent over varying depths of the aquifer (up to ~250 m bgl) despite the existence of different aquifer storeys. This observation is reasonable when considering as one of the primary recharge mechanisms an inflow from slope infiltrations of streambeds together with water mixing along the river course and subsurface flow path (check graphical abstract, Figure 4.1). The temperature profiles of wells J8 and LC2 indicate that very likely different aquifer storeys were sampled because of a change in the temperature gradient (Figure 4.8). However, due to the constantly rising temperature profiles at wells J5 and JF, here vertical flows could occur and lead to water mixing within the wells. Nevertheless, the deviation of a deep and shallow sample from J8 could indicate a mixing of water from CP 4 and 5 (Figure 4.8). Such a mixing, in turn, would be in accordance with the spatial distribution of observed regional groundwater

compartments. Based on a binary isotopic mixing model—incorporating water from the Puquio de Nunez area and groundwater from the fan apex of the Chacarillas fan—the shallow sample at well J8 consists of a water mix of 50:50 from both reservoirs. The deeper sample at J8 is almost identical to groundwater from the Puquio de Nunez area.

The spatial extension of the identified regional isotopic CP 4 also demonstrates that the groundwater which is recharged at Altos de Pica through rainfall is passing the Longacho Hinge (conservatively treated as an impermeable barrier; (Rojas and Dassargues 2007; Rojas et al. 2010)) and finally discharging into the PdT Aquifer (Figure 4.3a). A recent geophysical survey (gravity and TEM measurements) supports that the bedrock of the Longacho Hinge dips section-wise deeper into the underground, facilitating pathways for a shallow inflow from the Andean slope through sedimentary units into the PdT Aquifer (DGA 2013).

4.5.4. Recharge mechanisms

The isotopic assessment allows for some conclusions regarding recharge mechanisms of the PdT Aquifer. An indication that can be derived from the spatial isotope distribution is that alluvial fan recharge in response to flooding is probably negligible for the Juan de Morales and the Chacarillas alluvial fans. It was proven that water, flooding the Chacarillas alluvial fan after storm events, is rapidly enriching in $\delta^{18}O$ by ~1.2‰/day due to evaporation, and is relatively enriched with values above −4‰ $\delta^{18}O$ (Figure 4.6a) (Aravena et al. 1989). Furthermore, it is known that evaporation affects percolating waters up to 2 m bgl in the Atacama Desert (Houston 2006a).

Infiltrating floodwater caused by storms should, therefore, exhibit significantly higher $\delta^{18}O$ and $\delta^{2}H$ values when compared to water recharged along the river course and fan apex. As can be seen from Figure 4.6a, floodwater at the Chacarillas fan recently sampled after flooding, can isotopically not be correlated with shallow groundwater at the well J8 (water level at well J8 is ~39 m bgl). On the contrary, as visualized in Figure 4.3a and Figure 4.6a,c the isotopic composition of water below the alluvial fans of the Chacarillas (CP 5) and Juan de Morales (CP 3) catchments demonstrates lower $\delta^{18}O$ and $\delta^{2}H$ values than exhibits the water of the relevant basins upstream. This finding is very likely due to

groundwater flowing in from adjacent catchments as also indicated by the groundwater level contour lines (Figure 4.2b). The water of CP 2 can be found below the Juan de Morales alluvial fan and water of CP 4 below the Chacarillas alluvial fan (Figure 4.3a). The inflow from other basins is confirmed by a preliminary comparison of respective electrical conductivities of groundwater (Figure 4.6). Water below the Juan de Morales fan, for example, corresponds with values of 1500–3500 µS/cm to resources in CP 2. In this context, $\delta^{18}O$-data and electrical conductivity measurements propose that shallow groundwater at well J8 (Chacarillas alluvial fan) is the result of a mixing of a recharge provided from the lower stream segment of the Chacarillas river and the Puquio de Nunez area (CP 4) (Figure 4.6a).

Due to the apparent absence of the isotopic imprint of fractionated floodwater on shallow groundwater around alluvial fans, flash floods might not be in the long-term a significant source of recharge. The absence of ^{3}H in shallow groundwater at alluvial fans (<0.09 TU) emphasizes this conclusion because modern rainwater exhibits ^{3}H values of 3 to 10 TU in the region (Aravena et al. 1999). The respective shallow groundwater must, therefore, show residence times above 50 years. This finding implies that modern floodwater may be lost in majority to evaporation. Accordingly, earlier detected ^{3}H amounts in groundwater of the PdT were always associated with sites of agricultural activity and were attributed to isotope exchange with the atmosphere during watering and irrigation-return flow (Fritz et al. 1981). However, a more detailed study of the different alluvial fans could provide more evidence for the presented conclusion. Recharge conditions may also vary from fan to fan.

Nevertheless, the understanding that at the Chacarillas alluvial fan there is no significant recharge occurring from floodwater is in contradiction with Houston (2002). He argues—based on the interpretation of a hydraulic head rise at well J8 (total depth ~200 m bgl)—that a regular in situ recharge from the alluvial fan takes place, with a minimum average annual recharge equivalent to around 200 L/s. However, the phenomenon of the hydraulic head rise at well J8 could be explained solely by a short-term hydraulic head propagation (pressure) induced by recharge occurring at the sloping stream bed and fan apex of the Chacarillas river (as depicted in the graphical abstract). Such a continuous propagation of pressure signals is controlled by the aquifers hydraulic diffusivity and was recently demonstrated to occur in the Quisma basin (Tóth 2009; Scheihing et al. 2017). Due to the low specific storage of confined aquifers, which receive a

focused recharge at the basins margin (see graphical abstract), the pressure signal could propagate within weeks in the PdT Aquifer. This signal propagation could cause a slightly delayed water level rise at well J8 in response to distant recharge events, which can be easily misinterpreted as an in situ recharge (a hydraulic head time series analysis to demonstrate this effect exceeds the framework of this article but may be subject to a later study).

Another factor that supports the absence of alluvial fan recharge is the presence of thick (>20 m) unsaturated and clayey sediment layers at the alluvial fans of the Juan de Morales and Chacarillas basins. These unsaturated top layers were identified earlier by remote sensing imagery, drilling profiles and extensive TEM measurements carried out in the PdT (Jica 1995; Urqueta et al. 2017). Clayey top sediments show resistivities in the magnitude of 700–1000 Ωm compared to ~20 Ωm of the saturated aquifer section and ~100 Ωm for sediments of the vadose zone (Jica 1995). A regular percolation from alluvial fans (4-year return period of floods, 4.2) would need to result in thick vadose zones connecting clayey surface sediments at alluvial fans with the aquifer, which is not the case. This argumentation line yields another indication towards the conclusion that no regular and significant recharge occurs from the discussed alluvial fans.

Despite the vital recharge area Altos de Pica (~4000 m asl, section 4.5.3) in the Quisma basin (CP 4), it is proposed that the principal recharge facilitated into the PdT Aquifer occurs along the lower segments of rivers that discharge into the sedimentary basin. That is derived from the relation between catchment-specific $\delta^{18}O$ values and their sample altitudes (Figure 4.6). For CP 2 and 5 the $\delta^{18}O$ values of groundwater from the PdT Aquifer match with the $\delta^{18}O$ values of river and spring water of the corresponding catchments at altitudes between ~2200 m and 1000 m asl (Figure 4.6a). This matching implies that the water was recharged at these altitudes because isotopic fractionation by evaporation stopped at some point downstream. Major north-south striking faults in the region could reduce a prominent lateral groundwater inflow from higher elevations which is supported by the presence of several springs along the Andean Precordillera (Figure 4.2b, section 4.2, (Nester 2008; Scheihing et al. 2017)).

However, due to a lacking evaporative enrichment trend in data of CP 3 here, recharge areas providing higher fractions of lateral groundwater inflow to the PdT Aquifer could include streambed sections at higher elevations (Figure 4.6c and Figure 4.1). That is underlined by the fact that respective waters show highest D_{ex} values for the region (Figure 4.4c), which implies a minor

fractionation by evaporation along the river course and hence possibly higher recharge elevations.

Another factor that influences the D_{ex} value is whether a basins geologic characteristic facilitates the opportunity for interflow to take place along the streambed (reduced evaporation of river water). The importance of interflow is demonstrated by the fact that D_{ex} values from the Chacarillas basin are the lowest for the region (Figure 4.4c) and its host formations are in great parts impermeable Jurassic and Cretaceous quartzous sandstones (Chacarilla formation) or marine sedimentary rocks (Majala formation) (Blanco and Tomlinson 2013). Whereas streams in the Juan de Morales basin run mainly above Oligocene to Miocene sedimentary rocks (Altos de Pica formation) with thin layers of ignimbrites (Tambillo ignimbrite) that tend to weather easily (Blanco and Landino 2012; Scheihing et al. 2017).

However, overall it is known that a focused recharge occurring beneath ephemeral streams is in many arid environments the principal recharge mechanism (Scanlon et al. 2006; Guo et al. 2015). The derived conclusions imply that diffuse recharge at higher elevation is—in the mentioned cases—of minor importance. The presence of thick dry deposits (up to 500 m thickness and 4000 m asl (Blanco and Landino 2012; Blanco and Tomlinson 2013; Scheihing et al. 2017)) along the Andean Precordillera, that form ravines through which rivers discharge, supports that because a diffuse recharge would demand of infiltrating rainfall fractions to penetrate these dry layers. That is not the case. Hence, focused recharge along ephemeral rivers fed by direct runoff is much more likely. Only the Altos de Pica area appears to facilitate geological conditions for a substantial diffuse recharge along the Andean Precordillera to the PdT Aquifer, due to its relatively plainly deposited and well-fractured ignimbrites (Acosta and Custodio 2008; Uribe et al. 2015; Scheihing et al. 2017). However, further research is recommended to substantiate the elaborated conclusions.

4.6. Conclusions

Earlier introduced assumptions about why collectively examined groundwater isotope samples from the Pampa del Tamarugal (PdT) Aquifer plot parallel to the local meteoric water line need to be reconsidered. A correlation of isotope data from the PdT with data from the nearby Andean Altiplano excludes a variation of

isotope values in precipitation due to a change of regional climatic conditions. Other mechanisms are proposed to explain the isotope characteristics of meteoric water in the PdT. These mechanisms comprise rainout (amount effects) and altitude effects at the Andean eastern windward side and a mixing of air masses with different isotopic compositions at the transition zone from Precordillera to Altiplano (western and eastern vapor sources). It is proposed that exceptionally high topographic elevations can function as barriers for eastern air masses and inhibit the mentioned vapor mixing processes. The described topographically controlled effects could lead to specific isotope value ranges in precipitations of relevant basins. Hence, there is evidence that rainwater precipitating over PdT catchments can show distinct $\delta^{18}O$ value spectra that in total cover a range from −19 to −7‰. Once precipitated, meteoric waters undergo an isotopic evolution that involves evaporation-driven fractionation and subsurface groundwater mixing. There is, however, no evidence for hydrothermal isotopic water-rock interactions in the investigated cases. Overall, it is likely that similar mechanisms control isotope values of groundwater in other basins of the Atacama Desert.

Due to the observed basin-specific isotope characteristics in the PdT, it is possible to use $\delta^{18}O$ and $\delta^{2}H$ as tracers to delineate six major aquifer compartments. These compartments are consistent with flow directions indicated by regional groundwater level contour lines. The recharge areas of the mentioned compartments can be spatially correlated with different Precordilleran slope catchments. Furthermore, there is isotopic evidence that water recharged at Altos the Pica (~4000 m asl)—in the Quisma basin—passes the regional Longacho Hinge and provides a recharge into the PdT Aquifer.

However, isotopically ($\delta^{18}O$, $\delta^{2}H$, ^{3}H) there is no proof that regular flash floods reaching the alluvial fans of the Juan de Morales and Chacarillas catchments contribute significantly to groundwater recharge. In this context, there are indications that the main recharge facilitated by the Chacarillas and Tarapacá rivers is infiltrating along their lower stream segments between ~2200 and 1000 m asl as focused recharge.

4.7. Acknowledgment

We thank Compañía Minera Doña Inés de Collahuasi for the permission to publish internal isotope data. We appreciate the support of the Museum of Natural History of Berlin for carrying out stable isotope analysis in the framework of the Geo.X-initiative. This study was financed by CIDERH and CONICYT (National Commission of Scientific Research and Technology Chile) and the German Academic Exchange Service (DAAD). The authors also thank Juan Salas and Fernando Urbina, of the local DGA (Dirección General de Aguas, Chile) office in Iquique, for their field assistance and the permission to sample respective wells maintained by the DGA.

4.8. References

Acosta O, Custodio E (2008) Impactos ambientales de las extracciones de agua subterránea en el Salar del Huasco (norte de Chile) (Environmental impacts of groundwater production in the Salar del Huasco basin (Northern Chile)). Boletín Geológico y Minero:33–50

Aravena R, Suzuki O (1990) Isotopic Evolution of River Water in the Northern Chile Region. Water Resour. Res. 26:2887–2895. doi: 10.1029/WR026i012p02887

Aravena R, Suzuki O, Peña H, Grilli A, Salazar C, Orphanopoulos D, Rauert W (1989) Estudios de hidrología isotopica en Latino America (Isotope hydrology studies in Latin America): Estudio de hidrología isotopica en el area del Salar de Llamara, Desierto de Atacama, Chile (Isotope hydrology study in the Salar de Llamara area, Atacama Desert, Chile). http://www.iaea.org/inis/collection/nclcollectionstore/_public/21/031/21031083.pdf. Accessed 30 May 2016

Aravena R (1995) Isotope Hydrology and Geochemistry of Northern Chile Groundwaters. Bull. Inst. fr. études andines

Aravena R, Suzuki O, Peña H, Pollastri A, Fuenzalida H, Grilli A (1999) Isotopic composition and origin of the precipitation in Northern Chile. Applied Geochemistry 14:411–422. doi: 10.1016/S0883-2927(98)00067-5

Blanco N, Landino M (2012) Carta Mamina - Región de Tarapacá (Geological map Mamina - Tarapacá Region). map scale 1:100.000. Sernageomin, Santiago, Chile

Blanco N, Tomlinson AJ (2013) Carta Guatacondo - Región de Tarapacá (Geological map Guatacondo - Tarapacá Region). map scale 1:100.000, 156th edn. Sernageomin, Santiago

Chávez RO, Clevers JGPW, Decuyper M, Bruin S de, Herold M (2016) 50 years of water extraction in the Pampa del Tamarugal basin: Can Prosopis tamarugo trees survive in the hyper-arid Atacama

Desert (Northern Chile)? Journal of Arid Environments 124:292–303. doi: 10.1016/j.jaridenv.2015.09.007

Clark ID, Fritz P (1999) Environmental isotopes in hydrogeology, [2. print., corr.]. Lewis Publ, Boca Raton

Coplen TB (2011) Guidelines and recommended terms for expression of stable-isotope-ratio and gas-ratio measurement results. Rapid Commun. Mass Spectrom. 25:2538–2560. doi: 10.1002/rcm.5129

Cortecci G, Boschetti T, Mussi M, Lameli CH, Mucchino C, Barbieri M (2005) New chemical and original isotopic data on waters from El Tatio geothermal field, northern Chile. Geochem. J. 39:547–571. doi: 10.2343/geochemj.39.547

DGA (2013) Levantamiento de Información Geofísico en la Región de Tarapacá (Geophysical study of the region Tarapacá). Con potencial consultores LTDA. documentos.dga.cl/SUB5485v1.pdf. Accessed 13 May 2016

DGA (2017) Información Oficial Hidrometeorológica y de Calidad de Aguas en Línea (Oficial online information; hydrometeorology and water quality). http://snia.dga.cl/BNAConsultas/reportes. Accessed 20 July 2017

Frigge M, Hoaglin DC, Iglewicz B (1989) Some Implementations of the Boxplot. The American Statistician 43:50. doi: 10.2307/2685173

Fritz P, Suzuki O, Silva C, Salati E (1981) Isotope hydrology of groundwaters in the Pampa del Tamarugal, Chile. Journal of Hydrology 53:161–184. doi: 10.1016/0022-1694(81)90043-3

Galli C, Dingman R. (1965) Geology and Ground-Water Resources of the Pica Area Tarapaca Province, Chile. https://pubs.er.usgs.gov/publication/b1189. Accessed 13 May 2016

Gayo EM, Latorre C, Santoro CM, Maldonado A, Pol-Holz R de (2012a) Hydroclimate variability in the low-elevation Atacama Desert over the last 2500 yr. Clim. Past 8:287–306. doi: 10.5194/cp-8-287-2012

Gayo EM, Latorre C, Jordan TE, Nester PL, Estay SA, Ojeda KF, Santoro CM (2012b) Late Quaternary hydrological and ecological changes in the hyperarid core of the northern Atacama Desert (~21°S). Earth-Science Reviews 113:120–140. doi: 10.1016/j.earscirev.2012.04.003

Guo X, Feng Q, Liu W, Li Z, Wen X, Si J, Xi H, Guo R, Jia B (2015) Stable isotopic and geochemical identification of groundwater evolution and recharge sources in the arid Shule River Basin of Northwestern China. Hydrol. Process. 29:4703–4718. doi: 10.1002/hyp.10495

Gupta P, Noone D, Galewsky J, Sweeney C, Vaughn BH (2009) Demonstration of high-precision continuous measurements of water vapor isotopologues in laboratory and remote field deployments using wavelength-scanned cavity ring-down spectroscopy (WS-CRDS) technology. Rapid Commun Mass Spectrom 23:2534–2542. doi: 10.1002/rcm.4100

Herrera C, Custodio E, Chong G, Lamban LJ, Riquelme R, Wilke H, Jodar J, Urrutia J, Urqueta H, Sarmiento A, Gamboa C, Lictevout E (2016) Groundwater flow in a closed basin with a saline shallow lake in a volcanic area: Laguna Tuyajto, northern Chilean Altiplano of the Andes. Sci Total Environ 541:303–318. doi: 10.1016/j.scitotenv.2015.09.060

Herrera C, Gamboa C, Custodio E, Jordan T, Godfrey L, Jódar J, Luque JA, Vargas J, Sáez A (2017) Groundwater origin and recharge in the hyperarid Cordillera de la Costa, Atacama Desert, northern Chile. Sci Total Environ 624:114–132. doi: 10.1016/j.scitotenv.2017.12.134

Houston J (2002) Groundwater recharge through an alluvial fan in the Atacama Desert, northern Chile: mechanisms, magnitudes and causes. Hydrol. Process. 16:3019–3035. doi: 10.1002/hyp.1086

Houston J (2006a) Evaporation in the Atacama Desert: An empirical study of spatio-temporal variations and their causes. Journal of Hydrology 330:402–412. doi: 10.1016/j.jhydrol.2006.03.036

Houston J (2006b) The great Atacama flood of 2001 and its implications for Andean hydrology. Hydrol. Process. 20:591–610. doi: 10.1002/hyp.5926

Houston J (2006c) Variability of precipitation in the Atacama Desert: its causes and hydrological impact. Int. J. Climatol. 26:2181–2198. doi: 10.1002/joc.1359

Hren MT, Bookhagen B, Blisniuk PM, Booth AL, Chamberlain CP (2009) ?18O and ?: D of streamwaters across the Himalaya and Tibetan Plateau: Implications for moisture sources and paleoelevation reconstructions. Earth and Planetary Science Letters 288:20–32. doi: 10.1016/j.epsl.2009.08.041

Jayne RS, Pollyea RM, Dodd JP, Olson EJ, Swanson SK (2016) Spatial and temporal constraints on regional-scale groundwater flow in the Pampa del Tamarugal Basin, Atacama Desert, Chile. Hydrogeol J. doi: 10.1007/s10040-016-1454-3

Jica (1995) The study on the development of water resources in Northern Chile. http://sad.dga.cl/. Accessed 13 May 2016

Jordan TE, Nester PL (2012) The Pampa del Tamarugal forearc basin in Northern Chile. Tectonics of Sedimentary Basins - Recent Advances:369–381

Jordan TE, Kirk-Lawlor NE, Blanco NP, Rech JA, Cosentino NJ (2014) Landscape modification in response to repeated onset of hyperarid paleoclimate states since 14 Ma, Atacama Desert, Chile. Geological Society of America Bulletin 126:1016–1046. doi: 10.1130/B30978.1

Kendall C (ed) (2006) Isotope tracers in catchment hydrology, 1. ed., reprint. Elsevier, Amsterdam u.a.

Kitanidis PK (1997) Introduction to geostatistics: Applications to hydrogeology. Cambridge University Press, Cambridge, New York

Lin Y, Clayton RN, Groning M (2010) Calibration of delta(17)O and delta(18)O of international measurement standards - VSMOW, VSMOW2, SLAP, and SLAP2. Rapid Commun Mass Spectrom 24:773–776. doi: 10.1002/rcm.4449

Magaritz M, Aravena R, Peña H, Suzuki O, Grilli A (1989) Water chemistry and isotope study of streams and springs in northern Chile. Journal of Hydrology 108:323–341. doi: 10.1016/0022-1694(89)90292-8

Magaritz M, Aravena R, Peña H, Suzuki O, Grilli A (1990) Source of Ground Water in the Deserts of Northern Chile: Evidence of Deep Circulation of Ground Water from the Andes. Groundwater. doi: 10.1111/j.1745-6584.1990.tb01706.x

Nester PL (2008) Basin and Paleoclimate Evolution of the Pampa del Tamarugal Forearc Valley, Atacama Desert, Northern Chile.

https://ecommons.cornell.edu/bitstream/handle/1813/10484/Nester2008.pdf?sequence=1&isAllowed=y. Accessed 5 May 2017

Placzek C, Quade J, Patchett PJ (2006) Geochronology and stratigraphy of late Pleistocene lake cycles on the southern Bolivian Altiplano: Implications for causes of tropical climate change. Geological Society of America Bulletin 118:515–532. doi: 10.1130/B25770.1

Placzek C, Quade J, Betancourt JL, Patchett PJ, Rech JA, Latorre C, Matmon A, Holmgren C, English NB (2009) Climate in the dry central Andes over geologic, millennial and interannual timescales. Annals of the Missouri Botanical Garden 96:386–397. doi: 10.3417/2008019

PUC (2009) Levantamiento Hidrogeológico para el Desarrollo de nuevas fuentes de Agua en áreas prioritarias de la zona norte de Chile, Regiones XV, I, II y III (Hydrogeological study for the development of new sources of water resources in northern zones of Chile, regiones XV, I, II and III). documentos.dga.cl/REH5161v4.pdf. Accessed 13 May 2016

Quade J, Rech JA, Betancourt JL, Latorre C, Quade B, Rylander KA, Fisher T (2008) Paleowetlands and regional climate change in the central Atacama Desert, northern Chile. Quaternary Research 69:343–360. doi: 10.1016/j.yqres.2008.01.003

Risacher F, Alonso H, Salazar C (1999) Geoquimica de Aguas en cuencas cerradas I, II y III Regiones Chile (Geochemistry of water resources in closed basins, regions I, II and III of Chile): Volume I and II. http://documentos.dga.cl/CQA1921v1.pdf. Accessed 30 May 2016

Rojas R, Dassargues A (2007) Groundwater flow modelling of the regional aquifer of the Pampa del Tamarugal, northern Chile. Hydrogeol J 15:537–551. doi: 10.1007/s10040-006-0084-6

Rojas R, Batelaan O, Feyen L, Dassargues A (2010) Assessment of conceptual model uncertainty for the regional aquifer Pampa del Tamarugal – North Chile. Hydrol. Earth Syst. Sci. 14:171–192. doi: 10.5194/hess-14-171-2010

Salazar C, Rojas L, Pollastri A (1998) Evaluación de Recursos Hidricos en el Sector de Pica - Evaluation of water resources in the Pica area: Hoya de la Pampa del Tamarugal I Region. http://documentos.dga.cl/SUB1658.djvu. Accessed 30 May 2016

Scanlon BR, Keese KE, Flint AL, Flint LE, Gaye CB, Edmunds WM, Simmers I (2006) Global synthesis of groundwater recharge in semiarid and arid regions. Hydrol. Process. 20:3335–3370. doi: 10.1002/hyp.6335

Scheihing K, Tröger U (2017) Local climate change induced by groundwater overexploitation in a high Andean arid watershed, Laguna Lagunillas basin, northern Chile. Hydrogeol J 16:1817. doi: 10.1007/s10040-017-1647-4

Scheihing KW, Moya CE, Tröger U (2017) Insights into Andean slope hydrology: Reservoir characteristics of the thermal Pica spring system, Pampa del Tamarugal, northern Chile. Hydrogeol J 119:33. doi: 10.1007/s10040-017-1533-0

Terzer S, Wassenaar LI, Araguás-Araguás LJ, Aggarwal PK (2013) Global isoscapes for δ18O and δ2H in precipitation: Improved prediction using regionalized climatic regression models. Hydrol. Earth Syst. Sci. 17:4713–4728. doi: 10.5194/hess-17-4713-2013

Tóth J (2009) Gravitational systems of groundwater flow: Theory, evaluation, utilization, 1. publ. Cambridge Univ. Press, Cambridge u.a.

Uribe J, Muñoz JF, Gironás J, Oyarzún R, Aguirre E, Aravena R (2015) Assessing groundwater recharge in an Andean closed basin using isotopic characterization and a rainfall-runoff model: Salar del Huasco basin, Chile. Hydrogeol J. doi: 10.1007/s10040-015-1300-z

Urqueta H, Jódar J, Herrera C, Wilke H-G, Medina A, Urrutia J, Custodio E, Rodríguez J (2017) Land surface temperature as an indicator of the unsaturated zone thickness: A remote sensing approach in the Atacama Desert. Sci Total Environ 612:1234–1248. doi: 10.1016/j.scitotenv.2017.08.305

Valdés-Pineda R, Pizarro R, García-Chevesich P, Valdés JB, Olivares C, Vera M, Balocchi F, Pérez F, Vallejos C, Fuentes R, Abarza A, Helwig B (2014) Water governance in Chile: Availability, management and climate change. Journal of Hydrology 519:2538–2567. doi: 10.1016/j.jhydrol.2014.04.016

Vuille M, Werner M (2005) Stable isotopes in precipitation recording South American summer monsoon and ENSO variability: observations and model results. Climate Dynamics 25:401–413. doi: 10.1007/s00382-005-0049-9

Yonge CJ, Goldenberg L, Krouse HR (1989) An isotope study of water bodies along a traverse of southwestern Canada. Journal of Hydrology 106:245–255. doi: 10.1016/0022-1694(89)90075-9

5. Synthesis

While the central findings were discussed in the framework of the self-contained articles, the following chapter aims to delineate the broader context and connection of the developed conclusions. Subsequently, future topics of research will be outlined.

5.1. Summary of major findings

The main findings presented in the three self-contained articles are as follows:

(1) In chapter 2, based on a case study in the Laguna Lagunillas basin, it is demonstrated that shallow groundwater in catchments of the high arid Andes can have a regulating function on the local climate. An ongoing overexploitation of given groundwater resources can cause mean monthly minimum (mmin) temperatures to fall continuously and mean monthly maximum (mmax) temperatures to rise abruptly (critical drawdown: ~2 m bgl). Strongest air temperature anomalies were found to occur in Andean winter nights with a difference of up to 8°C compared to a nearby reference station, and during summer days, with a mean temperature increase of 2.7°C compared to pre-change conditions.

(2) Inter-basin groundwater flow from the Andean Altiplano to the Pampa del Tamarugal (PdT), through deep basement fractures, is very likely not occurring. For the most prominent candidate of such an inter-basin flow (Salar del Huasco basin-Pica Oasis) a hydrological time series analysis as well as reflection seismic data and geothermic considerations, demonstrate that the concept cannot be proven true (chapter 3). By contrast, geothermal and

hydrologic characteristics can be sufficiently explained by a groundwater system that is recharged in the Andean Precordillera (Altos de Pica).

(3) Pressure signals induced by recharge in the Andean Precordillera can propagate rapidly over tens of kilometers with a constant lag in the relevant confined and sloping aquifers. Such a signal propagation is facilitated by the aquifer's hydraulic diffusivity, which largely depends on the specific storage. This effect is not to be confused with the arrival of the recharged fluid-mass, which can exhibit mean residence times of a few thousand years (chapter 3).

(4) Stable isotope values in precipitations over Andean slope catchments that discharge into the PdT are mainly controlled by the mixing of easterly and westerly vapor sources in the mountainous transition zone from the Andean Altiplano to the Precordillera. Catchment dependent topographic features can be a major controlling factor of this process, by either facilitating or inhibiting a mixing of these easterly and westerly air masses with different isotopic compositions. This effect is consistently reflected in isotope characteristics of respective groundwater resources (chapter 4).

(5) The principal recharge facilitated into the PdT-Aquifer is probably infiltrating along the lower stream segments of discharging rivers; isotopically there is no evidence of an alluvial fan recharge after flash-floods in the investigated cases (chapter 4).

5.2. Conclusive discussion

The different derived conclusions are of high importance for the hydrological understanding of the Atacama Desert and related water management considerations for the area of work.

In their sedimentary valleys, high Andean arid catchments often hold undeveloped groundwater resources that – in most cases – are related to shallow aquifers, which are accompanied by superficial salt flats (Risacher et al. 2003). In the search for additional water supply sources, these undeveloped aquifers are an attractive alternative to overexploited conventional aquifers (PUC 2009). While it is known that water mining in the arid Andes can have devastating effects on related groundwater-fed ecosystems (Larraín and Poo 2010; Yáñez Fuenzalida and Molina Otárola 2008; BHP Billiton 2015), it is possible to demonstrate an associated yet hitherto disregarded effect. There is evidence that

the removal of shallow groundwater in high Andean arid catchments, can have a severe impact on local mean minimum and mean maximum air temperatures (chapter 2). The observed groundwater-climate feedbacks appear to be controlled by the water's ability to store and conduct heat energy (from either solar or geothermal sources), as well as the absorption of solar energy due to evaporation processes (Scheihing and Tröger 2017). This fact should raise attention among the different stakeholders who are in charge of managing water resources in the arid Andes, as well as holding concern for climatologists and ecologists. It indicates that the many shallow aquifers found in the high arid Andes play a crucial role in regulating local climates which, in sum, could also have an impact at a regional scale.

There have been several attempts to model the effects of large lakes on regional climates (Thiery et al. 2015; Williams et al. 2015; Hostetler et al. 1993; Gula and Peltier 2012; MacKay et al. 2009). In the broader area of work, only 60 km east of the Laguna Lagunillas basin, the world's largest salt flat is found with an extension of more than 10,000 km^2, namely the Salar de Uyuni (in Bolivia). The Salar de Uyuni exhibits near-surface groundwater in great parts and it is also known for its lithium-rich brines (Sieland 2014). The regulating importance of these shallow water resources regarding the local and regional climate are worth examining to better understand the significance of groundwater-climate feedbacks on regional scales and particularly to assess the possible environmental impacts of lithium-rich brine extractions (lowering of near-surface groundwater levels) (An et al. 2012; Gruber et al. 2011; Ogawa et al. 2014; Hodson 2015).

However, the results emphasize the necessity to assure sustainable water productions schemes of shallow aquifers in the arid Andes. A drawdown of near-surface groundwater below 2 m bgl and beyond can have an ongoing effect on mean minimum temperatures (Scheihing and Tröger 2017). Systematic groundwater exploitation over greater extents in the Andes should thus be bound to relevant obligations, detailed monitoring programs, and conservative recharge estimations to prevent eventual climatic feedbacks on a broader scale.

A hitherto undeveloped high Andean aquifer is found in the Salar del Huasco basin. A long-lived question concerning its hydrogeological connection to the plane Atacama Desert was sufficient reason to reject requests for water extraction rights to date (chapter 1.2). Investigations, as presented in chapter 3, have inquired into the open question concerning a possible inter-basin flow

(Magaritz et al. 1989; Magaritz et al. 1990; Jayne et al. 2016; Jica 1995; Fritz et al. 1981; Uribe et al. 2015). A seismic, hydrological and hydrochemical assessment of the respective groundwater system prompted the conclusion that a hydraulic connection through deep faults cannot be proven correct (chapter 3). Particularly the low reservoir temperature – as derived by geothermometers – and the short-term hydraulic pressure response to recharge events in the Andean Precordillera, justify disregarding the concept (Scheihing et al. 2017). This conclusion is in accordance with the considerations of Uribe et al. (2015), who came to the same conclusion based on water balance considerations for the Salar del Huasco basin. Nevertheless, the applied methodology by Scheihing et al. (2017) and Uribe et al. (2015) might not be sensitive to very low portions of leaking and later uprising deep groundwater through deep fractures (> 2 km) that would mix with resources from the investigated slope reservoir. However, such low portions would be negligible in terms of water management.

There is another argument against a provided recharge into the PdT by profound uprising waters from the Altiplano, which can be derived from drilling profiles of two very deep (~2500 and ~1200 m bgl) exploratory drillings placed a few kilometers east of the Salar de Pintados (Figure 1.1b, drillings were executed by the Chilean oil company ENAP in 1961). They reveal that groundwater in the deep sedimentary basin of the PdT – at depths higher than 500 m bgl – is without exception brackish (from company internal drilling profiles). Hence, low saline water (<1500 µS/cm), as found in the central PdT-Aquifer (Jica 1995), cannot originate from deep uprising groundwater. The results of chapter 4 provide an implicit explanation for the presence of respective low-saline resources. It was demonstrated that water that is recharged at the Andean Precordillera (Altos de Pica) passes the localities Pica and Puquio Nunez (electrical conductivity <600 µS/cm) and the regional Longacho Hinge, and discharges section-wise into the PdT-Aquifer. The Longacho Hinge was conservatively treated as an impermeable barrier (Rojas and Dassargues 2007; Rojas et al. 2010). This assumption is found to be incorrect and should be revised in future hydrogeological models. Besides, this point could have been one of the main constraints in the model of Rojas et al. (2010).

Furthermore, another incorrect understanding is the idea of a substantial groundwater recharge occurring through alluvial fans, which was likewise respected in the conceptual models of Rojas et al. (2010) (Houston 2002). This idea was introduced based on an analysis of water table fluctuations at well J8

(total depth: ~200 m). In chapter 4 it was stressed – based on a sizeable stable isotope dataset and ^{3}H samples – that isotopically there is no evidence of alluvial fan recharge in the PdT (Scheihing et al. 2018). At the same time, the observed rise of the groundwater level in well J8 could be explained, by a short-term hydraulic response of the sloping confined aquifer to focused recharge events along the lower stream segments of the Chacarillas river (including the fan apex). Such a short-term hydraulic response (with a constant lag to recharge) is controlled by the aquifers' hydraulic diffusivity and was proven to occur in the area of work (chapter 3). Spring discharge amounts and groundwater level variations at Pica and Puquio Nunez exhibit a constant-lag response of 20-24 months regarding recharge events in the Andean Precordillera (Scheihing et al. 2017).

It is noteworthy that the recharge amounts (in mean 200 l/s) derived by Houston (2002) relied on the water-table-fluctuation method, which in turn strongly depends on the aquifer's storage coefficient (Healy and Scanlon 2010). Houston (2002) rejected a relatively low storage coefficient (0.001) as derived by a single-well pumping test (Jica 1995), arguing that the pumping test's time series would exhibit a dual porosity response and instead proposed a value of 0.08, justifying it based on literature values. The estimated recharge amounts calculated by Houston (2002) might thus rely on false assumptions and are doubtable. From the author's perspective, it is more likely that the hydraulic head fluctuation in well J8 is dominated by the deeper confined aquifer, which naturally exhibits a much lower storage coefficient and hence is much more sensitive to pressure changes induced by distant recharge events (Tóth 2009). The water-table-fluctuation method cannot be applied to confined aquifers (Healy and Scanlon 2010).

There is more evidence to reject the concept of alluvial fan recharge that can be derived from the resistivity log of well J8, which was measured when constructing the well. From Figure 5.1 it can be understood that between 14-30 m bgl there persists a 16-m thick clay layer, which exhibits a very strong resistivity maximum (950 Ωm) (Jica 1995). If a percolation after flash-flood events occurred with a return period of four years, as argued by Houston (2002), the respective clay layer would need to be water soaked. Another, deeper clay layer that bears water (59-108 m bgl), consistently shows no resistivity anomaly (values below 30 Ωm, Figure 5.1).

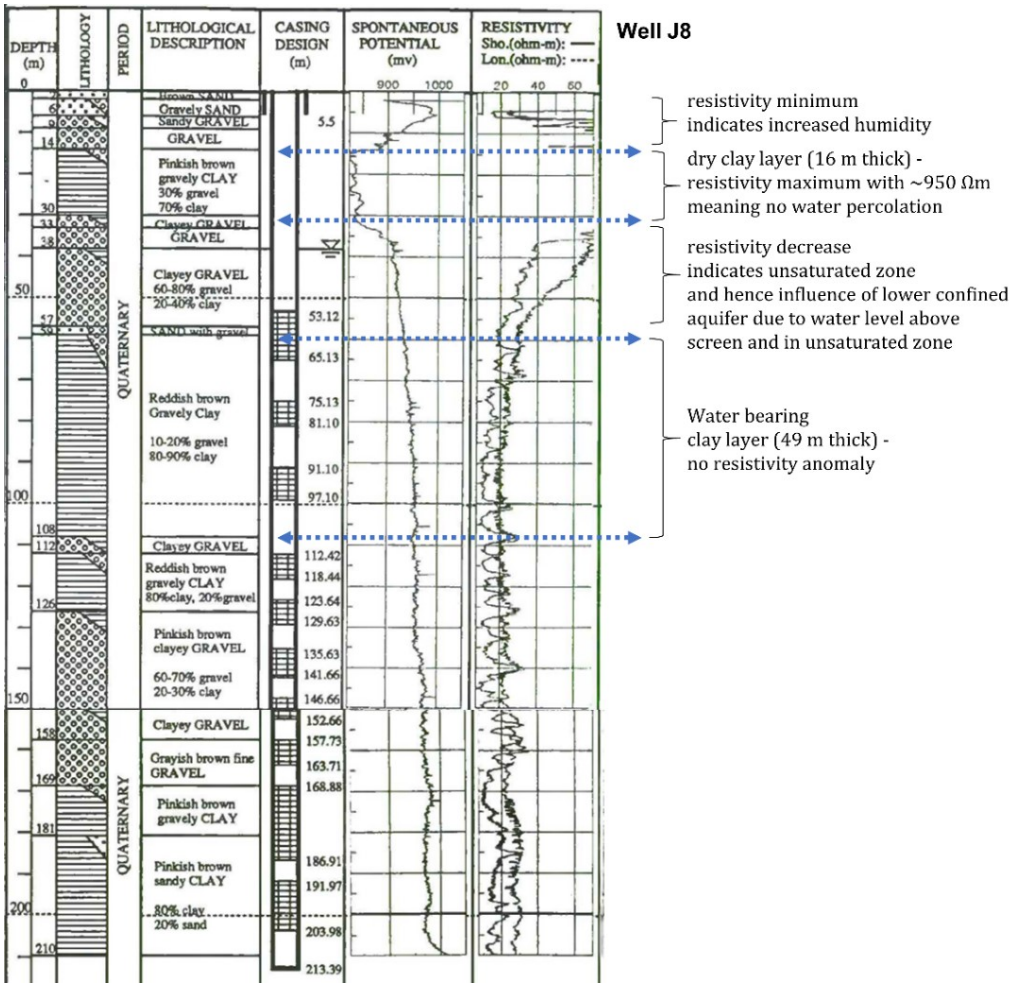

Figure 5.1 Well profile, spontaneous potential and resistivity log of well J8 (modified after Jica (1995))

Hence, the resistivity maximum provides evidence that the upper clay layer is dry and that eventually infiltrated water from top sediments cannot pass this barrier. The elaborated argumentation yields a fundamental insight because it implies that regularly arriving flood water –in the investigated cases - is lost in great parts by evaporation. Having clarified this hydrological process, future research efforts in water resources management should consider quantifying the water loss by flood water evaporation at alluvial fans and – if feasible – develop solutions to optimize the usage of this water fraction, which can be substantial.

In the context of an anthropogenic climate change, climate models project a decrease of precipitation over the central Andes by up to 30%, while predicting an increase in the frequency of extreme La Niña and El Niño conditions (Minvielle and Garreaud 2011; Cai et al. 2014; Cai et al. 2015). As the El Niño and La Niña phenomena are linked to a higher probability of storm events in the arid Andes (Houston 2006), respective precipitation patterns are likely to become more

extreme, which favors the occurrence of flash-flood events. Nevertheless, even in recent years a variety of places in northern Chile and western Peru have suffered from severe flooding events, with hundreds of affected people (Floodlist 2017). Managing the extremes between sudden floods and water scarcity might be one of the most urgent and promising areas in water management endeavors west of the Andean rain shadow.

However, the fact that the confined part of the PdT-Aquifer can demonstrate short-term hydraulic responses to distant recharge events (in the case of chapter 3: 32 km distance and 3000 m elevation difference) is a crucial insight in terms of understanding its hydrological functioning. Such hydraulic feedbacks were also reported – for example – in the Yucca Mountain Region of Nevada and California (USA) (Fenelon and Moreo 2002). Sloping confined hydrogeological systems can be found in large parts of the Atacama Desert, which is typically linked to the hydrology of the arid Andes. Hence, this novel finding is likely to hold importance for a variety of akin basins. It can be used to predict water level fluctuations by – for example – entertaining lumped hydrologic models in conjunction with other hydrologic or meteorological time series. While distributed hydrogeologic models are the most commonly-applied models in groundwater resources management, lumped hydrologic models offer a similarly precise prediction ability of groundwater levels in many cases (Mackay et al. 2014; Long 2015; Kazumba et al. 2008). Particularly in data scarce and geologic complex areas with high conceptual uncertainties, lumped hydrologic models can represent a more suitable alternative when compared to distributed models.

Nevertheless, the earlier-mentioned insight leads also to a hitherto unidentified concept for a managed artificial recharge scheme. Theoretically, it would be possible to build infiltration wells in the Andean Precordillera at Altos de Pica (~4000 m asl) and thereby recharge the PdT-Aquifer at 1000 m asl. The impact of such an artificial recharge should be perceptible after 24 months by a rise of groundwater levels at the Andean foothills. As understood from the isotopic assessment in chapter 4, this water finally reaches the central PdT-Aquifer and will very likely also stimulate the respective hydraulic head. Nevertheless, whether this idea is feasible would need to be subject to a future assessment.

In any case, the consideration shows that the conservatively established limits of the PdT-Aquifer must be revised. To date, the defined eastern limit of the PdT-Aquifer has not reached higher than ~1300 m asl (Jica 1995). At least around Pica and Puquio Nunez, the correct aquifer limit lies in the Andean Precordillera, in

the Altos de Pica recharge area. This conclusion also has implications for assessing the total volume of the aquifer's groundwater resources, which will be in sum considerably higher than the initially calculated 27 km^3 (Jica 1995).

Finally, it is worthwhile taking a closer look at the regional isotopic assessment carried out in chapter 4. The understanding that there are vapor mixing processes occurring in the central Andes of air masses that exhibit different isotopic characteristics is not new (Vuille and Werner 2005; Aravena et al. 1999). However, the local importance that catchment-dependent topographic features can have in controlling this vapor mixing processes has previously not been considered. Based on a thorough isotope analysis of groundwaters in the arid Andes, it was demonstrated that long-term mean stable isotope values of precipitations can be considerably influenced by mountainous barriers that inhibit the mixing of easterly and westerly air masses at the lee side. Additionally, they can force other isotope-altering effects such as altitude or amount effects at the luv side. These insights allow disregarding several other suspected reasons for the distinct isotopic patterns in groundwater of the PdT, such as a change of climatic conditions or thermal water-rock interactions because they fail to explain the observed spatial correlations (chapter 4). The methodology applied to yield this understanding relies on robust and fundamental isotopic considerations, but overall it can reveal these interrelations due to the substantial number of samples and the vast area covered.

In terms of water management in the PdT, the phenomenon of locally varying isotope characteristics in precipitations due to distinct topographic features allows for using stable isotopes as a useful tracer and leads to the conclusion, that recharge facilitated by the investigated slope catchments primarily occurs as focused recharge along the lower stream segment of the rivers (with exception of the Altos de Pica recharge area) (Scheihing et al. 2018). This insight holds importance for the conceptual hydrogeological understanding of the PdT-Aquifer, particularly when intending to model the basin.

Altogether, the presented thesis clarifies several aspects concerning the hydrological functioning of the PdT-Aquifer and related arid Andean groundwater systems. Furthermore, it introduces unconsidered hydrological processes that are of relevance also for other hydrogeological sites in the Atacama Desert. Consequently, most promising future topics of research will be elaborated.

5.3. Topics of further research

A crucial technology in accounting for the water balance of arid catchments and shallow aquifers are remote sensing approaches to estimate the real evapotranspiration, termed the surface energy balance algorithm (SEBAL) or surface energy balance system (SEBS) (Bastiaanssen et al. 1998; Su 2002). These algorithms rely on publicly-accessible satellite data that feature daytime thermal infrared imagery (like MODIS, ASTER or Landsat data), as well as ground-based measurements of fundamental meteorological parameters, such as wind speed. Although various sites in northern Chile would be applicable for such an assessment, there is only one study on the subject (focusing on the Salar de Atacama) (Kampf and Tyler 2006). Particularly the estimation of real evapotranspiration from the area around the Salar de Pintados and Salar de Bellavista – which marks a terminal water trap for waters from the PdT-Aquifer – would yield a vital component of the groundwater system's hydrologic budget. Moreover, in terms of hydrogeologically-closed arid Andean basins such as the Salar del Huasco basin, the remotely-sensed estimation of real evapotranspiration would allow deriving reasonable estimates of total recharge amounts, as evaporation is here supposed to be the only water outflow (Uribe et al. 2015; Gowda et al. 2009; Zhang et al. 2011).

The methodology might also be suitable for estimating the water loss by real evaporation from alluvial fans after flash-floods. The primary constraint here is the high resolution needed and the availability of applicable satellite imagery. Such intents should be supported by the installation of gauging stations that can continuously measure discharge amounts even under extreme conditions. A major problem, for now, is that many installed gauging stations fail to record extreme flooding events because respective discharge amounts are out of scale (Lictevout and Gocht 2017). However, determining the real evapotranspiration based on high-resolution satellite imagery could be a cornerstone for future intentions to hydrogeologically model respective groundwater systems.

In chapter 2, it has been demonstrated that in the arid Andes nocturnal heat fluxes from shallow groundwater to the lower atmosphere can have a regulating impact on the local climate. The calculation of remotely-sensed surface energy balances – based on thermal infrared nighttime imagery – could provide an estimation of these heat fluxes from shallow arid Andean aquifers to the lower atmosphere and might allow inferring the importance of geothermal heat

sources in this process. The consequently resolvable relationship between groundwater levels, heat fluxes and air temperatures in a variety of arid Andean catchments, would thus be another promising future subject of research.

Apart from that, recently there have been some remote sensing approaches to hydrologically model runoff and streamflow of ungauged basins (Poortinga et al. 2017). Such an approach could be tested for accuracy based on the gauged Tarapacá river basin in the area of work. If the approach proves applicable to arid Andean slope catchments, it could provide an useful tool for deriving water losses by flash-floods of other ungauged basins and allow more precisely estimating eventual recharge amounts from stream beds.

5.4. References

An JW, Kang DJ, Tran KT, Kim MJ, Lim T, Tran T (2012) Recovery of lithium from Uyuni salar brine. Hydrometallurgy 117-118:64–70. doi: 10.1016/j.hydromet.2012.02.008

Aravena R, Suzuki O, Peña H, Pollastri A, Fuenzalida H, Grilli A (1999) Isotopic composition and origin of the precipitation in Northern Chile. Applied Geochemistry 14(4):411–422. doi: 10.1016/S0883-2927(98)00067-5

Bastiaanssen W, Menenti M, Feddes RA, Holtslag A (1998) A remote sensing surface energy balance algorithm for land (SEBAL). 1. Formulation. Journal of Hydrology 212-213:198–212. doi: 10.1016/S0022-1694(98)00253-4

BHP Billiton (2015) BHP Billiton Chile Sustainability report 2014. http://www.bhpbilliton.com/~/media/bhp/documents/society/reports/2014/csr-eng150518sustainabilityreport2014bhpbillitonchileoperations.pdf. Accessed 17 May 2016

Cai W, Borlace S, Lengaigne M, van Rensch P, Collins M, Vecchi G, Timmermann A, Santoso A, McPhaden MJ, Wu L, England MH, Wang G, Guilyardi E, Jin F-F (2014) Increasing frequency of extreme El Niño events due to greenhouse warming. Nature Climate change 4(2):111–116. doi: 10.1038/nclimate2100

Cai W, Wang G, Santoso A, McPhaden MJ, Wu L, Jin F-F, Timmermann A, Collins M, Vecchi G, Lengaigne M, England MH, Dommenget D, Takahashi K, Guilyardi E (2015) Increased frequency of extreme La Niña events under greenhouse warming. Nature Climate change 5(2):132–137. doi: 10.1038/nclimate2492

Floodlist (2017) News list on floodings in Chile. http://floodlist.com/tag/chile. Accessed 1 June 2017

Fritz P, Suzuki O, Silva C, Salati E (1981) Isotope hydrology of groundwaters in the Pampa del Tamarugal, Chile. Journal of Hydrology 53(1-2):161–184. doi: 10.1016/0022-1694(81)90043-3

Gowda PH, Senay GB, Howell TA, Marek TH (2009) Lysimetric Evaluation of Simplified Surface Energy Balance Approach in the Texas High Plains. Applied Engineering in Agriculture 25(5):665–669. doi: 10.13031/2013.28855

Gruber PW, Medina PA, Keoleian GA, Kesler SE, Everson MP, Wallington TJ (2011) Global Lithium Availability. Journal of Industrial Ecology 15(5):760–775. doi: 10.1111/j.1530-9290.2011.00359.x

Gula J, Peltier WR (2012) Dynamical Downscaling over the Great Lakes Basin of North America Using the WRF Regional Climate Model: The Impact of the Great Lakes System on Regional Greenhouse Warming. J. Climate 25(21):7723–7742. doi: 10.1175/JCLI-D-11-00388.1

Healy RW, Scanlon BR (2010) Estimating groundwater recharge. Cambridge University Press, Cambridge, New York

Hodson H (2015) Lithium dreams. New Scientist 228(3043):38–41. doi: 10.1016/S0262-4079(15)31421-4

Hostetler SW, Bates GT, Giorgi F (1993) Interactive coupling of a lake thermal model with a regional climate model. J. Geophys. Res. 98(D3):5045–5057. doi: 10.1029/92JD02843

Houston J (2002) Groundwater recharge through an alluvial fan in the Atacama Desert, northern Chile: mechanisms, magnitudes and causes. Hydrol. Process. 16(15):3019–3035. doi: 10.1002/hyp.1086

Houston J (2006) Variability of precipitation in the Atacama Desert: its causes and hydrological impact. Int. J. Climatol. 26(15):2181–2198. doi: 10.1002/joc.1359

Jayne RS, Pollyea RM, Dodd JP, Olson EJ, Swanson SK (2016) Spatial and temporal constraints on regional-scale groundwater flow in the Pampa del Tamarugal Basin, Atacama Desert, Chile. Hydrogeol J. doi: 10.1007/s10040-016-1454-3

Jica (1995) The study on the development of water resources in Northern Chile. http://sad.dga.cl/. Accessed 13 May 2016

Kampf SK, Tyler SW (2006) Spatial characterization of land surface energy fluxes and uncertainty estimation at the Salar de Atacama, Northern Chile. Advances in Water Resources 29(2):336–354. doi: 10.1016/j.advwatres.2005.02.017

Kazumba S, Oron G, Honjo Y, Kamiya K (2008) Lumped model for regional groundwater flow analysis. Journal of Hydrology 359(1-2):131–140. doi: 10.1016/j.jhydrol.2008.06.021

Larraín S, Poo P (2010) Conflictos por el agua en Chile - Entre los derechos humanos y las reglas de mercado (Water conflicts in Chile - between human rights and the rules of the free market), 1a ed.

Lictevout E, Gocht M (2017) Hydrometric network design in hyper-arid areas: Example of Atacama Desert (North Chile). Hydrol Res:nh2017004. doi: 10.2166/nh.2017.004 [s.n], Santiago, Chile

Long AJ (2015) RRAWFLOW: Rainfall-Response Aquifer and Watershed Flow Model (v1.15). Geosci. Model Dev. 8(3):865–880. doi: 10.5194/gmd-8-865-2015

Mackay JD, Jackson CR, Wang L (2014) A lumped conceptual model to simulate groundwater level time-series. Environmental Modelling & Software 61:229–245. doi: 10.1016/j.envsoft.2014.06.003

MacKay MD, Neale PJ, Arp CD, Senerpont Domis LN de, Fang X, Gal G, Jöhnk KD, Kirillin G, Lenters JD, Litchman E, MacIntyre S, Marsh P, Melack J, Mooij WM, Peeters F, Quesada A, Schladow SG, Schmid

M, Spence C, Stokesr SL (2009) Modeling lakes and reservoirs in the climate system. Limnol. Oceanogr. 54(6part2):2315–2329. doi: 10.4319/lo.2009.54.6_part_2.2315

Magaritz M, Aravena R, Peña H, Suzuki O, Grilli A (1989) Water chemistry and isotope study of streams and springs in northern Chile. Journal of Hydrology 108:323–341. doi: 10.1016/0022-1694(89)90292-8

Magaritz M, Aravena R, Peña H, Suzuki O, Grilli A (1990) Source of Ground Water in the Deserts of Northern Chile: Evidence of Deep Circulation of Ground Water from the Andes. Groundwater(4). doi: 10.1111/j.1745-6584.1990.tb01706.x

Minvielle M, Garreaud RD (2011) Projecting Rainfall Changes over the South American Altiplano. J. Climate 24(17):4577–4583. doi: 10.1175/JCLI-D-11-00051.1

Ogawa Y, Koibuchi H, Suto K, Inoue C (2014) Effects of the Chemical Compositions of Salars de Uyuni and Atacama Brines on Lithium Concentration during Evaporation. Resource Geology 64(2):91–101. doi: 10.1111/rge.12030

Poortinga A, Bastiaanssen W, Simons G, Saah D, Senay G, Fenn M, Bean B, Kadyszewski J (2017) A Self-Calibrating Runoff and Streamflow Remote Sensing Model for Ungauged Basins Using Open-Access Earth Observation Data. Remote Sensing 9(1):86. doi: 10.3390/rs9010086

PUC (2009) Levantamiento Hidrogeológico para el Desarrollo de nuevas fuentes de Agua en áreas prioritarias de la zona norte de Chile, Regiones XV, I, II y III (Hydrogeological study for the development of new water resources in northern zones of Chile, regiones XV, I, II and III). documentos.dga.cl/REH5161v4.pdf. Accessed 13 May 2016

Risacher F, Alonso H, Salazar C (2003) The origin of brines and salts in Chilean salars: a hydrochemical review. Earth-Science Reviews 63(3-4):249–293. doi: 10.1016/S0012-8252(03)00037-0

Rojas R, Dassargues A (2007) Groundwater flow modelling of the regional aquifer of the Pampa del Tamarugal, northern Chile. Hydrogeol J 15(3):537–551. doi: 10.1007/s10040-006-0084-6

Rojas R, Batelaan O, Feyen L, Dassargues A (2010) Assessment of conceptual model uncertainty for the regional aquifer Pampa del Tamarugal – North Chile. Hydrol. Earth Syst. Sci. 14(2):171–192. doi: 10.5194/hess-14-171-2010

Scheihing K, Tröger U (2017) Local climate change induced by groundwater overexploitation in a high Andean arid watershed, Laguna Lagunillas basin, northern Chile. Hydrogeol J 16:1817. doi: 10.1007/s10040-017-1647-4

Scheihing KW, Moya CE, Tröger U (2017) Insights into Andean slope hydrology: Reservoir characteristics of the thermal Pica spring system, Pampa del Tamarugal, northern Chile. Hydrogeol J 119(2):33. doi: 10.1007/s10040-017-1533-0

Scheihing K, Moya C, Struck U, Lictevout E, Tröger U (2018) Reassessing Hydrological Processes That Control Stable Isotope Tracers in Groundwater of the Atacama Desert (Northern Chile). Hydrology 5:3. doi: 10.3390/hydrology5010003

Sieland R (2014) Hydraulic Investigations of the Salar de Uyuni, Bolivia. https://www.researchgate.net/publication/281061345_Hydraulic_Investigations_of_the_Salar_de_Uyuni_Bolivia?enrichId=rgreq-58d468dabf9704e98e047a010f96c002-

XXX&enrichSource=Y292ZXJQYWdlOzI4MTA2MTM0NTtBUzoyNjM3NTE0MzM3MTU3MTJAMTQzOTg5NDY1MDM1OQ%3D%3D&el=1_x_2&_esc=publicationCoverPdf. Accessed 28 May 2017

Su Z (2002) The Surface Energy Balance System (SEBS) for estimation of turbulent heat fluxes. Hydrol. Earth Syst. Sci. 6(1):85–100. doi: 10.5194/hess-6-85-2002

Thiery W, Davin EL, Panitz H-J, Demuzere M, Lhermitte S, van Lipzig N (2015) The Impact of the African Great Lakes on the Regional Climate. J. Climate 28(10):4061–4085. doi: 10.1175/JCLI-D-14-00565.1

Tóth J (2009) Gravitational systems of groundwater flow: Theory, evaluation, utilization, 1. publ. Cambridge Univ. Press, Cambridge u.a.

Uribe J, Muñoz JF, Gironás J, Oyarzún R, Aguirre E, Aravena R (2015) Assessing groundwater recharge in an Andean closed basin using isotopic characterization and a rainfall-runoff model: Salar del Huasco basin, Chile. Hydrogeol J. doi: 10.1007/s10040-015-1300-z

Vuille M, Werner M (2005) Stable isotopes in precipitation recording South American summer monsoon and ENSO variability: observations and model results. Climate Dynamics 25(4):401–413. doi: 10.1007/s00382-005-0049-9

Williams K, Chamberlain J, Buontempo C, Bain C (2015) Regional climate model performance in the Lake Victoria basin. Clim Dyn 44(5-6):1699–1713. doi: 10.1007/s00382-014-2201-x

Yáñez Fuenzalida N, Molina Otárola R (2008) La gran minería y los derechos indígenas en el norte de Chile [The big mining and the rights of indiginous people in northern Chile], 1. ed. Ciencias humanas. Estado y pueblos indígenas. LOM, Santiago

Zhang X-c, Wu J-W, Wu H-y, Li Y (2011) Simplified SEBAL method for estimating vast areal evapotranspiration with MODIS data. Water Science and Engineering(1):24–35. doi: 10.3882/j.issn.1674-2370.2011.01.003

List of Figures

List of Tables

6. Annexes

Annex 1 Acknowledgments

Annex 2 Outline of the author's contribution

Annex 3 Supplementary data (online)

6.1. Acknowledgments

Many people contributed to the work presented in this thesis, which is an outcome of the cooperation between the Department of Applied Geosciences of the Technical University of Berlin, Germany, and the Center of Research and Development of Water Resources in Iquique, Chile (CIDERH). I would like to thank my mentor Prof. Dr. Uwe Tröger for his unconditional support from the very beginning of the project, when planning the research proposal and acquiring funds, until the end, when finalizing the thesis. Furthermore, I would like to thank very much Dr. Claudio Moya, Dr. Ulrich Struck and Elisabeth Lictevout, that coauthored some of the presented work. I also thank Prof. Dr. Stefan Wohnlich and Prof. Dr. Matthias Barjenbruch for being part of the examination committee. Furthermore, I am grateful for the support of Jorge Olave, Damián Córdoba, Sonia Eloi, José Aguilera, Fernando Arancibia and the staff of CIDERH for their support regarding field work and the allocation of data.

I appreciate the project funding by the German Academic Exchange Service (DAAD) and the National Commission for Scientific and Technological Research, Chile (CONICYT), as well as the provision of data by the Compañía Minera Doña Inés de Collahuasi (CMDIC) and the Empresa Nacional del Petróleo Chile (ENAP). Some more people I would like to thank: Christian Antileo, John Houston, Benoit Viguier, Juan Salas, Fernando Urbina, Martin Appold, Sue Duncan, Eric Sproles, Claudio Custodio and all anonymous reviewers. Thank you.

6.2. Outline of the author's contribution to the self-contained articles of the thesis (Angaben zum Eigenanteil)

Chapter 2 – first author

Local climate change induced by groundwater overexploitation in a high Andean arid watershed, Laguna Lagunillas basin, northern Chile
The author developed the research idea. Data acquisition, literature revision and the methodological execution was done by the author. The interpretation of the results was done by the author, supported by suggestions of the coauthor Uwe Tröger. Writing and editorial handling were done by the author.

Chapter 3 – first author

Insights into Andean slope hydrology: reservoir characteristics of the thermal Pica spring system, Pampa del Tamarugal, northern Chile
The research idea was developed by the author and the co-author, Uwe Tröger. Data acquisition, literature revision and the methodological execution was done by the author. The interpretation of the results was done by the author, supported by suggestions of both coauthors, Claudio E. Moya and Uwe Tröger. Writing and editorial handling of the manuscript were done by the author.

Chapter 4 – first author

IV. Reassessing hydrological processes that control stable isotope tracers in groundwater of the Atacama Desert (northern Chile)
The research idea was developed by the author and co-author, Uwe Tröger. Data acquisition, literature revision and the methodological execution was done by the author. Laboratory work was done by the coauthor Ulrich Struck. The interpretation of the results was done by the author, supported by suggestions of Uwe Tröger, Claudio E. Moya and Elisabeth Lictevout. Writing and editorial handling of the manuscript were done by the author.

6.3. Supplementary data (online)

Supplementary material including the full isotope dataset and cross-validation plots of kriging models presented in chapter 4 can be found online at https://doi.org/10.3390/hydrology5010003.